

**SYNTHESIS AND DEVELOPMENT OF PHOSPHORUS LIGANDS IN THE
APPLICATION OF RHODIUM-CATALYZED HYDROFORMYLATION**

By

XIN ZHENG

A dissertation submitted to the
Graduate School-New Brunswick
Rutgers, The State University of New Jersey

In partial fulfillment of the requirements

For the degree of

Doctor of Philosophy

Graduate Program in Chemistry and Chemical Biology

Written under the direction of

Professor Xumu Zhang

And approved by

New Brunswick, New Jersey

October, 2015

ABSTRACT OF THE DISSERTATION

SYNTHESIS AND DEVELOPMENT OF PHOSPHORUS LIGANDS IN THE APPLICATION OF RHODIUM-CATALYZED HYDROFORMYLATION

By XIN ZHENG

Dissertation Director:

Professor Xumu Zhang

Rhodium-catalyzed hydroformylation reaction is one of the most powerful homogeneous catalytic processes in the synthesis of aldehydes that can be widely applied in pharmaceuticals and fine chemicals. The design and synthesis phosphorus ligands combine with rhodium precursor used as catalysts is essentially important in the development of this reaction. This dissertation mainly focuses on the design, synthesis and application of efficient phosphorus ligands in rhodium-catalyzed hydroformylation.

Asymmetric hydroformylation reaction (AHF), especially rhodium-catalyzed AHF has played a central role to construct chiral aldehydes in only one step. Although tons of chiral phosphorus ligands have been reported, few of them exhibited practicable enantioselectivities and regioselectivities. We report a new family of highly tunable bisphospholane ligands in the application of series of terminal and internal olefins, affording up to 88% for styrene derivatives, 93% ee for vinyl acetate

derivatives, 93% ee for dihydrofuran and 96% for dihydropyrrole. A systematic screening different substituents on the ligand showed that *ortho* chloride on phenyl moiety was the successful structure, achieving the highest regio- and enantioselectivity.

To expand the scope of substrates, especially the more challenging 1,1-disubstituted olefins, we first report the asymmetric hydroformylation of 1,1-disubstituted allylphthalimides by employing chiral ligand 1,2-bis[(2*S*,5*S*)-2,5-diphenylphospholano]ethane [(*S,S*)-Ph-BPE] to yield a series of β^3 -aminoaldehydes with up to 95% enantioselectivity. This asymmetric procedure provides an efficient alternative route to prepare chiral β^3 -amino acids and alcohols that are key structural elements of γ -aminobutyric acid.

Hydroaminomethylation is the tandem reaction of hydroformylation/hydrogenation. This efficient reaction is utilized to build nitrogen-containing compounds, which are interesting in pharmaceuticals and fine chemicals. In this chapter, we disclose the synthesis of 4-aryl-2,3-dihydropyrrole derivatives by rhodium-catalyzed intramolecular hydrominometylation reaction with up to 99% yield.

ACKNOWLEDGEMENTS

First, I would like to express my deepest gratitude to my dissertation advisor Professor Xumu Zhang, for introducing the world of organometallic chemistry to me, for inspiring my potential, for their support, guidance, encouragement, and patience.

I would also like to thank my dissertation committee members, Prof. Alan Goldman, Prof. Leslie Jimenez, and Dr. Gao Shang for taking time off of their busy schedule to review dissertation and attending my defense.

There is no way for me to come this far without the help from people I met during these years. They gave me essential assistance in my graduate study as well as my research. I would like to thank all of those who supported and assisted in any respect during my doctoral study, especially, Dr. Bonan Cao, Dr. Kun Xu, Dr. Tanglin Liu and Dr. Xiaowei Zhang for their generous help, invaluable discussion and closely cooperation. A special thanks is due to Dr. Thomas Emge for X-Ray crystallography expertise.

My thanks also go to my colleagues in the past and present at Zhang's group, for providing a pleasant and friendly working environment.

I would like to express special thanks to my parents. Their endless love and support has always been a great encouragement for me to finish my Phd study.

Finally, I offer my thanks to the financial support from Chemistry and Chemical Biology Department at Rutgers University.

TABLE OF CONTENTS

Abstract	ii
Acknowledgements	iv
Table of Contents	v
List of Schemes	viii
List of Tables	x
List of Figures	xi
Chapter 1. An Introduction to Rhodium-Catalyzed Hydroformylation	1
1.1. Overview	1
1.2. Mechanism for rhodium-catalyzed hydroformylation	5
1.3. The development of hydroformylation catalysts	6
1.4. Phosphorus ligands for Rh-catalyzed asymmetric hydroformylation	9
1.4.1. Bisphosphite ligands for Rh-catalyzed asymmetric hydroformylation	9
1.4.2. Bisphosphine ligands for Rh-catalyzed asymmetric hydroformylation	11
1.4.3. Phosphine-phosphite ligands for Rh-catalyzed asymmetric hydroformylation	13
1.4.4. Phosphine-phosphoramidite ligands for Rh-catalyzed asymmetric hydroformylation	16
1.4.5. Phospholane ligands for Rh-catalyzed asymmetric hydroformylation	17
1.4.6. Monophosphorus ligands for Rh-catalyzed asymmetric hydroformylation	20
1.5. Objective	22
References	22
Chapter 2. Synthesis and Application of Easily Accessible and Tunable Bisphospholane Ligands for Asymmetric Hydroformylation	29

2.1. Introduction	29
2.2. Results and Discussion	31
2.3. Conclusion	49
2.4. Experimental Section	49
2.4.1. General Remarks	49
2.4.2. General procedure for ligand synthesis and AHF reactions	50
2.4.3. Characterization of the ligands	51
2.4.4 GC and HPLC analysis of the chiral aldehydes	60
2.4.5. Single crystal X-ray diffraction structure of ligand 1c (CCDC 955452)	70
2.4.6. Single crystal structure of complex A (CCDC 955453)	71
Reference	72
Chapter 3. Rh-catalyzed Asymmetric Hydroformylation of 1,1-Disubstituted Allylphthalimides	78
3.1. Introduction	78
3.2. Results and Discussion	81
3.3. Conclusion	88
3.4. Experiment Section	88
3.4.1. General Remarks	88
3.4.2. General Procedure for the Synthesis of Substrates 1a-1i	89
3.4.3. General Procedure for the Asymmetric Hydroformylation of Allylphthalimides	89
References	99
Chapter 4. Synthesis of 4-Aryl-2,3-Dihydropyrrole Derivative by Rh-Catalyzed Intramolecular Hydroaminomethylation Reaction	104

4.1. Introduction	104
4.2. Results and Discussion	107
4.3. Conclusion	111
4.4. Experimental Section	111
4.4.1. General Remarks	111
4.4.2. General procedure for hydroaminomethylation reactions	112
References	122

LIST OF SCHEMES

1.1.	Hydroformylation reaction	1
1.2.	Hydrofromylation of propylene and the application thereof	2
1.3.	The application of asymmetric hydroformylation reaction in total synthesis	3
1.4.	Effect of alkene substitution on the reaction rate of hydroformylation reaction	3
1.5.	The mechanism of hydroformylation reaction	6
1.6.	Structures of DIOP, DIPAMP, TPPTS, Bisbi and UCC ligand	8
1.7.	Structures of fourth generation hydroformylation ligands	9
1.8	Chiral diphosphite ligands for asymmetric hydroformylation	11
1.9	Chiral diphosphine ligands for asymmetric hydroformylation	12
1.10	The AHF of 1,1-disubstituted olefin by DIOP	12
1.11	The AHF of 1,1-disubstituted olefin by (R,R)-BenzP*	13
1.12	The AHF of 3,3-disubstituted cyclopropenes	13
1.13	[Rh(CO) ₂ (R,S)-Binaphos] complex	14
1.14	Binaphos and its derivatives	15
1.15	Bobphos ligand	16
1.16	Phosphine-phosphoramidite ligands for AHF	16
1.17	Phospholane ligands for AHF	18
1.18	Monophosphorus ligands for AHF	20
1.19	Enantioselective hydroformylation of allylic amines	21
1.20	Enantioselective hydroformylation of 2-substituted homoallylic alcohols	21
2.1.	Different approach to the bis-diazaphospholate ligands	30

2.2	The application of β^2 -amino aldehyde to the synthesis	37
2.3.	Structures of biologically active products	39
2.4.	Conversion of AHF of <i>N</i> -Boc pyrrolidine into β -proline	40
2.5.	The application of 3-carbaldehyde to the total synthesis	45
2.6.	NMR data of complex B $[\text{RhH}(\text{CO})_2(\text{P}^{\wedge}\text{P})]$ obtained at 298K	47
2.7.	Equilibrium between ee and ea complexes	48
3.1.	The AHF of 1,1-disubstituted alkenes by ligand 1 and DIOP	79
3.2.	The AHF of α -alkylacrylates by ligand BenzP*	79
3.3.	Synthesis of (+)-3-isobutyl GABA. ¹⁰ a) nPr_2NH , HOAc; b) KCN, ROH; c) 1).KOH, MeOH 2). H_2 , Ni 3).HOAc; d) 1) IPA, H_2O 2) recryst e) 1) THF/ H_2O 2) recryst	80
3.4.	Chiral ligands for the asymmetric hydroformylation reaction	81
3.5.	Biologically active compounds containing isopropyl moiety	87
3.6.	Synthesis of β^3 -amino acids and alcohols	87
4.1.	Structure of biologically active alkaloids with pyrrolidine moieties	104
4.2.	Transformation of 3-aryl dihydropyrrole into bioactive alkaloids	105
4.3.	General catalytic cycle for hydroaminomethylation	106

LIST OF TABLES

1.1.	Relative reaction rate for hydroformylation employing Wilkinson's catalyst	4
1.2.	AHF screening of a library of bisdiazaphospholane ligands	18
2.1.	Ligand screening for AHF of styrene	32
2.2.	AHF of styrene derivatives	34
2.3.	AHF of vinyl acetate derivatives	35
2.4.	AHF of <i>N</i> -allylsulfonamides and <i>N</i> -allylamides	36
2.5.	AHF of other allylic substrates	38
2.6.	AHF of 15 with different ligands	40
2.7.	Optimization of selected ligands for the AHF of 2,3-dihydrofuran 15	42
2.8.	Expanding the scope of cyclic olefins	44
2.9.	AHF of vinyl amide and other 1,2-disubstituted olefins	46
3.1.	Asymmetric hydroformylation of 1a	82
3.2.	Syngas pressure screening for the Rh-catalyzed asymmetric hydroformylation of 1a ^a	83
3.3.	Solvent screening for the Rh-catalyzed asymmetric hydroformylation of 1a ^a	84
3.4.	Asymmetric hydroformylation of allylphthalimide ^a	86
4.1.	Rh-catalyzed hydroaminomethylation of 1a with different ligands ^a	107
4.2.	Optimization of reaction conditions ^a	108
4.3.	Expanding the scope of substrates ^a	110

LIST OF FIGURES

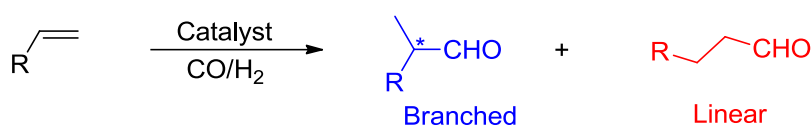
2.1.	X-ray crystal structure of complex A [Rh(1c)acac]	46
2.2	X-ray crystal structure of 1c	47

Chapter 1

An Introduction to Rhodium-Catalyzed Hydroformylation

1.1 Overview

Hydroformylation is recognized as one of the most important homogenous catalytic processes. It has been extensively applied in fine chemicals and pharmaceuticals in past decade. The merit of this methodology is atomic economy to transform olefins into aldehydes in only one step (Scheme 1-1).¹

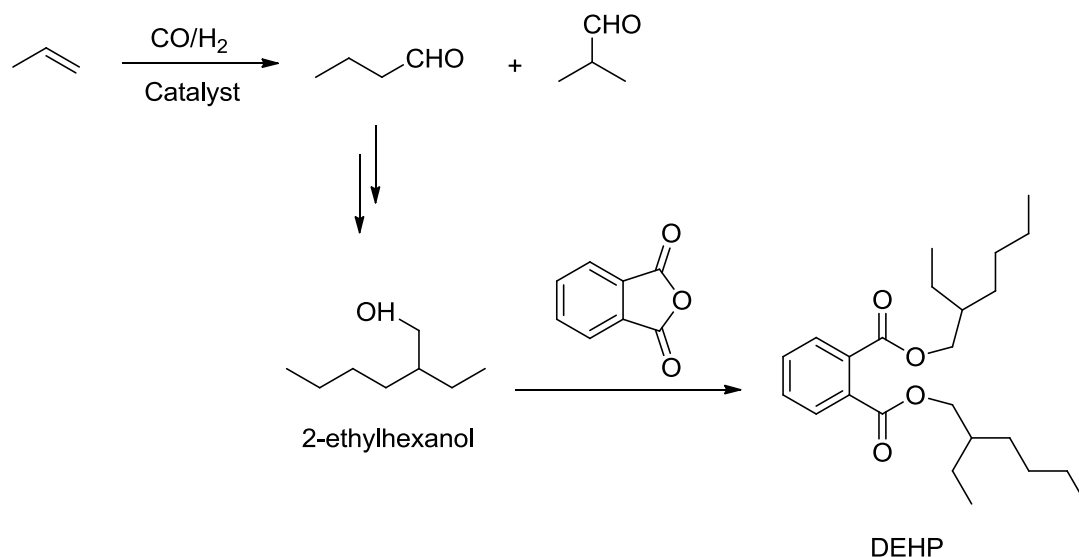


Scheme 1-1. Hydroformylation reaction

Hydroformylation reaction was first discovered by Otto Roelen in 1938 with cobalt as a metal precursor. The harsh reaction conditions with low reactivity did not attract chemists on this reaction at that time.² In the middle of 1960's, Wilkinson and coworkers first employed $\text{RhCl(PPh}_3)_3$ as the catalyst for hydrogenation³. Later, they reported rhodium-catalyzed hydroformylation using modified alkylphosphines and arylphosphines.⁴ These complexes formed by phosphine ligands with rhodium precursor substantially increased reaction activity and selectivity at milder conditions comparing with cobalt catalysts.⁴ Thus, modern research on hydroformylation focuses mainly on phosphorus ligands modified rhodium catalysts and their applications.⁵

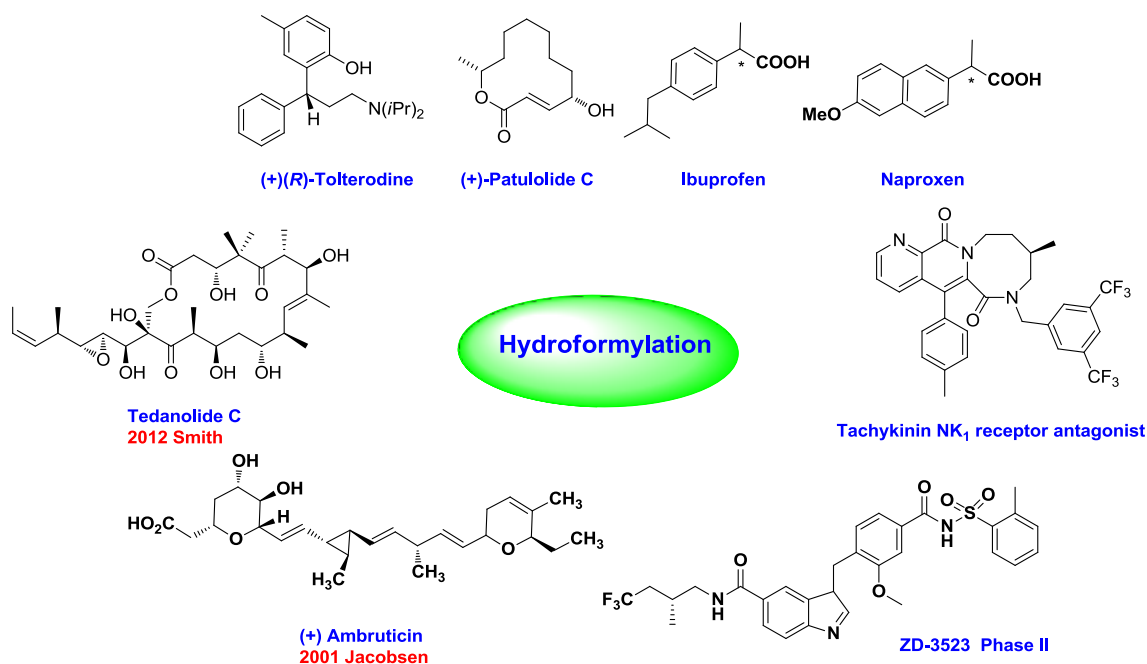
Nowadays, over 10 million tons of oxo products are produced based on rhodium-catalyzed hydroformylation every year. In industry, it is highly demand of normal aldehydes, especially for the preparation of polymer plasticizers and detergents. For instance, the hydroformylation of propylene to *n*-butanal has been put

into large-scale production. Most importantly, its product can be transformed into 2-ethylhexanol through consecutive aldol condensation and reduction to form bis(2-ethylhexyl)phthalate (DEHP), which is a critical intermediate to make PVC with approximately annual output of three billion kilograms (Scheme 1-2).¹



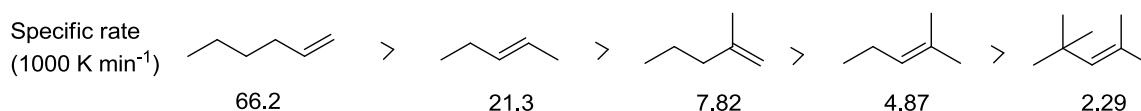
Scheme 1-2. Hydroformylation of propylene and the application thereof

Asymmetric hydroformylation (AHF) products are of great importance for the drug intermediates. These chiral aldehydes can be further transformed into alcohols, amines, esters, carboxylic acid derivatives.^{1,6} The enantiomerically pure aldehydes are valuable building block for the synthesis of various biologically active compounds and natural products.⁷ For instance, the anti-inflammatory drugs such as Ibuprofen and Naproxen can be synthesized from the key intermediate chiral 2-arylpropanoic acid, affording by AHF of vinylarenes, followed by oxidation reaction. The asymmetric hydroformylation of diene has been applied in total synthesis of Ambruticin and Patuloide C by Jacobsen and Smith, respectively (Scheme 1-3).^{7d, 7i}



Scheme 1-3. The application of asymmetric hydroformylation reaction in total synthesis

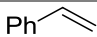
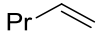
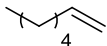
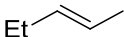
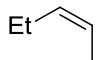
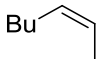
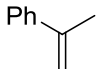
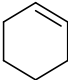
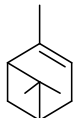
The rate of hydroformylation reaction depends significantly on the substitution of alkenes. The least reactive systems are internal alkenes, such as trisubstituted olefins. Tetrasubstituted derivatives are completely inert toward this reaction. Cycloalkenes are less reactive and more challenging to control regioselectivities than the corresponding acyclic alkenes (Scheme 1-4).^{7k, 7l}



Scheme 1-4. Effect of alkene substitution on the reaction rate of hydroformylation reaction

In Table 1-1, it shows the relative reactivity of a diverse set of alkene substrates catalyzed by Wilkinson's catalyst $[\text{HRh}(\text{CO})(\text{PPh}_3)_3]$ gave valuable insight for the study of this reaction.^{7m, 7n}

Table 1-1. Relative reaction rate for hydroformylation employing Wilkinson's catalyst

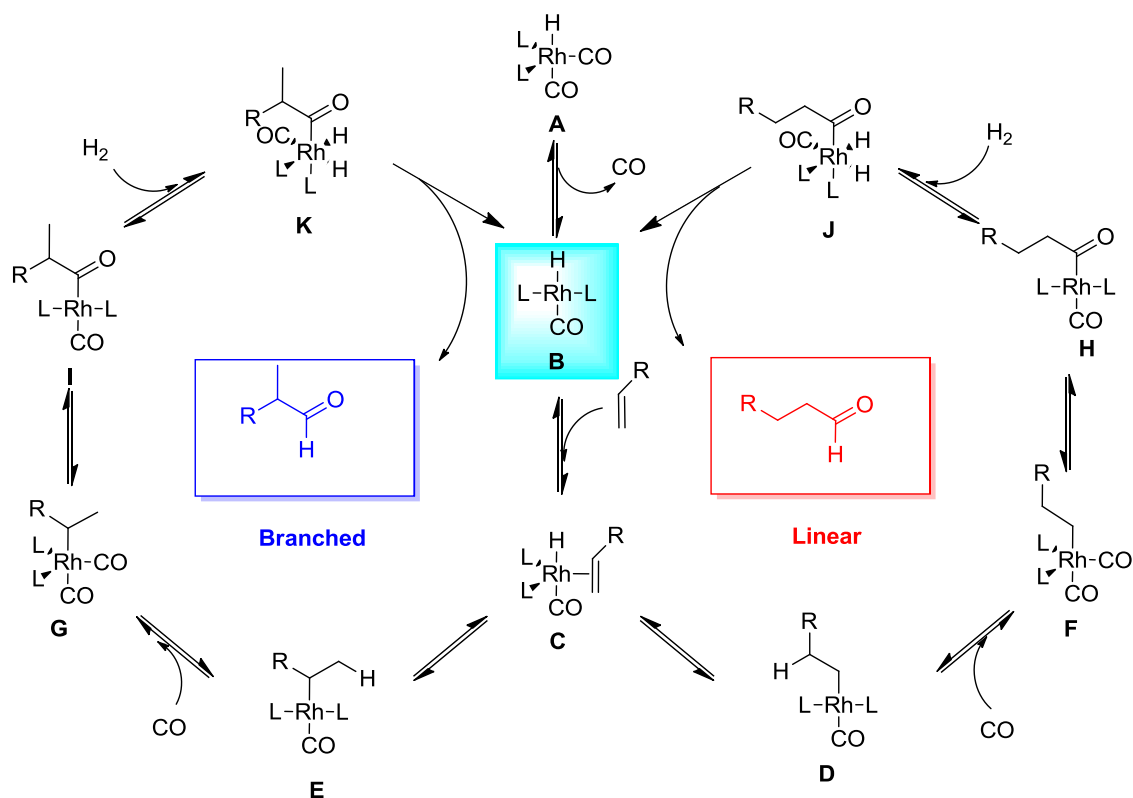
No	Alkene	Relative rate
1		4.32
2		3.73
3		3.50
4		0.15
5		0.15
6		0.12
7		0.06
8		<0.05
9		<0.05

The scope of this chapter is to review recent literature examples on the development of phosphorus ligands in the rhodium-catalyzed hydroformylation reaction.

1.2 Mechanism for rhodium-catalyzed hydroformylation

The first proposed mechanism was so-called dissociative mechanism by Breslow and Heck (Scheme 1-5)^{1f, 6} for cobalt-catalyzed hydroformylation reaction. It is also applicable for rhodium-catalyzed hydroformylation with chelating mono-phosphines or diphosphines.

This mechanism starts from different Rh(I)-sources under syngas pressure and in the presence of phosphorus ligands to form the trigonal bipyramidal 18-electron complex **A**. And then, the dissociation of one carbon monoxide from complex **A** generates unsaturated 16-electron square planar complex **B**, the key active catalyst specie, which subsequently coordinates with an olefin to the Rh center in the equatorial position, forming a trigonal bipyramidal hydrido olefin complex **C**. Next, the hydride insertion into C-C double bond generates either tetragonal alkyl rhodium complexes **D** or **E**, leading to linear or branched mechanism, respectively. Thus, this is crucial importance step to determine the regio- and enantioselectivity of the hydroformylation reaction.



Scheme 1-5. The mechanism of hydroformylation reaction

Next, the coordination of one carbon monoxide to the Rh center generates 18-electron trigonal bipyramidal complexes **F** and **G**, respectively, which is followed by carbon monoxide migratory insertion into the alkyl group yields tetragonal acyl complexes **H** and **I**. Oxidative addition of dihydrogen followed by reductive elimination liberates the isomeric linear and branched aldehydes and regenerates the catalyst **B** for another catalytic cycle.

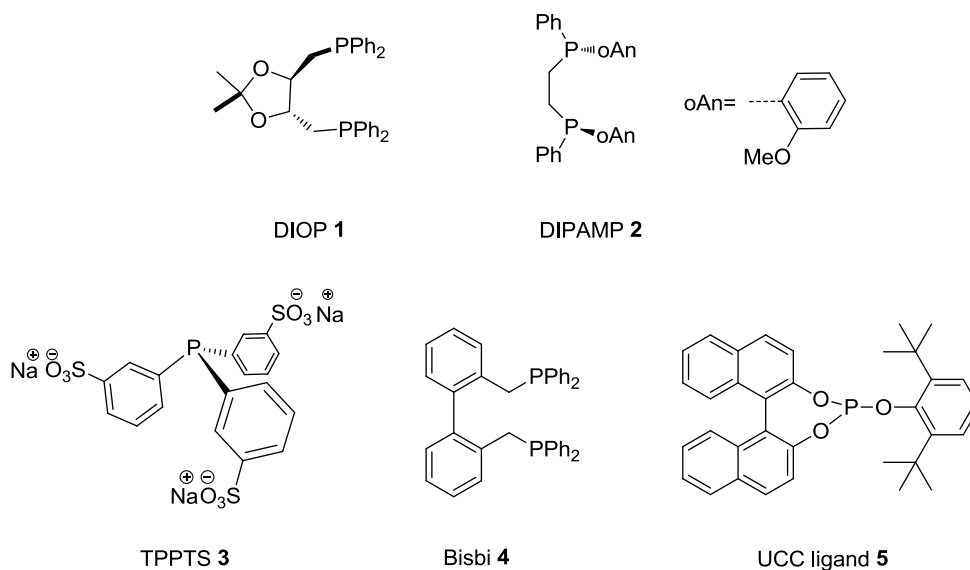
1.3 The development of hydroformylation catalysts

Phosphorus ligands have been applied for hydroformylation reaction for nearly half century. The effects of phosphine ligands in organic catalysis have been well known for quite a long time.

The first generation of hydroformylation catalysts was $[\text{CoH}(\text{CO})_4]$ without phosphine ligand⁸. The reaction conditions were harsh with low reactivity. This process mainly gave linear aldehyde. The early example of phosphine-catalyzed alkene hydroformylation reaction using cobalt as metal precursor was reported by Shell⁹ in 1964. In 1965, Wilkinson and co-workers employed arylphosphines with rhodium as catalysts and run reactions at very mild conditions³.

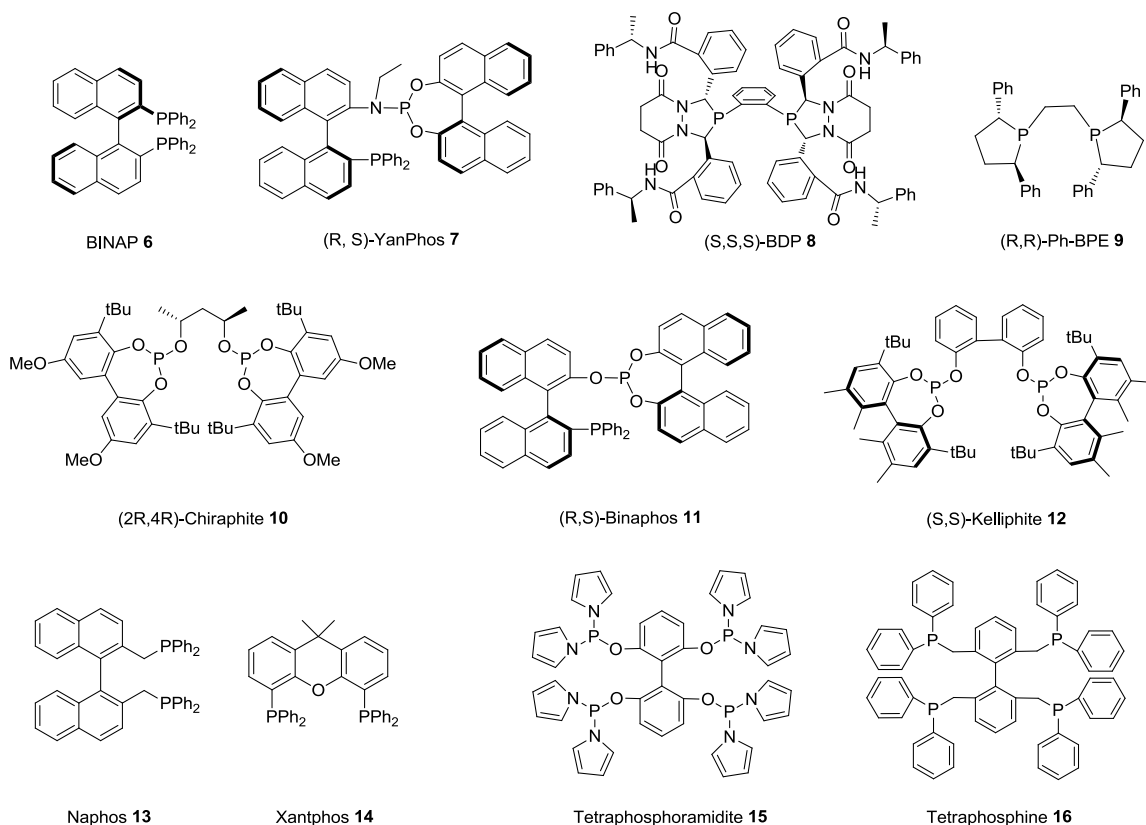
The second generation catalyst was rhodium triphenylphosphine catalyst. This type of catalyst is much faster even under milder reaction conditions comparing with cobalt catalysts. Also, it increased the utility of feedstock. The disadvantage of this rhodium triphenylphosphine catalyst was the low reactivity for the hydroformylation of internal olefins.

The representative catalyst of third generation was the water-soluble rhodium-tppts **3** system. This process was reported in 1984 by Celanese. In 1995, it has been applied for the hydroformylation of 1-butene.¹⁰ At the meantime, bidentate phosphine and phosphite ligands have also been extensively applied in rhodium catalyzed hydroformylation reaction, which comprised Kagan's DIOP,¹¹ Knowles' DIPAMP,¹² Eastman's Bisbi¹³ and UCC ligand **5** (Scheme 1-6).



Scheme 1-6. Structures of DIOP, DIPAMP, TPPTS, Bisbi and UCC ligand

In recent years, many biphosphines, biphosphites, phosphine-phosphite, phosphine-phosphoramidite and bisphosphacyclic ligands have been reported and applied in hydroformylation reaction. Some are efficient for asymmetric hydroformylation; some are highly selective for linear hydroformylation. The most successful ligands of asymmetric hydroformylation in the fourth generation comprise Noyori's BINAP;¹⁴ Binaphos **11**, introduced by Takaya;¹⁵ BDP **8**, developed by Landis' group;¹⁶ Ph-BPE **9**, designed by Dow chemical;¹⁷ Yanphos **7**, reported by Zhang's group;¹⁸ Chiraphite^{19a-b} **10** and Kellphite^{19c} **12** (Scheme 1-7). For linear hydroformylation reaction, the excellent ligands include van Leeuwen's Xantphos **14**²⁰, Beller's Naphos²¹ **13** and Zhang group's tetraphosphine **16** and tetraphosphoramidate **15** ligands (Scheme 1-7).²²



Scheme 1-7. Structures of fourth generation hydroformylation ligands

1.4 Phosphorus ligands for Rh-catalyzed asymmetric hydroformylation

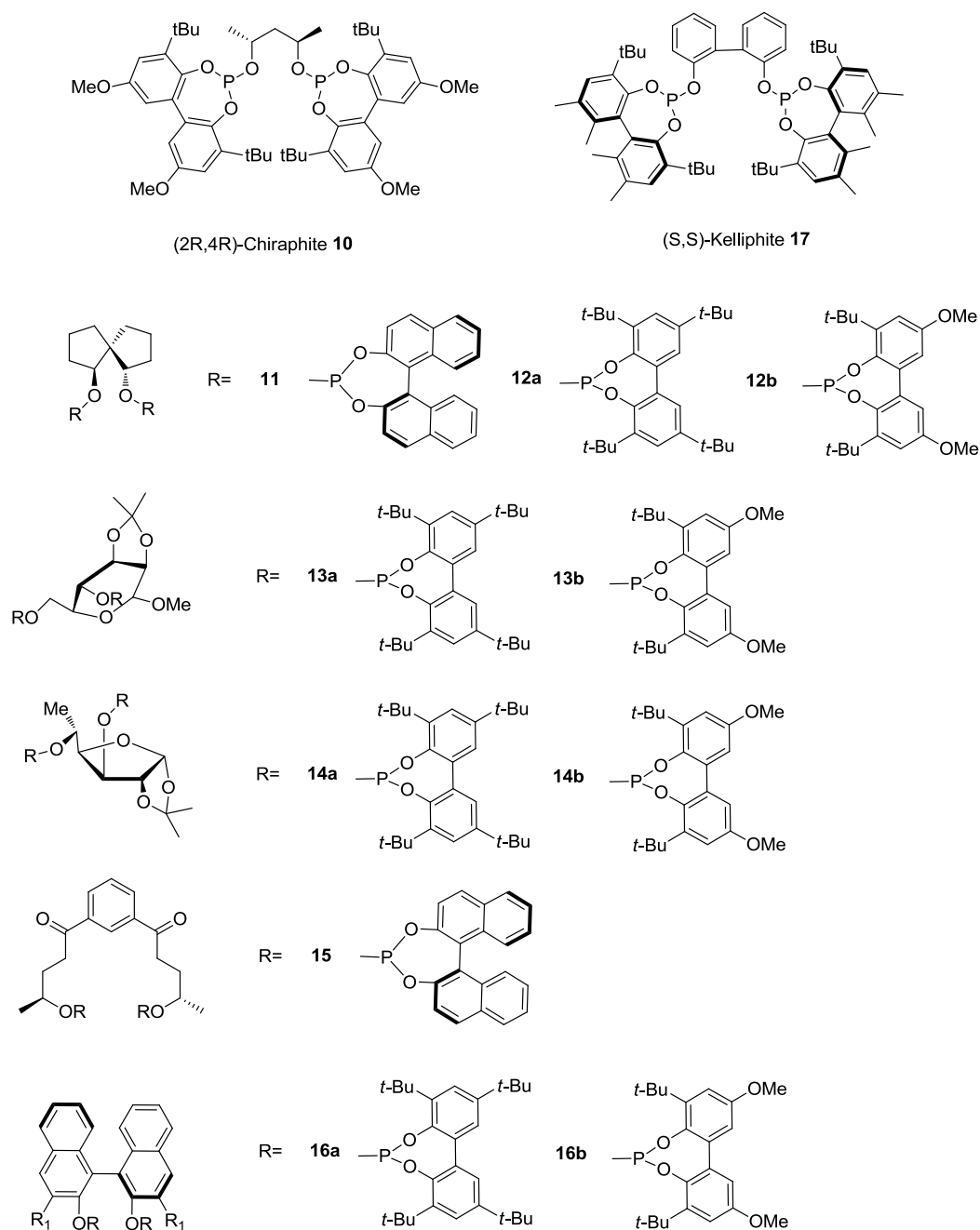
Asymmetric hydroformylation provides enantiomerically enriched aldehydes from inexpensive feedstock directly. However, even thousands of ligands have been reported, successful examples are few and limited to be applied in industry. The challenging aspects are 1) low reactivity at ambient temperature 2) difficulty to control the regio- and enantioselectivity simultaneously 3) limited scope of substrates. Thus, ligand design is super critical for this methodology. We will discuss the AHF ligands by classification as follow.

1.4.1 Bisphosphite ligands for Rh-catalyzed asymmetric hydroformylation

Phosphite ligands are very active in hydroformylation reaction because of their superior π -acceptor properties. The pioneering work by Babin and Whiteker in 1992 introduced highly enantioselective hydroformylation ligand, (R,R)-Chiraphite **10** (Scheme 1-8).²³ It is a bulky diphosphite ligand with a chiral (2R, 4R)-pentane-2,4-diol backbone. (R,R)-Chiraphite **10** offers more than 90% enantioselectivity in the AHF of styrene under mild reaction conditions. The *t*-butyl groups made this ligand more steric hinder and transferred the chiral information to the non-chiral biphenyl moieties. Decreasing the temperature led to a slight increase of enantiomeric excess in the expense of lower conversion. The electron-withdrawing property of diphosphite ligands enable the AHF to be conducted at relatively low temperature, resulting in higher enantioselectivity. Thus, optically active diols became useful bridges for the synthesis of chiral diphosphate ligands. Diversity of chiral diphosphite ligands have been synthesized, along with different chiral elements in the phosphite moiety. For

instance, Chan and coworkers employing chiral spiro [4.4]nonane-1,6-diol as backbone for diphosphite ligands **11** and **12**, achieving up to 65% ee for the AHF of styrene.²⁴

Sugar derivatives have also been used in asymmetric catalysis due to easily accessible. The first diphosphite ligand based on sugar backbone was reported by van Leeuwen and coworkers. This ligand **13** afforded moderate enantioselectivities (65 % ee) in the AHF of styrene and its derivatives.²⁵ A series of furanoside backbone diphosphite ligands such as ligands **14**, explored by Diéguez and coworkers, providing up to 91% enantioselectivities in the AHF of styrene and its derivatives.²⁶ Other optically active diol such as macrocyclic used for ligand **15**, reported by Freixa and coworkers, giving up to 76 % ee in the AHF of styrene.²⁷ Recently, our group developed a family of diphosphite ligands **16** based on chiral BINOL backbone.²⁸ Moderate enantioselectivities (up to 80% ee) and excellent regioselectivities (b/l up to 98/2) have been achieved in the AHF of vinyl acetate. Additionally, Kelliphite **17**, bearing a non-chiral 2,2'-biphenol backbone and chiral phosphite moieties,²⁹ was developed by Dow Chemical for the AHF of allylic cyanide and vinyl acetate with up to 80% enantioselectivity.



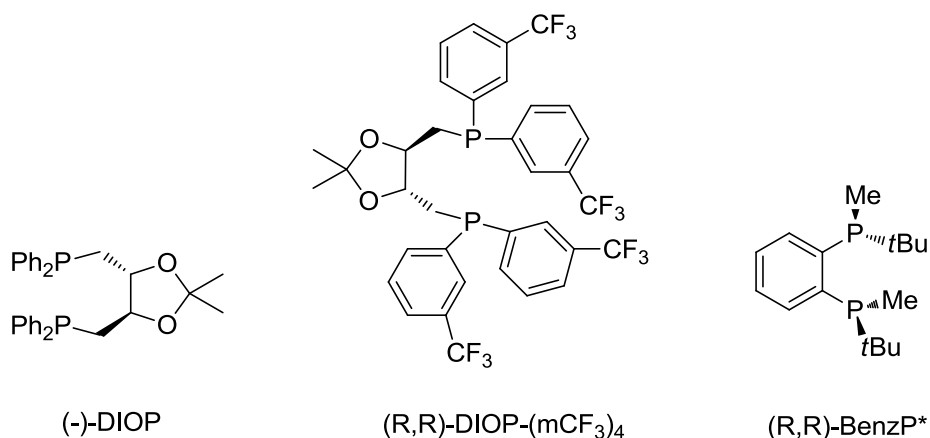
Scheme 1-8. Chiral diphosphite ligands for asymmetric hydroformylation

1.4.2 Bisphosphine ligands for Rh-catalyzed asymmetric hydroformylation

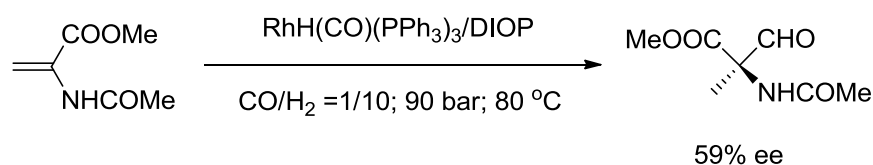
The bisphosphine ligands are less efficient for asymmetric hydroformylation than the bisphosphite ligands. The most classic ligand is (R,R)-DIOP. The use of DIOP with rhodium catalyst precursors was first reported in 1973 for the AHF of

aromatic olefins^{1b}. Among these substrates, it gave up to 23% ee and 69/31 branched to linear ratio for styrene in the absence of solvent. The modified DIOP ligand (Scheme 1-9) with the phenyl ring of the PPh₂ moiety provided 100% conversion with up to 42% ee for vinyl acetate^{1b}.

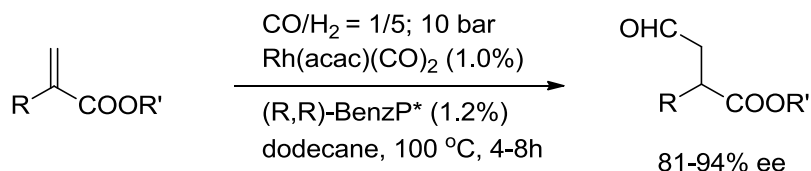
The rhodium-DIOP system can provide quaternary stereogenic center in the AHF of amido acrylate in 100% conversion at mild temperature with up to 59% enantioselectivity (Scheme 1-10)^{1b}. The excellent hydrogenation ligand (R,R)-BenzP* has been studied for the AHF of functionalized 1,1-disubstituted olefins under mild condition with up to 94% ee (Scheme 1-11). This methodology directly generated 1,4-dicarbonyl building blocks with an α -tertiary stereogenic center.^{30a}



Scheme 1-9. Chiral diposphine ligands for asymmetric hydroformylation

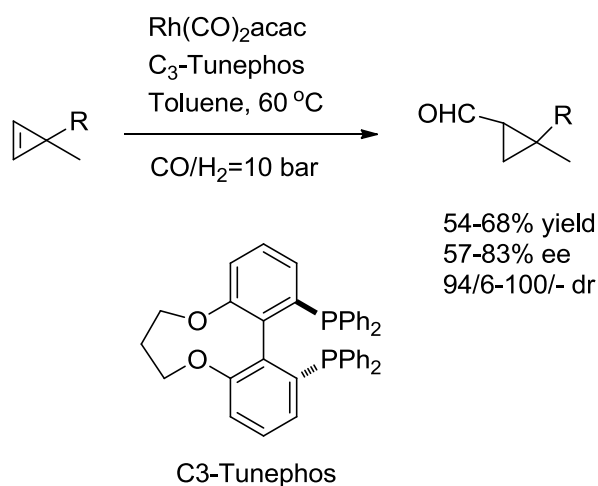


Scheme 1-10. The AHF of 1,1-disubstituted olefin by DIOP



Scheme 1-11. The AHF of 1,1-disubstituted olefin by (R,R)-BenzP*

The first catalytic diastereo- and enantioselective hydroformylation of cyclopropenes by C₃-Tunephos has been developed. The reaction proceeded under mild reaction condition with up to 83% ee and 100 dr value (Scheme 1-12).^{30b}

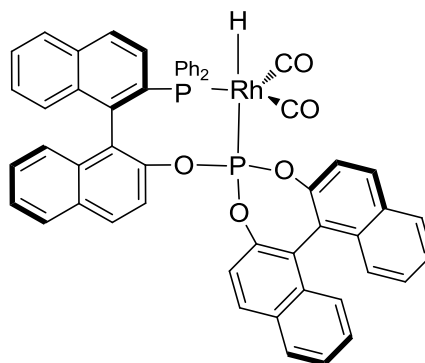


Scheme 1-12. The AHF of 3,3-disubstituted cyclopropenes

1.4.3 Phosphine-phosphite ligands for Rh-catalyzed asymmetric hydroformylation

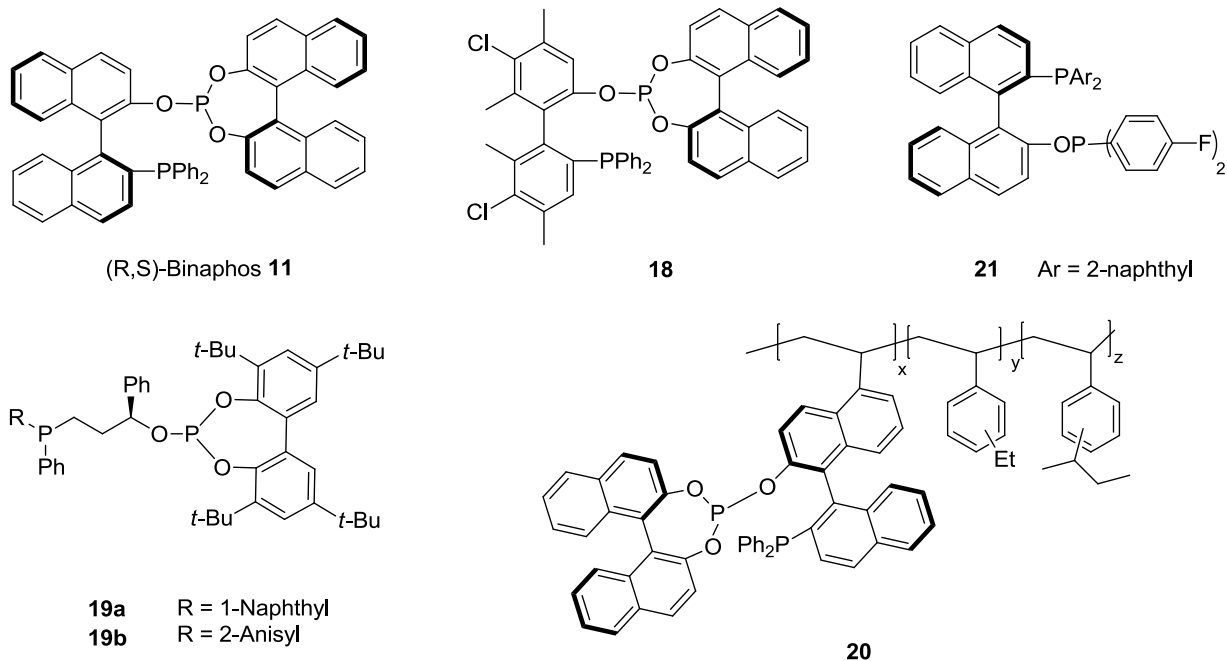
Since diphosphite ligands formed more stable hydroformylation catalysts than diphosphine ligands. In 1993, Takaya and Nozaki designed the chiral phosphine-phosphite ligand (R,S)-Binaphos **11**. As expected, this hybrid phosphine-phosphite ligand based on binaphthyl backbone provided much higher enantioselectivities than either diphosphine ligands or diphosphite ligands, along with more than 90% ee for a

wide variety of substrates. This ligand is recognized as the benchmark in asymmetric hydroformylation.³¹ The complex of $[\text{RhH}(\text{CO})_2(\text{R,S})\text{-Binaphos}]$ have been characterized by NMR spectroscopy. All the NMR data indicate that the hydride is oriented *cis* position to phosphine and *trans* to phosphite (Scheme 1-13).³²



Scheme 1-13. $[\text{RhH}(\text{CO})_2(\text{R,S})\text{-Binaphos}]$ complex

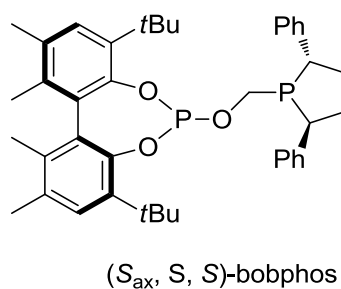
Due to excellent enantioselectivities of Binaphos **11**, van Leeuwen and coworkers designed a series of modified Binaphos ligands **19** (Scheme 1-14). The stereocenter is closer to the phosphite moiety and the substituents on phosphine are much more near to the metal center, resulting in slightly improved enantioselectivity.^{31c,33} The conformations of the bisphenol moiety at the phosphite are controlled by the substituent in the backbone, which also control the configuration of final products. The coordination mode of these ligands complexes are opposite to Binaphos complex. The phosphite moiety coordinated at an equatorial position and the phosphine at the apical position, which are important for achieving high enantioselectivity. For instance, Biphemphos **18**, bearing a chiral biphenyl backbone, afforded comparable enantioselectivity as Binaphos (Scheme 1-14).^{31b,34}



Scheme 1-14. Binaphos and its derivatives

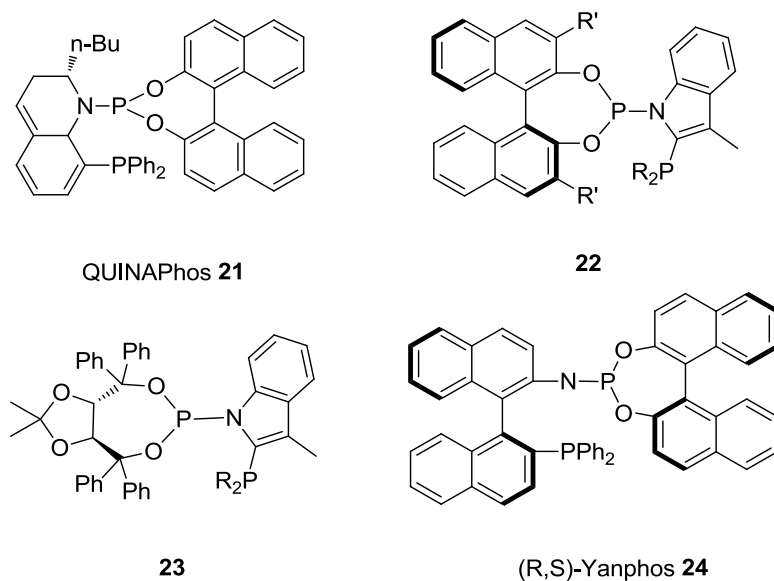
Binaphos **11** can be stabilized on polymer resin for recovery. Highly cross-linked polymer-supported Binaphos ligands **20** were effective for the hydroformylation of styrene (up to 89% ee).³⁵ Hydroformylation of 4-vinyl- β -lactam employing ligand **21** gave the β -methyl branched aldehyde in excellent yield with good regio- and diastereoselectivity.³⁶

Recently, Clarke and coworkers discovered a new phosphine-phosphite ligand (Sax, S, S)-bobphos (Scheme 1-15) that gave unexpectedly high levels of reactivity in the AHF of terminal alkyl olefins $RCH_2CH=CH_2$ with up to 92% ee.³⁷



Scheme 1-15. Bobphos ligand**1.4.4 Phosphine-phosphoramidite ligands for Rh-catalyzed asymmetric hydroformylation**

In 2000, Leitner and coworkers reported a new hybrid phosphine-phosphoramidite ligand (QUINAPhos **21**) (Scheme 1-16) based on 1,2-dihydroquinoline backbone. It presented up to 74% enantioselectivity in AHF of styrene.³⁸ After that, IndolPhos ligands **22** and **23**,³⁹ reported by Reek and coworkers, derived from Binol and Taddol, respectively, affording moderate to good enantioselectivities (up to 74 % ee) in the AHF of styrene, vinyl acetate, and allyl cyanide.

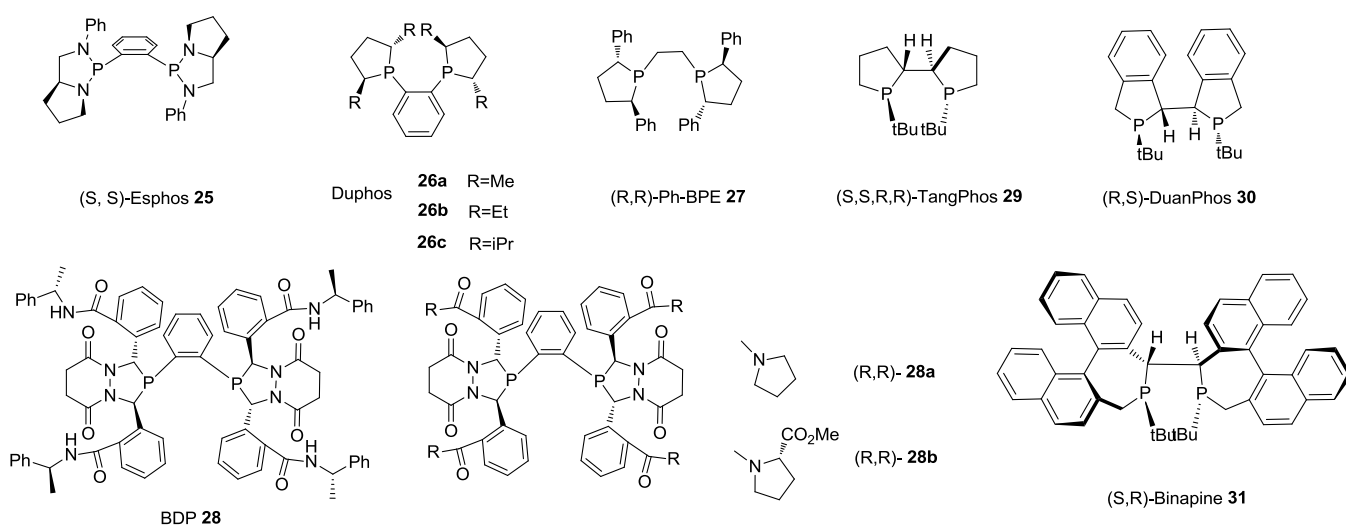
*Scheme 1-16.* Phosphine-phosphoramidite ligands for AHF

Inspired by the success of Binaphos **11**, Zhang group designed the phosphine-phosphoramidite analogue (Yanphos **24**).^{40a} The replacement of oxygen by nitrogen on Binaphos has significantly improved the rigidity and electron property. Molecular

modeling study demonstrated that the more rigid chiral environment in the complex of [RhH(CO)₂(R,S)-Yanphos] than [RhH(CO)₂(R,S)-Binaphos] due to introduction of a N-ethyl moiety. The (R,S)-Yanphos showed unprecedented high enantioselectivity for styrene derivatives (up to 99%), vinyl acetate derivatives (up to 98%) and allyl cyanide (up to 96%).^{40b} The reaction turnover number could lower at S/C = 10,000 remaining unchangeable reactivity (89% conv.) and enantioselectivity (98% ee) for the AHF of styrene. In addition, Yanphos is much more basic than Binaphos that remarkably reduced the racemization of final chiral products.

1.4.5 Phospholane ligands for Rh-catalyzed asymmetric hydroformylation

C₂-Symmetric phospholane-type ligand, (S,S)-Esphos **25** developed by Wills and coworkers in 2000, providing up to 90% enantioselectivity for AHF of vinyl acetate but no selectivity of styrene.⁴¹ After that, a series excellent phospholane ligands have been applied in AHF that comprise Duphos **26**,⁴² (R,R)-Ph-BPE **27**,⁴³ (S,S,S)-BDP **28**,^{44a} (S,S,R,R)-Tangphos **29**,^{45a} (R,S)-Duanphos **30**,⁴⁶ (S,R)-Binapine **31**^{45a} and so on (Scheme 1-17).



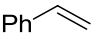
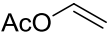
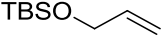
Scheme 1-17. Phospholane ligands for AHF

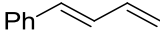
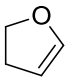
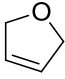
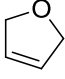
In 2005, Landis and coworkers first reported the synthesis of bis-3,4-diazaphospholane ligand (BDP **28**) in an efficient way and applied it in the hydroformylation of three classic substrates styrene, vinyl acetate, and allyl cyanide with modest regioselectivities (b/l 6.6:1, 37:1, and 4.1:1) and excellent enantioselectivities (82, 96, and 87%).^{44a} The same ligand was also used for the AHF of vinylcarboxamides and dialkylacrylamides with excellent enantioselectivities and regioselectivities. In particular, *N*-vinyl trifluoroacetamide underwent highly selective hydroformylation, providing the only α product with 99% ee.^{44f}

Allylic alkenes are considerably challenging substrates for AHF. In most cases, the linear aldehydes are the major products. This BDP ligand enables exceptionally high enantioselectivity for the AHF of *N*- and *O*-functionalized allyl substrates. The AHF of allyl alcohols processed in 95% enantioselectivity, although the b/l ratio still favored the linear aldehyde.^{44f}

Landis and coworkers further developed a small library of BDP ligands to test the influence of different steric bulky substitutes on the activity and selectivity of AHF (Table 1-2).^{44d}

Table 1-2. AHF screening of a library of bisdiazaphospholane ligands

Entry	Ligand	Substrate	b/l	ee(%)
1	28		18.3	87
2	28		53	98
3	28		2	96

4	28		-	97
5	28b		3.5	90
6	28a		<1:30	95
7	28b		<1:30	95

1,2-bis(2,5-diphenylphosphino)ethane (R, R)-Ph-BPE **27** is one of the excellent phospholane ligands, yielding up to 94 %, 82 % and 90 % ee for styrene, vinyl acetate and allyl cyanide respectively.⁴³ The improved reactivity of Ph-BPE compared with Me-, Et- and iPr-BPE was attributed to the presence of relatively electron-withdrawing phenyl rings, which represents a more reactive Rh-catalyst via facile carbon monoxide dissociation.

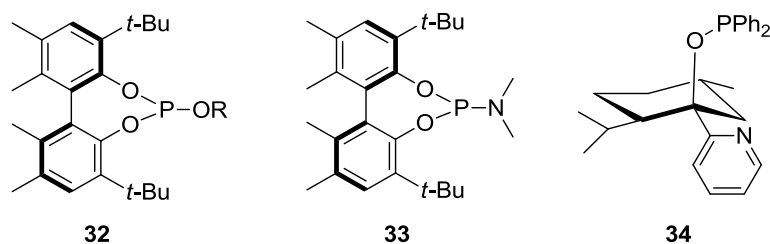
Some other asymmetric hydrogenation ligands previously developed by Zhang's group were also applied in AHF. The first highly enantioselective Rh-catalyzed hydroformylation of norbornene and its derivatives by (S,S,R,R)-Tangphos **29** has been reported, forming the *exo* aldehyde with up to 92% ee.^{45b} In contrast, Binaphos only gave moderate enantioselectivity up to 70% for the same substrate. Klosin and coworkers identified both (S,S,R,R)-Tangphos **29** and Binaphine **31** offered excellent enantioselectivities in AHF of three typical substrates. (S,S,R,R)-TangPhos **29** achieved up to 90 % ee for styrene, 93 % ee for allyl cyanide and 83 % ee for vinyl acetate, while (S,R)-Binaphine **31** provided up to 94 % , 94 % and 87 % respectively.^{45a}

Recently, Buchwald and coworkers investigated (R,S)-Duanphos **30** in the AHF of 1,1-disubstituted substrates, especially 3,3,3-trifluoroprop-1-en-2-yl acetate.

The final products were selectively formed quaternary aldehydes with up to 92% ee which are useful pharmaceutical intermediates.⁴³⁶

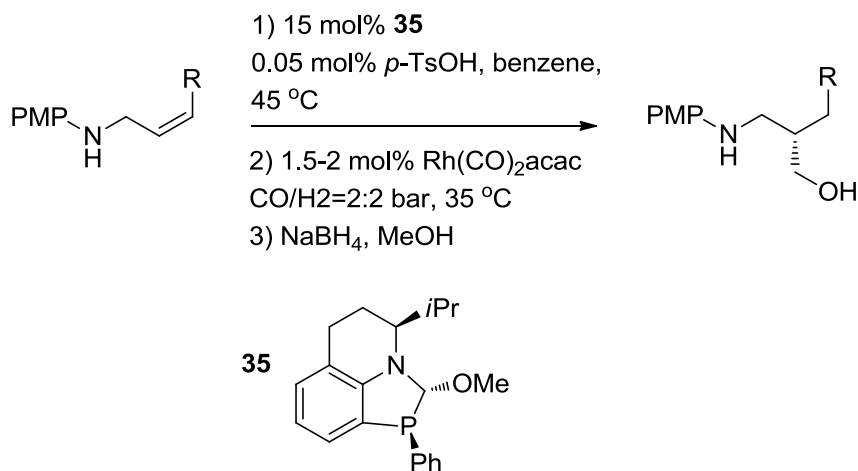
1.4.6 Monophosphorus ligands for Rh-catalyzed asymmetric hydroformylation

Monophosphorus ligands have been widely applied in linear selective hydroformylation but less in asymmetric hydroformylation reaction due to low enantioselectivity and reactivity. For instance, monophosphite ligand **32** (Scheme 1-18) gave 38 % ee, 8 % ee and 43 % ee for styrene, vinyl acetate and allyl cyanide respectively.⁴⁷ Ojima and coworkers designed ligand **33** provided more than 80% enantioselectivity for the AHF of allyl cyanide (Scheme 1-18).⁴⁸ The chiral bidentate *P, N* ligand reported by Faraone and coworkers performed excellent catalytic ability on methylacrylate with enantioselectivity up to 92%.⁴⁹



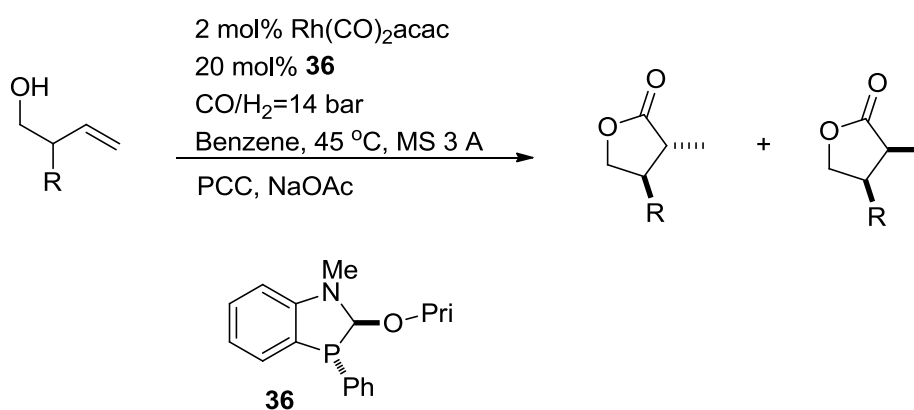
Scheme 1-18. Monophosphorus ligands for AHF

Recently, a new strategy of dynamic chiral catalytic directing group ligands was designed by Tan's group which allowed for simultaneous control of regioselectivity and enantioselectivity in the course of asymmetric hydroformylation of allylic amines by ligand **35** (Scheme 1-19). The products were directly reduced to generate the corresponding 1,3-aminoalcohols in moderate to good yields with up to 93% ee.⁵⁰



Scheme 1-19. Enantioselective hydroformylation of allylic amines

The directing ligand **36** was efficient for the AHF of 2-substituted homoallylic alcohols to achieve high anti-selectivity in the five-membered ring lactone with high yield and diastereoselectivity (Scheme 1-20).⁵¹



Scheme 1-20. Enantioselective hydroformylation of 2-substituted homoallylic alcohols

1.5 Objectives

Asymmetric hydroformylation is a very promising catalytic methodology in the application of organic synthesis to convert olefins into enantiomerically pure aldehydes. The challenging in AHF is to design new efficient chiral phosphorus ligands bearing suitable steric and electronic properties that can achieve both high enantioselectivity and regoselectivity at high temperature. Additionally, easily and tunable synthesis routes are also crucially important for screening and optimizing reaction conditions.

In practice, efforts towards this goals have been devoted into three aspects: a) design and synthesis of conformationally rigid, electron-withdrawing P-chiral ligands for AHF; b) testing the new ligands in the AHF of classical substrates and investigating the relationship of ligand structures; c) exploring more challenging substrates and further application of AHF in the synthesis of valuable chiral pharmaceuticals and fine chemicals. The detailed results will be discussed in the following chapters.

Reference

1. For recent reviews, see: a) Claver, C.; van Leeuwen, P. W. N. M. In *Rhodium Catalyzed Hydroformylation*; Eds: Claver, C.; van Leeuwen, P. W. N. M. Kluwer Academic Publishers, Dordrecht, The Netherlands, 2000; b) Agbossou, F.; Carpentier, J. F.; Mortreux, A. *Chem. Rev.* **1995**, 95, 2485; c) Herrmann, W. A.; Cornils, B. *Angew. Chem. Int. Ed.* **1997**, 36, 1048; d) Nozaki, K.; Ojima, I. in *Catalytic Asymmetric Synthesis*, 2nd ed, (Ed.: Ojima, I.), Wiley-VCH, New York, 2000, chapter 7; e) Breit, B.; Seiche, W. *Synthesis* **2001**, 1; f) Breit, B. *Angew. Chem. Int. Ed.* **2005**, 44, 6816; g) Godard, C.; Ruiz, A.;

- Diéguez, M.; Pàmies, O.; Claver, C. in *Catalytic Asymmetric Synthesis*, 3rd ed, (Ed.: Ojima, I.), WileyVCH, New York, 2010, chapter 10.
2. a) Roelen, O. (Chemische Verwertungsgesellschaft, mbH Oberhausen) German Patent DE 849548, 1938/1952; b) Roelen, O. (Chemische Verwertungsgesellschaft, mbH Oberhausen) U.S. Patent 2327066, 1943.
 3. Young, J. F.; Osborn, J. A.; Jardine, F. A.; Wilkinson, G. *J. Chem. Soc., Chem. Comm.* **1965**, 131.
 4. a) Evans, D. A.; Osborn, J. A.; Wilkinson, G. *J. Chem. Soc. A*, **1968**, 3133; b) Brown, C. K.; Wilkinson, G. *J. Chem. Soc. A* **1970**, 17, 2753; c) Wilkinson, G. *Bull. Soc. Chim. Fr.* **1968**, 5055; d) Osborn, J. A.; Jardine, F. H.; Young, J. F.; Wilkinson, G. *J. Chem. Soc. A* **1966**, 1711.
 5. Stille, J. K. In *Comprehensive Organic Synthesis*; Trost, B. M.; Fleming, I., Eds.; Pergamon: Oxford, 1991.
 6. Heck, R. F.; Breslow, D. S. *J. Am. Chem. Soc.* **1961**, 83, 4023.
 7. a) Botteghi, C.; Paganelli, S.; Schionato, A.; Marchetti, M. *Chirality*, **1991**, 3, 355; b) Jacob, R. T. et al. *J. Med. Chem.* **1994**, 37, 128; c) Gladiali, S.; Bayön, J. C.; Claver, C. *Tetrahedron: Asymmetry*, **1995**, 6, 1453; d) Liu, P.; Jacobsen, E. N. *J. Am. Chem. Soc.* **2001**, 123, 10772; e) Botteghi, C. et al. *Org. Pro. Res & Dev.* **2002**, 6, 379; f) Vries, J. G. Et.al. *Adv. Synth. Catal.* **2003**, 345, 478. Diéguez, M.; Pàmies, O.; g) Claver, C. *Tetrahedron: Asymmetry* **2004**, 15, 2113; h) Gual, A.; Godard, C.; Castellón, S.; Claver, C. *Tetrahedron: Asymmetry* **2010**, 21, 1135. 29; i) Smith, T. E.; Fink, S. J.; Levine, Z. G.; McClelland, K. A.; Zackheim, A. A.; Daub, M. E. *Org. Lett.* **2012**, 14, 1452; j) Burke, S. D. et.al. *Org. Lett.* **2012**, 14, 1180; k) Wender, I.; Metlin, S.; Ergun, S.; Sternberg, H.W.; Greenfield, H. *J. Am. Chem. Soc.* **1956**, 78, 5401; l) Heil,

- B.; Marko', L. *Chem. Ber.* **1969**, *102*, 2238; m) Brown, C.K. ; Wilkinson, G. *J. Chem. Soc. A* **1970**, *17*, 2753; n) Brown, C. K.; Wilkinson, G. *Tetrahedron Lett.* **1969**, *22*, 1725.
8. Frohning, C. D.; Kohlpaintner, C. W. page 29, in *Applied Homogeneous Catalysis with Organometallic Compounds*, eds. Cornils B.; Herrmann, W. A., VCH, Weinheim, 1996, Vol 1 and 2.
 9. Slauch, L. H.; Mullineaux, R. D. U.S. Pat. 3,239,569 and 3,239,570, 1996 (to shell); *Chem. Abstr.* **1964**, *64*, 15745 and 19420. *J. Organomet. Chem.* **1968**, *13*, 469.
 10. Cornils, B.; Kuntz, E. G. *J. Organomet. Chem.* **1995**, *502*, 177.
 11. Poulin, J. C.; Dang, T. P.; Kagan, H. B. *J. Organomet. Chem.* **1975**, *84*, 87.
 12. a) Knowles, W. S.; Sabacky, M. J. *J. Chem. Soc., Chem. Commun.* **1971**, 481;
b) Knowles, W. S.; Sabacky, M. J.; Vineyard, B. D., and Weinkauff, J. *J. Am. Chem. Soc.* **1975**, *97*, 2567.
 13. Devon, T. J.; Phillips, G. W.; Puckette, T. A.; Stavinoha, J. L.; Vanderbilt, J. J. US Patent 4 694 109, 1987.
 14. Miyashita, A.; Yasuda, A.; Tanaka, H.; Toriumi, K.; Ito, T.; Souchi, T.; Noyori, R. *J. Am. Chem. Soc.* **1980**, *102*, 7932.
 15. Sakai, N.; Mano, S.; Nozaki, K.; Takaya, H. *J. Am. Chem. Soc.* **1993**, *115*, 7033.
 16. Clark, T. P.; Landis, C. R.; Freed, S. L.; Klosin, J.; Abboud, K. A. *J. Am. Chem. Soc.* **2005**, *127*, 5040.
 17. Iwata, M.; Yazaki, R.; Chen, I. H.; Sureshkumar, D.; Kumagai, N.; Shibasaki, M.; *J. Am. Chem. Soc.* **2011**, *133*, 5554.
 18. Yan, Y.; Zhang, X. *J. Am. Chem. Soc.* **2006**, *128*, 7198.

19. a) Babin, J. E.; Whiteker, G. T. (Union Carbide Corporation), WO 9303839, 1993; b) Whiteker, G. T.; Briggs, J. R.; Babin, J. E.; Barner, B. A. Chemical Industries, Vol. 89, Marcel Dekker, New York, 2003, 359; c) Cobley, C. J. ; Gardner, K. ; Klosin, J.; Praquin, C.; Hill, C.; Whiteker, G. T.; Zanotti-Gerosa, A.; Petersen, J. L.; Abboud, K. A. *J. Org. Chem.* **2004**, 69, 4031.
20. a) van der Veen, L. A.; Kamer, P. C. J.; van Leeuwen, P. W. N. M. *Angew. Chem. Int. Ed.* **1999**, 38, 336; b) van der Veen, L. A.; Kamer, P. C. J. ; van Leeuwen, P. W. N. M. *Organometallics* **1999**, 18, 4765; c) Bronger, R. P. J.; Kamer, P. C. J.; van Leeuwen, P. W. N. M. *Organometallics* **2003**, 22, 5358.
21. Klein, H.; Jackstell, R.; Wiese, K.-D.; Borgmann, C.; Beller, M. *Angew. Chem. Int. Ed.* **2001**, 40, 3408.
22. Yu, S.; Zhang, X.; Yan, Y.; Cai, C.; Dai, L.; Zhang, X. *Chem. Eur. J.* **2010**, 16, 4938.
23. a) Babin, J. E.; Whiteker, G. T. (Union Carbide Corporation), WO 9303839, 1993; b) Whiteker, G. T.; Briggs, J. R.; Babin, J. E.; Barner, B. A. Chemical Industries, Vol. 89, Marcel Dekker, New York, 2003, 359.
24. a) Jiang, Y.; Xue S.; Yu, K.; Li, Z.; Deng, J.; Mi, A.; Chan, A. S.C. *Tetrahedron: Asymmetry* **1998**, 9, 3185; b) Jiang, Y.; Xue S.; Yu, K.; Li, Z.; Deng, J.; Mi, A.; Chan, A. S.C. *J. Organometallic Chem.* **1999**, 586, 159.
25. Buisman, G. J. H.; Martin, M. E.; AngeliqueKlootwijk, E. J. V.; Kamer, P. C. J.; van Leeuwen, P. W. N. M. *Tetrahedron: Asymmetry*, **1995**, 6, 719.
26. a) Diéguez, M.; Pamies, O.; Ruiz, A.; CastilloÂn, S.; Claver, C. *Chem. Eur. J.* **2001**, 7, 3086; b) Diéguez, M.; Pamies, O.; Ruiz, A.; Claver, C. *New J. Chem.*, **2002**, 26, 827; c) Diéguez, M.; Pamies, O.; Claver, C. *Chem. Commun.*, **2005**, 1221.

27. Freixa, Z.; Bay_on, J. C. *J. Chem. Soc., Dalton Trans.* **2001**, 2067.
28. Zou, Y.; Yan, Y.; Zhang, X. *Tetrahedron Lett.*, **2007**, 48, 4781.
29. Cobley, C. J. ; Gardner, K. ; Klosin, J.; Praquin, C.; Hill, C.; Whiteker, G. T.; Zanolli-Gerosa, A.; Petersen, J. L.; Abboud, K. A. *J. Org. Chem.* **2004**, 69, 4031.
30. a) Wang, X.; Buchwald, S. L. *J. Am. Chem. Soc.* **2011**, 133, 19080; b) Sherrill, W. M.; Rubin, M. *J. Am. Chem. Soc.* **2008**, 130, 13804.
31. a) Sakai, N.; Mano, S.; Nozaki, K.; Takaya, H. *J. Am. Chem. Soc.* **1993**, 115, 7033; b) Nozaki, K.; Sakai, N.; Nanno, T.; Higashijima, T.; Mano, S.; Horiuchi, T.; Takaya, H. *J. Am. Chem. Soc.* **1997**, 119, 4413; c) Horiuchi, T.; Ohta, T.; Shirakawa, E.; Nozaki, K.; Takaya, H. *J. Org. Chem.* **1997**, 62, 4285; d) Horiuchi, T.; Shirakawa, E.; Nozaki, K.; Takaya, H. *Organometallics* **1997**, 16, 2981; e) Nozaki, K.; Matsuo, T.; Shibahara, F.; Hiyama, T. *Adv. Synth. Catal.* **2001**, 343, 61; f) Shibahara, F.; Nozaki, K.; Hiyama, T. *J. Am. Chem. Soc.* **2003**, 125, 8555.
32. Vaska, L. J. *J. Am. Chem. Soc.* **1996**, 7, 33.
33. Nozaki, K.; Matsuo, T.; Shibahara, F.; Hiyama, T. *Adv. Synth. Catal.* **2001**, 343, 61.
34. Higashizima, T.; Sakai, N.; Nozaki, K.; Takaya, H. *Tetrahedron Lett.* **1994**, 35, 2023.
35. a) Nozaki, K. ; Itoi, Y. ; Shibayara, F. ; Shirakawa, E. ; Ohta, T. ; Takaya, H. ; Hiyama, T. *J. Am. Chem. Soc.* **1998**, 120, 4051; b) Nozaki, K. ; Shibahara, F. ; Itoi, Y. ; Shirakawa, E. ; Ohta, T. ; Takaya, H. ; Hiyama, T. *Bull. Chem. Soc. Jpn.* **1999**, 72, 1911.

36. a) Nozaki, K.; Li, W.; Horiuchi, T.; Takaya, H. *J. Org. Chem.* **1996**, *61*, 7658;
 b) Takaya, H.; Sakai, N.; Nozaki, K., et al. U.S. Patent 5, 530, 150, 1996; *Chem. Abstr.* **1996**, *125*, 143006; c) Takaya, H.; Sakai, N.; Tamao, K.; et al. EP614870 **1994** *Chem. Abstr.* **1994**, *123*, 198277.
37. Noonan, G.; Fuentes, J. A.; Cobley, C. J.; Clarke, M. L. *Angew. Chem. Int. Ed.* **2012**, *51*, 2477.
38. Francio, G.; Faraone, F.; Leitner, W. *Angew. Chem. Int. Ed.*, **2000**, *39*, 1428.
39. Wassenaar, J.; de Bruin, B.; Reek, J. N. H. *Organometallics* **2010**, *29*, 2767.
40. a) Yan, Y.; Zhang, X. *J. Am. Chem. Soc.* **2006**, *128*, 7198; b) Zhang, X.; Cao, B.; Yan, Y.; Yu, S.; J, B.; Zhang, X. *Chem. Eur. J.* **2010**, *16*, 871.
41. a) Breeden, S.; Cole-Hamilton, D. J.; Foster, D. F.; Schwarz, G. J.; Wills, M. *Angew. Chem. Int. Ed.*, **2000**, *39*, 4106; b) Clarkson, G. J.; Ansell, J. R.; Cole-Hamilton, D. J.; Pogorzelec, P. J.; Whittell, J.; Wills, M. *Tetrahedron: Asymmetry* **2004**, *15*, 1787.
42. Burk, M. J. *J. Am. Chem. Soc.* **1991**, *113*, 8518.
43. a) Axtell, A. T.; Cobley, C. J.; Klosin, J.; Whiteker, G. T.; Zanotti-Gerosa, A.; Abboud, K. A. *Angew. Chem. Int. Ed.* **2005**, *44*, 2; b) Pilkington, C.; Zanotti-Gerosa, A. *Org. Lett.* **2003**, *5*, 1273.
44. a) Clark, T. P.; Landis, C. R.; Freed, S. L.; Klosin, J.; Abboud, K. *J. Am. Chem. Soc.* **2005**, *127*, 5040; b) Axtell, A. T.; Cobley, C. J.; Klosin, J.; Whiteker, G. T.; Zanotti-Gerosa, A.; Abboud, K. A. *Angew. Chem. Int. Ed.* **2005**, *44*, 5834; c) Thomas, P. J.; Axtell, A. T.; Klosin, J.; Peng, W.; Rand, C. L.; Clark, T. P.; Landis, C. R.; Abboud, K. A. *Org. Lett.* **2007**, *9*, 2665; d) Adint, T. T.; Wong, G. W.; Landis, C. R. *J. Org. Chem.* **2013**, *78*, 4231; e) Adint, T. T.; Landis, C. R. *J. Am. Chem. Soc.* **2014**, *136*, 7943; f) McDonald,

- R. I.; Wong, G. W.; Neupane, R. P.; Stahl, S. S.; Landis, C. R. *J. Am. Chem. Soc.* **2010**, *132*, 14027.
45. a) Axtell, A. T.; Klosin, J.; Abboud, K. A. *Organometallics* **2006**, *25*, 5003; b) Huang, J.; Bunel, E.; Allgeier, A.; Tedrow, J.; Thomas Storz, T.; Preston, J.; Correll, T.; Manley, D.; Soukup, T.; Jensen, R.; Syed, R.; Moniz, G.; Larsen, R.; Martinelli, M.; Paul J. Reider, P.J. *Tetrahedron Lett.* **2005**, *46*, 7831.
46. Wang, X.; Buchwald, S. L. *J. Am. Chem. Soc.* **2011**, *133*, 19080.
47. a) Cobley, C. J.; Klosin, J.; Qin, C.; Whiteker, G. T. *Org. Lett.* **2004**, *6*, 3277; b) Cobley, C. J.; Gardner, K.; Klosin, J.; Praquin, C.; Hill, C.; Whiteker, G. T.; Zanotti-Gerosa, A. *J. Org. Chem.* **2004**, *69*, 4031.
48. Hua, Z.; Vassar, V. C.; Choi, H.; Ojima, I. *Proc. Natl. Acad. Sci.*, **2004**, *101*, 5411.
49. Arena, C. G.; Nicolò, F.; Drommi, D.; Bruno, G.; Faraone, F. *J. Chem. Soc. Chem. Commun.* **1994**, 2251.
50. Worthy, A. D.; Joe, C. L.; Lightburn, T. E.; Tan, K. L. *J. Am. Chem. Soc.* **2010**, *132*, 14757.
51. Lightburn, T. E.; Dombrowski, M. T.; Tan, K. L. *J. Am. Chem. Soc.* **2008**, *130*, 9210.

Chapter 2

Synthesis and Application of Easily Accessible and Tunable Bisphospholane Ligands for Asymmetric Hydroformylation

2.1 Introduction

Asymmetric hydroformylation (AHF) of alkenes is essentially attractive for its high atom economy,¹ thus rendering it to be an outstanding methodology in the application of homogeneous catalysis on an industrial scale.² AHF is underdeveloped due to the difficulty in simultaneously controlling regio- and enantioselectivities at high reaction temperature.³ This useful and efficient methodology can afford a series of synthetically important chiral aldehydes, which are directly inaccessible by other synthetic methods.⁴

A significant breakthrough was the introduction of Binaphos by Tayaka and coworkers in 1997.⁵ Later on, a variety of bisphosphite and phosphine-phosphite ligands developed by the groups of Whiteker,⁶ Will,⁷ van Leeuwen,⁸ Claver,⁹ Reek,¹⁰ Tan,¹¹ Buchwald,¹² Clark,¹³ Ding,¹⁴ Zhang,¹⁵ and others¹⁶ brought the research of AHF to a new level. Meanwhile, Klosin and coworkers showed that bisphosphine ligand 1,2-bis(2,5-diphenylphospholano)ethane (Ph-BPE), originally for asymmetric hydrogenation reaction, can also give good results for the AHF, even though the conversion is low-to-moderate.¹⁷

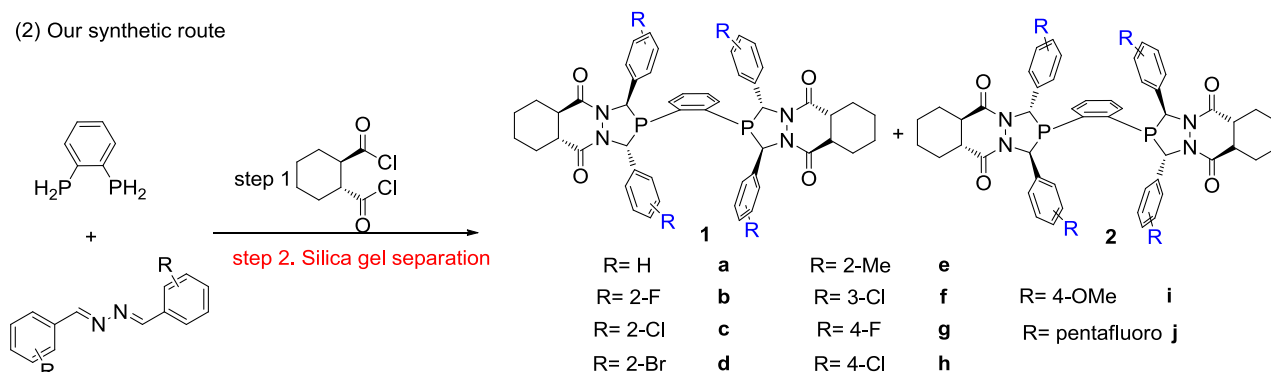
Although significant progress has been made in the past decade, the following challenges still restrict the application of AHF: 1) limited substrate scope; 2) high catalyst loading; 3) complex and multiple steps to synthesize the chiral ligands.

Recently, Landis and coworkers successfully developed an excellent bis(diazaphospholane) (BDP) ligand through a highly efficient method.¹⁸ This ligand showed highly selective for a broad range of substrates due to conformational rigidity and electron-deficient properties. But chiral separation by HPLC is the main drawback to easily access to BDP ligands. Additionally, only electron-withdrawing amide groups can be introduced to the *ortho*-positions of phenyl moieties (Scheme 2-1, [Eq. (1)]) is another disadvantage to tune this type of ligand. Giving few chiral phosphine ligands easily tunable, a modified preparation is highly necessary and will have a major impact in this field.

(1) Synthetic route of Landis's bisdiazaphospholane ligand



(2) Our synthetic route



Scheme 2-1. Different approach to the bis-diazaphospholane ligands

In asymmetric catalysis, a subtle change in the ligand can bring significantly affect the yields and the regio- and enantioselectivities. However, to the best of our

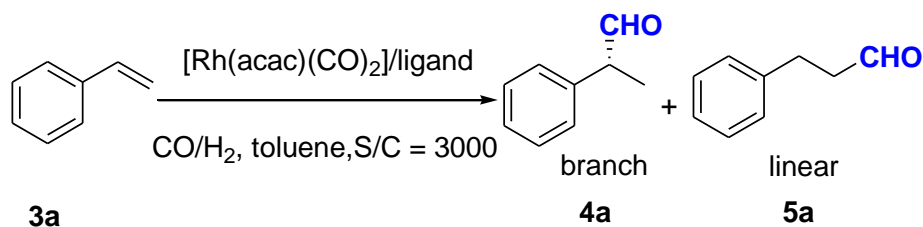
knowledge, examples on the systematically varying the steric and electronic properties of the ligands for AHF are very limited. Thus, in this chapter, we aim at synthesizing a series of tunable and highly efficient AHF catalysts without involving the HPLC separation; easily tunable of steric and electronic properties to match different types of substrates and then further practical applications in industry. The modified efficient synthetic route is in Scheme 2-1, [Eq. (2)]. With the participation of a commercially available and cheap chiral scaffold, a series of electronically and sterically varied ligands can be synthesized in one pot and separated through silica gel column easily. Moreover, the easily synthesized ligands can give good-to-excellent conversions, regio- and enantioselectivities for a broad range of mono- and disubstituted alkenes. For some substrate results, such as cyclic alkenes, are among the best in the current literature. In addition, mechanism studies on the precatalyst and catalytic resting-state species were also carried out.

2.2 Results and Discussion

Initial experiments were carried out to synthesize ligand **1**. In most cases, both of the two diastereomers can be synthesized in one pot and separated by flash column chromatography; however, when the R group was replaced by 4-F and 4-Cl, only one isomer of **2g** and **2h** were obtained respectively, and the exact reason is not clear yet. The absolute configuration of ligand **1c** was determined by single-crystal X-ray diffraction analysis.¹⁹ The stereochemistry of all other products (**1a-f**, **1i**) is assigned by analogy.²⁰ These easily synthesized ligands were then examined for the AHF of styrene (Table 2-1). First, the combination of ligand **1a**/[Rh(CO)₂(acac)] (acac=acetylacetonate) was employed as the catalyst, which can give excellent

conversion with a low catalyst loading (substrate-to-catalyst ratios (S/C)=3000, Table 2-1, entry 1).

Table 2-1. Ligand screening for AHF of styrene



Entry ^a	Ligand	Conversion(%) ^b	b/l ^c	ee(%) ^d
1	1a	99	16	70
2	1b	99	20	81
3	1c	99	24	85
4 ^e	1c	99	14	84
5	1d	99	17	75
6	1e	99	19	82
7	1f	99	13	61
8	1i	99	16	73
9	2g	99	9	30(S)
10	2h	99	9	52(S)
11	2j	99	4	20(S)
12	2c	99	19	24(S)
12 ^e	1c	98	11	81

^a All reactions were performed on a 1.0 mmol scale at 60 °C in toluene (0.5 mL) with 20 bar syngas ($\text{CO}:\text{H}_2 = 3:1$) with L:Rh = 3:1, S/C = 3000, and 8 h reaction time.

^b Determined by GC (β -DEX 225) with dodecane as internal standard.

^c Determined by ¹H NMR analysis.

^d Determined by Chiral GC (β-DEX 225).

^e The ratio of L/Rh was change to 2:1

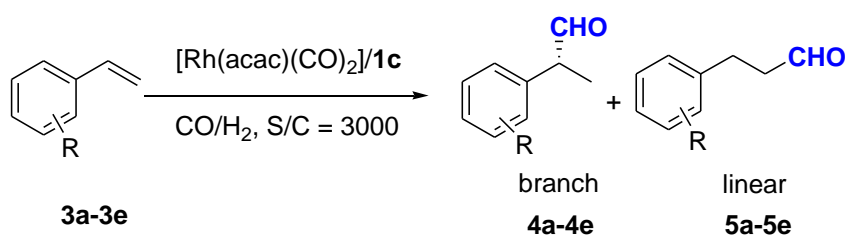
^f 80 °C, 150 psi of syngas (CO:H₂ = 1:1), S/C = 5000.

Encouraged by the preliminary results, a variety of electronically and sterically different ligands were examined. When the fluoride, chloride, bromide, and methyl groups were attached to the *ortho* positions of phenyl moieties, better regio- and enantioselectivities were obtained (Table 2-1, entries 2,3,5 vs. 1). It is known that the flexible ligand is not efficient for the asymmetric induction under high temperature; the introduction of a suitable group to the *ortho* position of phenyl moiety can possibly make the ligand more rigid, which has a benefit effect for the asymmetric induction. However, a substituent that is too bulky (e.g. 2-Br) has a negative effect on the enantioselectivity (Table 2-1, entries 2, 3 vs. 5). In terms of electronic properties of the substituents, the moderate electron-withdrawing group can increase the regio- and enantioselectivities (Table 2-1, entries 3 vs. 6). To investigate the steric effect of the ligand, the *ortho* chloride was replaced by *meta* chloride, lower regio- and enantioselectivities were obtained (Table 2-1, entry 7) Subsequently, the cooperative effect between the stereogenic centers of the cyclohexane backbone and the stereogenic phenyl moieties was demonstrated. Comparison of aldehyde configurations obtained with the diastereomers (Table 2-1, entries 3 vs. 12) indicated that the chirality of the product was predominantly controlled by the configuration of the aryl moieties, rather than the stereochemistry of the cyclohexane backbone. When ligand **1c** was evaluated under the standard AHF conditions reported by Landis (80 °C,

150 psi syngas, S/C= 5000),^{18a} 11:1 branched/linear (b/l) ratio and 81% ee value were obtained (Table 2-1, entry 12, Landis's result: 6.6:1 b/l ratio, 82% ee).

With optimized conditions in hands, the AHF of styrene derivatives also gave the desired products with excellent conversions, regio- and enantioselectivities (Table 2-2). In general, the electron-rich styrene derivatives have a negative effect on the conversion and stereoselectivities (Table 2-2, entries 2 and 3 vs. 1). The *ortho* substituents on the phenyl moiety have a positive effect on the asymmetric induction and regioselectivity (Table 2-2, entry 5).

Table 2-2. AHF of styrene derivatives



Entry ^a	R	Conversion(%) ^b	b/l ^c	ee(%) ^d
1	H	99	24	85
2	4-Me	98	20	80
3	4-OMe	93	20	77
4	4-F	99	19	83
5	2-F	99	58	88

^a All reactions were performed on a 1.0 mmol scale at 60 °C in toluene (0.5 mL) with 20 bar syngas (CO:H₂ = 3:1) with **1c**:Rh = 3:1, S/C = 3000, and 8 h reaction time.

^b Determined by GC (β-DEX 225) with dodecane as internal standard.

^c Determined by ¹H NMR analysis.

^d Determined by Chiral GC (β-DEX 225).

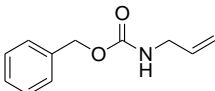
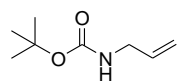
Entry ^a	R	Conversion(%) ^b	b/l ^c	ee(%) ^d
1	CH ₃	99	53	91
2	t-Bu	99	24	91
3	n-C ₇ H ₁₅	87	45	93
4	n-C ₉ H ₁₉	85	34	93
5	Ph	80	240	91

^d Determined by Chiral GC (β-DEX 225).

To further explore the application of the ligand, a series of *N*-allylsulfonamides and *N*-allylamides were tested for AHF (Table 2-4). For benzoyl (Bz)- and carbobenzyloxy (Cbz)-protected allylic amines **9d** and **9e**, excellent conversions and enantioselectivities were obtained (Table 2-4, entries 4 and 5). The protecting group in the resulting products can be easily deprotected, affording the synthetically useful chiral 1,3-aminoaldehyde in short synthetic steps. More importantly, *t*-butoxycarbonyl (Boc)-protected allylic amine **9f** can be hydroformylated under the standard conditions, providing the *N*-Boc-protected β^2 -amino aldehyde **10f** with good conversion and stereoselectivity (Table 2-4, entry 6).

Table 2-4. AHF of *N*-allylsulfonamides and *N*-allylamides

$ \begin{array}{c} \text{R}-\text{N}(\text{H})-\text{CH}_2\text{CH}=\text{CH}_2 \xrightarrow[\text{CO/H}_2, \text{ S/C} = 1000]{[\text{Rh}(\text{acac})(\text{CO})_2]/\text{1c}} \text{R}-\text{N}(\text{H})-\text{CH}_2-\text{CH}(\text{CHO})-\text{CH}_3 + \text{R}-\text{N}(\text{H})-(\text{CH}_2)_3-\text{CHO} \\ \text{9a-9f} \qquad \qquad \qquad \text{branch} \qquad \qquad \qquad \text{linear} \\ \qquad \qquad \qquad \text{10a-10f} \qquad \qquad \qquad \text{11a-11f} \end{array} $				
Entry ^a	Substrate	Conversion (%) ^b	b/l ^b	ee(%) ^d
1		92	9	88
2		92	6	88
3		99	6.5	91
4		99	18	92

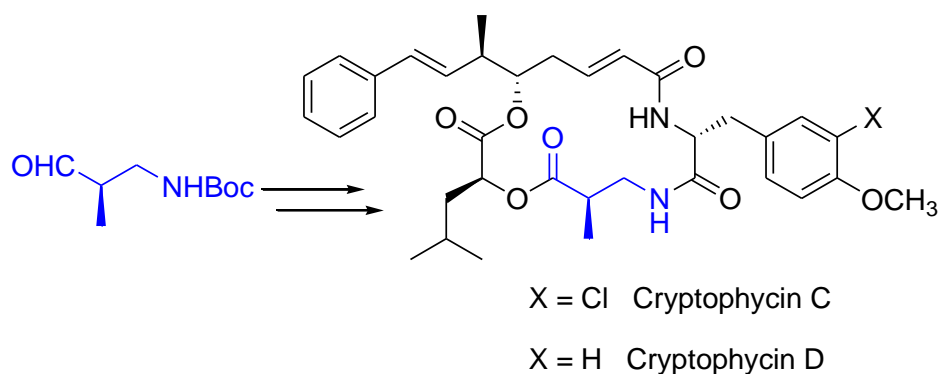
5		93	9.5	92
6		95	10	85

^a All reactions were performed on a 1.0 mmol scale at 40°C in toluene (0.5 mL) with 20 bar syngas (CO:H₂ = 3:1) with **1c**:Rh = 3:1, S/C = 1000, and 20 h reaction time.

^b Determined by ¹H NMR analysis.

^c Determined by HPLC or Chiral GC (β-DEX 225).

N-Boc-protected β²-amino aldehyde is a valuable structural motif, which can be transformed into many biologically important molecules. A prominent example is the promising cancer drug cryptophycin C and D, which can be obtained by utilizing this unit with the improved overall synthetic efficiency (Scheme 2-2).²¹

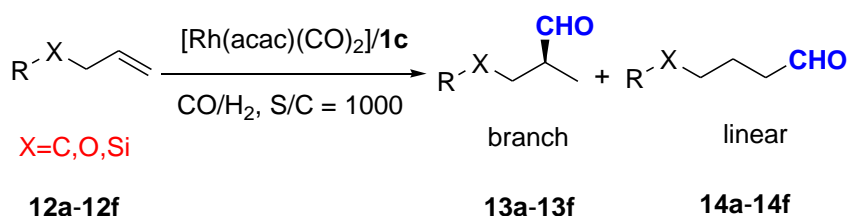


Scheme 2-2. The application of β²-amino aldehyde to the synthesis

Encouraged by the success of AHF of *N*-functionalized allyl substrates, *O*-, *Si*-functionalized and unfunctionalized allylic substrates were also tested. To our delight, various allylic substrates could undergo the AHF reaction to give the chiral aldehyde

with good conversion, moderate branch/linear ratio, and excellent *ee* values (up to 94% *ee*, Table 2-5). For *O*-functionalized substrates, moderate regioselectivity and good-to-excellent enantioselectivities were obtained (Table 2-5, entries 1-4). For the *Si*-functionalized and unfunctionalized allyl substrates allyltrimethylsilane **12e** and allylbenzene **12f**, good-to-excellent conversion and enantioselectivities were obtained (Table 2-5, entries 5 and 6), but showed preference for linear products.

Table 2-5. AHF of other allylic substrates



Entry ^a	Substrate	Conversion(%) ^b	b/l ^b	<i>ee</i> (%) ^c
1	TMSO-CH ₂ CH=CH ₂	99	2.4	94
2	TBSO-CH ₂ CH=CH ₂	99	2	83
3	PhO-CH ₂ CH=CH ₂	99	3	90
4	AcO-CH ₂ CH=CH ₂	67	3	92
5	TMS-CH ₂ CH=CH ₂	83	0.5	91
6 ^d	Ph-CH ₂ CH=CH ₂	99	1.1	90

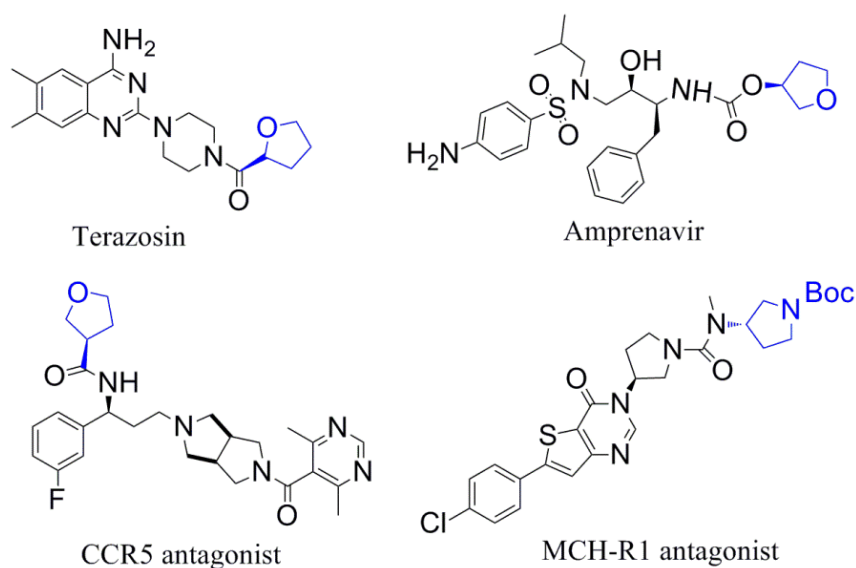
^a All reactions were carried out on a 1.0 mmol scale at 40 °C in toluene (0.5 mL) with 20 bar syngas (CO/H₂ = 3:1) with **1c**/Rh = 3:1, S/C = 1000, and 20 h reaction time.

^b Determined by ¹H NMR analysis.

^c Determined by HPLC or Chiral GC (β-DEX 225).

^d The reaction temperature is 80 °C.

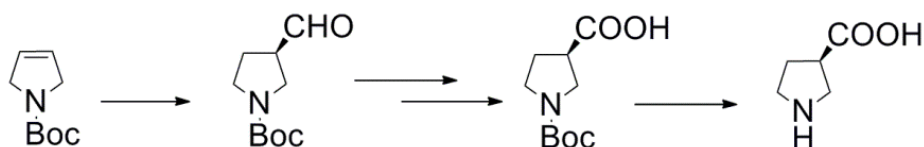
After investigating the reactivity of terminal alkenes, the AHF of more challenging of 1,2-disubstituted olefins, especially dihydrofuran (DHF) and pyrroline, were then examined. Their chiral products 2- and 3-carbaldehydes can be extensively applied in the synthesis of biologically active natural products and pharmaceuticals (Scheme 2-3).²²



Scheme 2-3. Structures of biologically active products

For instance, chiral 3-carbaldehyde is a potential synthetic intermediate for preparing Terazosin,^{22b} used as an enlarged prostate (BPH), and Amprenavir,^{22c} a high potent drug for the treatment of HIV protease inhibitor. Chiral 2-carbaldehyde can be used to synthesize CCR5 antagonist^{22d} that is currently being investigated in clinical trials for the treatment of HIV-1 infection. 3-Pyrrolidinecarboxylic acid is a key structural element in the synthesis of peptides and proteins.^{22e-g} Limited methodologies can access to this building block in short steps. The AHF of *N*-Boc pyrroline can directly access to chiral 3-carbaldehyde, subsequently oxidized into enantioenriched β -proline in only two steps (Scheme 2-4).^{22a} Furthermore, MCH-R1

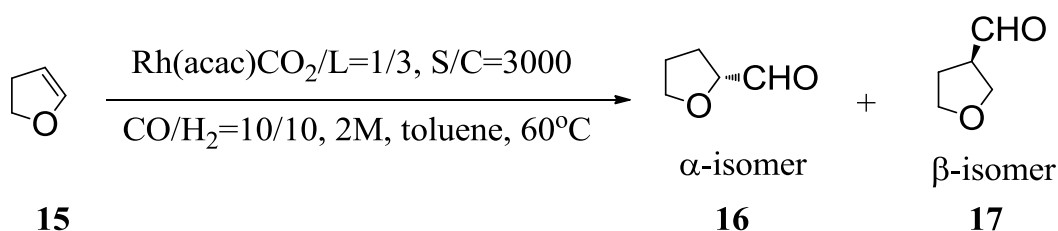
antagonist,^{22e} an anti-obesity agent, is also derived from the AHF of *N*-Boc pyrroline (Scheme 2-3).



Scheme 2-4. Conversion of AHF of *N*-Boc pyrroline into β -proline

Due to structure differences between terminal and internal olefins, we started with 2,3-DHF (**15**) as a model substrate to evaluate the effects of ligands on activity and selectivity. The reaction was performed in the presence of 0.1 mol% ligand at 60 °C under 20 bar syngas pressure (CO/H₂ = 10/10). In principle, 2-carbaldehyde (**16**) is the desired product and 3-carbaldehyde (**17**) is presented as a byproduct by isomerization.^{22a,23} In Table 2-6, the library of ligands accomplished better conversions and enantioselection, especially ligand **1c** with up to 92% enantioselectivity of α -carbaldehyde **16** (Table 2-6, entry 3).

Table 2-6. AHF of **15** with different ligands



Entry ^a	Ligand	Conv. (%) ^b	α/β	<i>ee</i> (%) ^c (α)	<i>ee</i> (%) ^c (β)
1	1a	91	0.93	71 (R)	87 (R)
2	1b	80	0.83	84 (R)	88 (R)
3	1c	99	1.00	92 (R)	71 (R)
4	1e	64	1.56	86 (R)	94 (R)
5	1f	73	0.73	72 (R)	86 (R)
6	1g	60	0.86	60 (R)	71 (R)
7	1h	49	0.64	60 (R)	68 (R)
8	1i	38	1.00	65 (R)	79 (R)
9	1j	7	0.09	38 (S)	0

^a All reaction were performed on a 1.0 mmol scale at 60 °C in toluene (0.5 mL) total 2M, with 20 bar syngas (CO:H₂ = 10/10), Rh/L= 1/3, S/C= 3000 and 20 h reaction time.

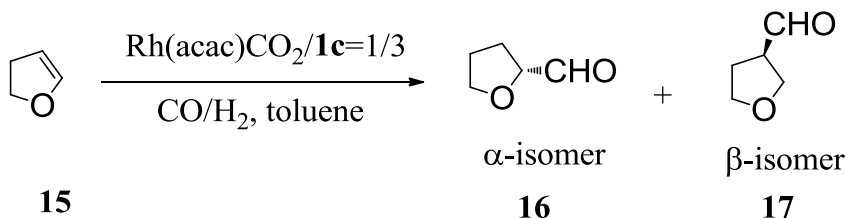
^b Determined by ¹H NMR analysis

^c Determined by Chiral GC (β -DEX 225)

Encouraged by preliminary results, we next varied the CO/H₂ partial syngas pressure with ligand **1c** (Table 2-7). Increasing CO partial pressure from 10 to 15 under the total pressure 20 bar, the *ee* value of α -isomer **17** increased to 93 % with slightly dropped of conversion (Table 2-7, entry 2). To the best of our knowledge, this

is the highest enantioselectivity of 2-carbaldehyde (**17**, 93%) ever reported in the AHF of 2,3-DHF. A lower CO to H₂ ratio therefore diminished enantioselectivity (86% *ee*) and regioselectivity (0.30) in aldehyde **17** (Table 2-7, entry 3). It is generally accepted that the competition of β -hydride elimination and CO insertion led to isomerization. Hence, higher CO partial pressure can suppress isomerization. Under optimal CO/H₂ ratio of 15/5, decreasing temperature (40 °C) or increasing molarity neither has a positive effect on both regio- and enantioselectivity (Table 2-7, entries 5-6). The comparable result was yielded using S/C=1000 (substrate to catalyst) (Table 2-7, entries 2 vs 7).

Table 2-7. Optimization of selected ligands for the AHF of 2,3-dihydrofuran **15**



Entry ^a	S/C	Temp (°C)	[M]	CO/H ₂ (bar)	Conv. (%) ^b	α/β	<i>ee</i> (%) ^c (α -isomer)	<i>ee</i> (%) ^c (β -isomer)
1	3000	60	2	10/10	99	1	92 (R)	71 (R)
2	3000	60	2	15/5	92	0.70	93 (R)	53 (R)
3	3000	60	2	5/15	99	0.30	86 (R)	77 (R)
4	3000	60	2	5/5	71	1.09	90 (R)	57 (R)

5	3000	60	3	15/5	92	0.87	88 (R)	78 (R)
6	3000	40	2	15/5	46	0.53	76 (R)	33 (R)
7	1000	60	2	15/5	>99	0.75	91 (R)	56 (R)

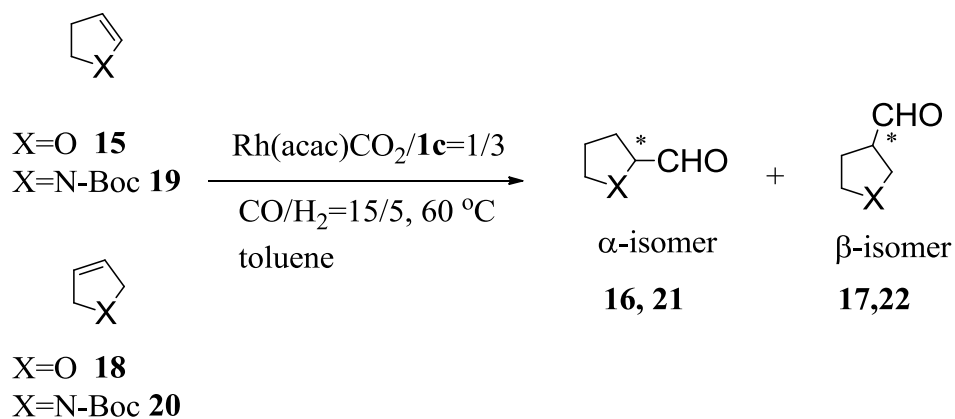
^a All reaction were performed on a 1.0 mmol scale at 60 °C or 40 °C in toluene with 20 bar syngas, Rh/L= 1/3 and 20 h reaction time.

^b Determined by ¹H NMR analysis

^c Determined by Chiral GC (β-DEX 225)

Next, we further expand the scope of cyclic olefins (Table 2-8). The AHF of 2,5-DHF (**18**) is challenging to get high β/α ratio and enantioselectivity of β-isomer because of competitive olefin isomerization to 2,3-DHF, then yielded 2-carbaldehyde (**16**) as a minor product.^{23e} The reaction afforded 166 of β/α ratio and 92% ee of β-isomer (Table 2-8, entry 2). The AHF of *N*-(*t*-butoxycarbonyl)-2-pyrroline **19** proceeded smoothly with 96% ee of the major product α-isomer (Table 2-8, entry 3). The AHF of *N*-(*t*-butoxycarbonyl)-3-pyrroline **20** provided exclusively β product with 92% enantioselectivity (Table 2-8, entry 4).

The resulting chiral 3-(S)-carbaldehyde **17** is a useful synthetic intermediate for 3-(S)-hydroxytetrahydrofuran by Baeyer-Villiger oxidation.²⁴ Following several steps, HIV protease inhibitor Amprenavir can be synthesized easily according to the literature.²⁵

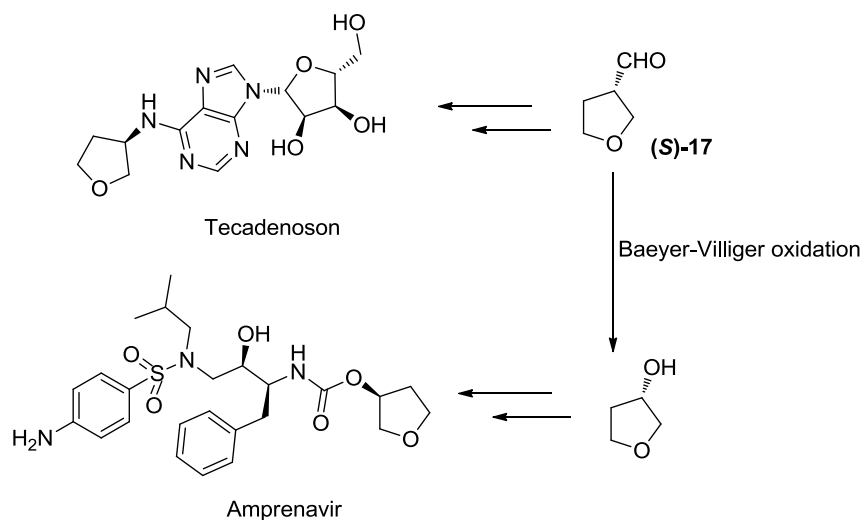
Table 2-8. Expanding the scope of cyclic olefins

Entry ^a	Compound	Conv _h (%) ^b	β/α	<i>ee</i> (%) ^c (α -isomer)	<i>ee</i> (%) ^c (β -isomer)
1	15	92	0.70	93 (R)	53 (R)
2	18	>99	166	-	92 (S)
3	19	>99	6.14	96 (R)	86 (R)
4	20	>99	-	-	92 (S)

^a All reaction were performed on a 1.0 mmol scale with ligand (0.1mol%), 3000:1 total substrate/Rh (S/C), in toluene for 20 h.

^b Determined by ¹H NMR analysis

^c Determined by Chiral GC (β-DEX 225)



Scheme 2-5. The application of 3-carbaldehyde to the total synthesis

Finally, other representative mono- and disubstituted olefins were also test for hydroformylation with **1c**/[Rh(acac)(CO)₂] catalytic system (Table 2-9). The reaction of vinyl amide produces the valuable 1,2-aminoaldehyde with 11/1 regioselectivity and 88% enantioselectivity in 92% conversion (Table 2-9, entry 1). Other disubstitued olefins gave moderate regioselectivities and good enantioselectivities (Table 2-9, entries 2-3).

A series of experiments were performed to investigate the mechanism of the catalytic system. First, ligand **1c** was mixed with [Rh(CO)₂(acac)] at room temperature, displacement of the two carbon monoxide ligands by the bidentate ligand afforded the square planar complex **A** [Rh(acac)(P[^]P)] , which was demonstrated by single-crystal X-ray diffraction analysis¹⁹ (bite angle: 84.9, CCDC 955453, Figure 2-1). The result is similar to Rh[Ph-BPE](acac) that bite angle is 85.5, indicating the excellent selectivity for hydroformylation of styrene and vinyl acetate. The crystallographic structure of **1c** is shown in Figure 2-2.

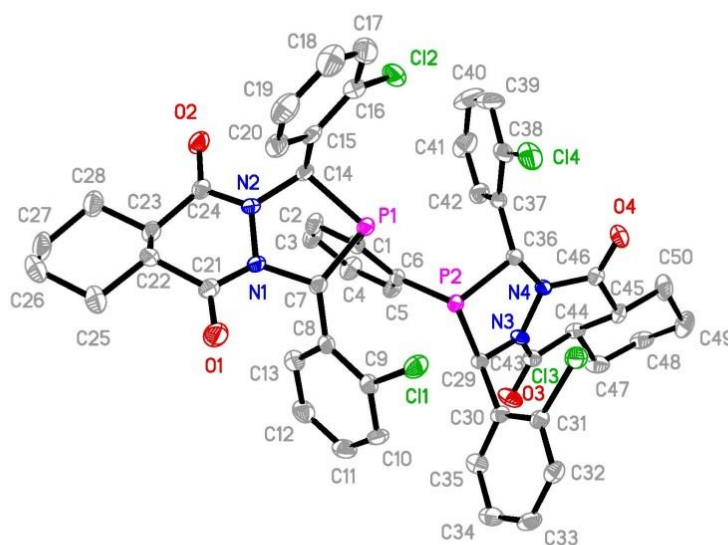
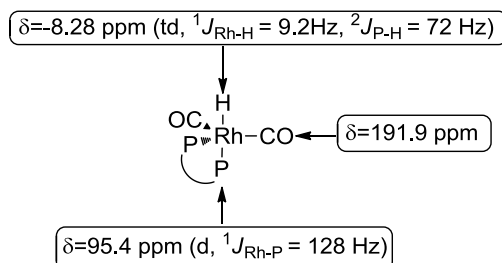
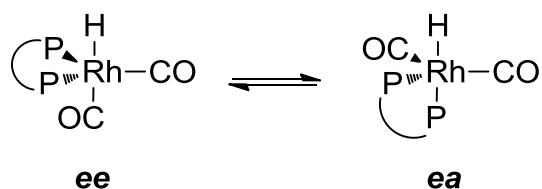


Figure 2-2. X-ray crystal structure of **1c**

Next, the resting-state species (complex **B** [Rh(H)(CO)₂(P[^]P)]) was prepared in situ by mixing one equivalent of ligand **1c** with the metal precursor [Rh(CO)₂(acac)] in toluene-d₈, and reacted under the same hydroformylation conditions (20 bar syngas (CO/H₂=3:1) at 60 °C for 10 h, without the existence of the substrate). The formation of the rhodium complex **B** was characterized by using NMR spectroscopy²⁶ (Scheme 2-6).



Scheme 2-6. NMR data of complex **B** [RhH(CO)₂(P[^]P)] obtained at 298K



Scheme 2-7. Equilibrium between **ee** and **ea** complexes

In the ^1H NMR spectroscopic experiment, a triplet of doublets peak of hydride signal was detected at high field ($\delta = -8.3$ ppm). The coupling constant between the phosphorus atom (P^1) and the hydride of 72 Hz was observed. The magnitude of this coupling constant (72 Hz) is bigger than the reported for the equatorial phosphorus atom (< 10 Hz), but smaller than the reported for the apical hydride with apical phosphorus atom (160-200 Hz).²⁷ From ^{13}C NMR, only single peak was detected single peak at 191.9 ppm. Double peaks were seen from ^{31}P NMR. From all of the data, we assumed one of the phosphane atoms (P^2) in ligand **1c** is in a *trans* position to the hydride in complex **B**. The complex is indeed a trigonal bipyramid but somewhat distorted. The steric bulky ligand makes P^1 in the equatorial plane bend toward the small hydride. This explains why the coupling constant is between a pure **ea** and **ee** fashion.

However, the X-ray crystal structure of complex **A** $[\text{Rh}(\mathbf{1c})\text{acac}]$ (Figure 2-1) clearly demonstrated the square planar structure, indicating that despite the steric bulk of this bisphospholane ligand *cis*-coordination in the Rh(I) complex was feasible.²⁷ Furthermore, the DFT calculations showed the energy difference between **ea** complex and **ee** complex was extremely small that was only 1.76 kJ/mol. Thus, there is a great possibility that the two fashions are in fast exchange during the high reaction temperature and can both contribute to the activity and selectivity (Scheme 2-7). More experiments are underway to get this mechanism clear.

2.3 Conclusion

An efficient method for the easy and tunable synthesis of a series of AHF ligands from low-cost, commercially available starting materials was developed. A systematic screening of the library of ligands on AHF showed that an appropriate electron withdrawing group attached to the *ortho* position of phenyl moieties in the ligand is essential to achieve the high regio- and enantioselectivities; however, too bulky substituent led to the decrease in enantioselectivities. With a low catalyst loading (S/C=1000:1 to 3000:1), a wide range of terminal and internal olefins, especially the challenging dihydrofuran and *N*-Boc-pyrroline substrates, underwent the hydroformylation reaction to give the synthetically useful chiral aldehydes with good to excellent regio- and enantioselectivities.

2.4 Experimental Section

2.4.1 General Remarks

All reagents were received from commercial source and used without further purification. All of the reactions were carried out in the nitrogen-filled glovebox. Purifications of the ligands were carried out by flash chromatography using silica gel.

^1H NMR, ^{13}C NMR and ^{31}P NMR spectra were recorded on a Bruker Avance (400 MHz) spectrometer with CDCl_3 as the solvent and tetramethylsilane (TMS) as the internal standard. Chemical shifts are reported in parts per million (ppm, δ scale) downfield from TMS at 0.00 ppm and referenced to the CDCl_3 at 7.26 ppm (for ^1H NMR) or 77.16 ppm (for deuteriochloroform). GC analysis was carried out on Agilent gas chromatography using chiral capillary columns. HPLC analysis was carried out on Agilent 1200 series. New compounds were further characterized by high resolution mass spectra (HRMS) on a Waters Q-ToF Ultima mass spectrometer with an

electrospray ionization source (University of Illinois, SCS, Mass Spectrometry Lab). Optical rotations $[\alpha]^{25}_D$ were measured on a JASCO P-2000 polarimeter. The single crystal X-ray analysis was carried out on Bruker-AXS Smart APEX CCD diffractometer.

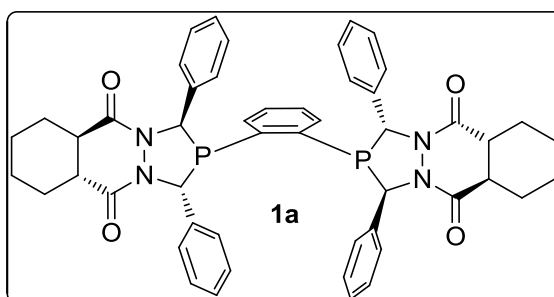
2.4.2 General procedures for ligand synthesis and AHF reactions

Generally procedure for ligand synthesis: To a Schlenk flask (100 mL) equipped with a magnetic bar was added 1,2-dibenzylidenehydrazine (2g, 10mmol) and dry THF (60 mL), then 1,2-cyclohexanedicarboxylic acid chloride (4g, 20mmol) in dry THF (20 mL) was added. The mixture was stirred at rt for 20 min, then was cooled to 0 °C. Subsequently, 1,2-diphosphinobenzene (1.1 mL, 5 mmol, 10% in hexane) was added to the mixture dropwise. The resulting mixture was allowed to warm to rt and stirred for 6h under nitrogen atmosphere. After the reaction was finished, NaHCO₃ (2M, 20 mL) was added at 0 °C. The mixture was extracted with ethyl acetate (3 × 20 mL). The combined organic phase was dried with Na₂SO₄ and evaporated in vacuum. Purification of the residue by flash column chromatography (EtOAc : Hex = 1:3-1:1) afforded the desired ligand 1a as a white solid (530 mg, 13% yield).

Generally procedure for AHF reactions: In a glovebox filled with nitrogen, to a 5 mL vial equipped with a magnetic bar was added ligand (0.003 mmol) and Rh(acac)(CO)₂ (0.001 mmol in toluene (0.2 mL)). After stirring for 10 min, substrate (1.0 mmol) and additional toluene was charged to bring the total volume of the reaction mixture to 0.5 mL. The vial was transferred into an autoclave and taken out of the glovebox. Carbon monoxide (15 bar) and hydrogen (5 bar) were charged in sequence. The reaction mixture was stirred at 60 °C (oil bath) for 20 h. The reaction was cooled and the pressure was carefully released in a well ventilated hood. The

conversion and branch/linear ratio were determined by ^1H NMR spectroscopy from the crude reaction mixture. The enantiomeric excesses of the products were determined by chiral GC analysis with a Supelco's Beta Dex 225 column from the crude reaction mixture, or by reducing them into alcohol with NaBH_4 and analyzing with HPLC.

2.4.3 Characterization of the ligands



^1H NMR (400M, CDCl_3) 1.33-1.42 (m, 4H), 1.78-1.86 (m, 6H), 2.09-2.33 (m, 10H), 6.15 (s, 2H), 5.77-5.82 (m, 4H), 6.60 (d, $J = 8$ Hz, 3H), 6.85 (t, $J = 7.6$ Hz, 4H), 6.97-7.08 (m, 4H), 7.14-7.16 (m, 4H), 7.28-7.41 (m, 9H).

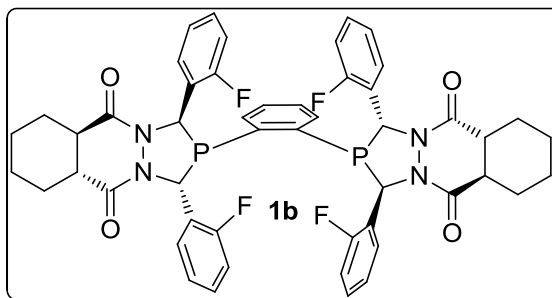
^{13}C NMR (100M, CDCl_3) 24.5, 24.6, 26.1, 26.9, 41.8, 42.6, 57.3 (m), 62.0 (t, $J = 19$ Hz), 125.9, 126.3 (t, $J = 4.2$ Hz), 127.2, 127.9, 128.3, 129.3, 130.3, 130.8, 136.3, 137.8 (t, $J = 9$ Hz), 139.0, 167.3, 169.7.

^{31}P NMR (162M, CDCl_3) -1.41.

HRMS (ESI): calcd for $\text{C}_{50}\text{H}_{48}\text{N}_4\text{O}_4\text{P}_2$ ($[\text{M}+\text{H}]$): 831.3151, found 831.3179.

$[\alpha]_{\text{D}}^{25} = 10.9^\circ$ ($c = 1.41$, acetone).

White solid (13 % yield); M.P. 185°C .



^1H NMR (400M, CDCl_3) 1.30-1.40 (m, 4H), 1.65 (m, 1H), 1.80-1.84 (m, 5H), 2.04-2.15 (m, 2H), 2.20-2.33 (m, 8H), 5.96 (s, 2H), 6.17 (t, $J = 10$ Hz, 2H), 6.36-6.43 (m, 4H), 6.56-6.61 (m, 2H), 6.89-6.95 (m, 2H), 7.08-7.24 (m, 10H), 7.33-7.38 (m, 2H).

^{13}C NMR (100M, CDCl_3) 24.4, 24.5, 26.0, 26.6, 41.5, 42.0, 52.6 (m), 56.7 (m), 115.2, 115.4, 116.1, 116.3, 123.3, 123.5, 123.7, 124.8 (d, $J = 3.3$ Hz), 125.6 (m), 126.9, 128.1, 128.7 (d, $J = 8.2$ Hz), 130.1, 130.2, 130.6, 138.9, 157.9 (d, $J = 87$ Hz), 160.4 (d, $J = 87$ Hz), 167.3, 169.1.

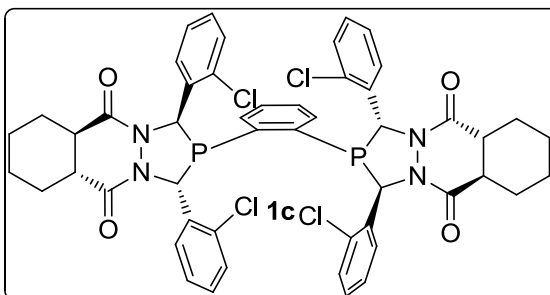
^{31}P NMR (162M, CDCl_3) 1.66

^{19}F NMR (376M, CDCl_3) – 114.8, -114.6 (t, $J = 364$ Hz).

HRMS (ESI): calcd for $\text{C}_{50}\text{H}_{44}\text{F}_4\text{N}_4\text{O}_4\text{P}_2$ ($[\text{M}+\text{H}]$): 903.2774, found 903.2781.

$[\alpha]_{\text{D}}^{25} = 28.5^\circ$ ($c = 0.33$, acetone).

White solid (11 % yield); M.P. 220



^1H NMR (400M, CDCl_3) 1.30-1.40 (m, 4H), 1.81-1.85 (m, 6H), 2.06-2.40 (m, 10H), 6.10 (s, 2H), 6.40-6.45 (m, 4H), 6.73-6.77 (m, 4H), 6.84-6.88 (m, 2H), 7.08-7.11 (m, 4H), 7.16-7.18 (m, 2H), 7.28-7.33 (m, 4H), 7.43-7.48 (m, 2H).

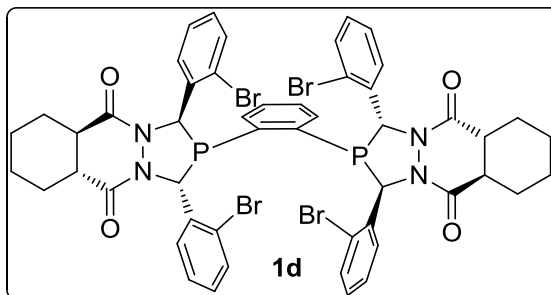
^{13}C NMR (100M, CDCl_3) 24.3, 26.0, 26.6, 29.7, 41.6, 42.1, 57.7 (m), 58.6 (t, $J = 17$ Hz), 125.8, 126.0, 127.7, 128.2, 128.8, 129.4, 129.6, 130.1, 130.4, 131.7, 132.7 (m), 133.7, 136.3 (t, $J = 10$ Hz), 139.8, 167.2, 169.3.

^{31}P NMR (162M, CDCl_3) 1.33.

HRMS (ESI): calcd for $\text{C}_{50}\text{H}_{44}\text{Cl}_4\text{N}_4\text{O}_4\text{P}_2$ ($[\text{M}+\text{H}]$): 967.1592, found 969.1703.

$[\alpha]_{\text{D}}^{25} = 30.8^\circ$ ($c = 0.33$, acetone).

White solid (11 % yield); M.P. 320°C .



^1H NMR (400M, CDCl_3) 1.30-1.43 (m, 4H), 1.80-1.83 (m, 5H), 2.04-2.11 (m, 3H), 2.20-2.37 (m, 8H), 6.15 (s, 2H), 6.42-6.47 (m, 4H), 6.77-6.82 (m, 4H), 6.93-6.96 (m, 2H), 7.08-7.11 (m, 3H), 7.18-7.24 (m, 4H), 7.36 (t, $J = 8$ Hz, 2H), 7.63 (d, $J = 8$ Hz, 3H).

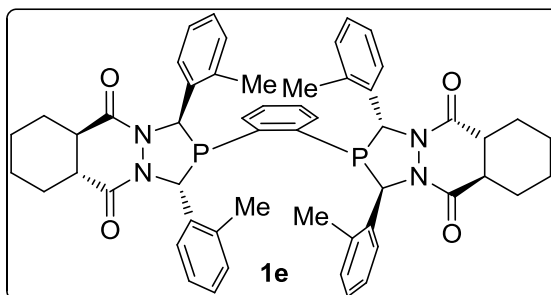
^{13}C NMR (100M, CDCl_3) 24.5, 26.2, 26.7, 29.8, 41.7, 42.2, 60.0 (m), 61.3 (t, $J = 17$ Hz), 122.6, 123.4 (m), 126.3, 126.7, 128.5, 128.6, 129.2, 129.9, 130.3, 132.0, 132.9, 133.8, 135.5, 138.3 (t, $J = 10$ Hz), 139.9, 167.4, 169.4.

^{31}P NMR (162M, CDCl_3) 2.75 (s)

HRMS (ESI): calcd for $\text{C}_{50}\text{H}_{44}\text{Br}_4\text{N}_4\text{O}_4\text{P}_2$ ($[\text{M}+\text{H}]$): 1142.9571, found 1146.9593 ($\text{M}+4$).

$[\alpha]_{\text{D}}^{25} = 30.1^\circ$ ($c = 0.31$, acetone).

White solid (7 % yield); M.P. 390°C .



^1H NMR (400M, CDCl_3) 1.30-1.43 (m, 4H), 1.73-1.85 (m, 6H), 1.92-2.00 (m, 3H), 2.13-2.14 (m, 3H), 2.18-2.27 (m, 10H), 2.42 (s, 6H), 5.92 (s, 2H), 6.05-6.11 (m, 4H), 6.51-6.55 (m, 4H), 6.83 (d, $J = 7.2\text{Hz}$, 2H), 6.91 (d, $J = 7.2$ Hz, 3H), 7.17-7.29 (m, 9H).

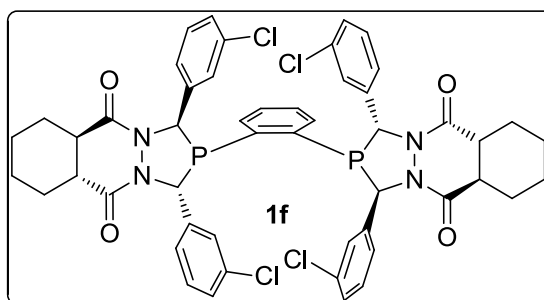
^{13}C NMR (100M, CDCl_3) 20.1 (t, $J = 5.8$ Hz), 20.3, 24.4, 24.5, 26.0, 26.7, 41.7, 42.0, 54.5 (m), 58.5 (t, $J = 18$ Hz), 124.7, 125.1, 125.2 (m), 126.8, 127.1, 128.3, 130.4, 130.5, 131.1, 134.7, 134.8, 135.6, 137.2 (t, $J = 9.1$ Hz), 139.6 (m), 167.1, 169.3.

^{31}P NMR (162M, CDCl_3) -0.42.

HRMS (ESI): calcd for $C_{54}H_{56}N_4O_4P_2$ ($[M+H]^+$): 887.3777, found 887.3799.

$[\alpha]_D^{25} = 36.5^\circ$ ($c = 0.4$, acetone).

White solid (12 % yield); M.P. 290°C.



1H NMR (400M, $CDCl_3$) 1.30-1.36 (m, 4H), 1.74-1.81 (m, 6H), 2.01-2.28 (m, 10H), 5.60 (t, $J = 10$ Hz, 2H), 5.76 (s, 2H), 6.39 (m, 2H), 6.53-6.55 (m, 2H), 6.80 (t, $J = 8$ Hz, 2H), 6.92-6.97 (m, 4H), 7.07-7.09 (m, 4H), 7.25-7.27 (m, 4H), 7.36-7.38 (m, 2H).

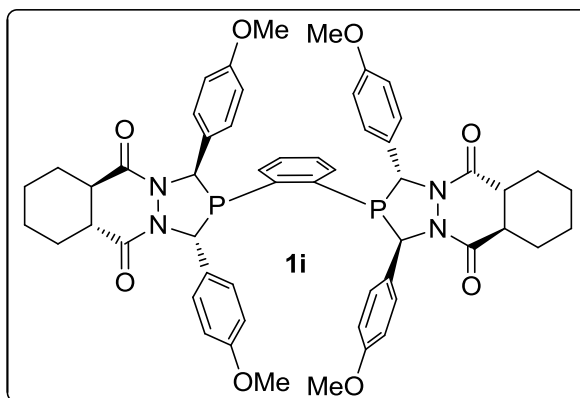
^{13}C NMR (100M, $CDCl_3$) 24.5, 24.6, 26.1, 26.9, 41.8, 42.8, 56.8 (m), 61.5 (t, $J = 17$ Hz), 124.1, 124.2, 124.6, 126.4, 126.9 (m), 127.6, 128.8, 129.2, 130.5, 130.7, 131.6, 134.1, 135.4, 138.2, 138.4, 139.4 (m), 167.6, 170.1.

^{31}P NMR (162M, $CDCl_3$) -0.18.

HRMS (ESI): calcd for $C_{50}H_{44}Cl_4N_4O_4P_2$ ($[M+H]^+$): 967.1592, found 969.1635.

$[\alpha]_D^{25} = 23.7^\circ$ ($c = 0.4$, acetone).

White solid (14 % yield); M.P. 200°C.



^1H NMR (400M, CDCl_3) 1.30-1.40 (m, 2H), 1.77-1.85 (m, 7H), 2.02-2.08 (m, 3H), 2.19-2.39 (m, 8H), 3.66 (s, 6H), 3.83 (s, 6H), 5.75-5.80 (m, 4H), 6.37-6.39 (m, 3H), 6.50-6.52 (m, 4H), 6.89-6.91 (m, 4H), 7.08-7.11 (m, 6H), 7.30-7.33 (m, 3H).

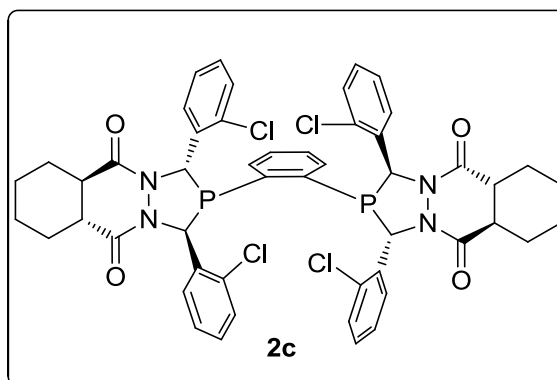
^{13}C NMR (100M, CDCl_3) 24.4, 24.6, 26.0, 26.8, 41.7, 42.4, 55.2, 55.4, 56.7, 61.4 (t, $J = 18\text{Hz}$), 113.2, 114.5, 127.1, 127.5 (t, $J = 4.4\text{ Hz}$), 128.2, 130.1, 130.6, 158.5, 159.5, 167.1, 169.7.

^{31}P NMR (162M, CDCl_3) -2.76.

HRMS (ESI): calcd for $\text{C}_{54}\text{H}_{56}\text{N}_4\text{O}_8\text{P}_2$ ($[\text{M}+\text{H}]$): 951.3573, found 951.3601.

$[\alpha]_{\text{D}}^{25} = 15.7^\circ$ ($c = 0.67$, acetone).

White solid (9 % yield); M.P. 295°C .



^1H NMR (400M, CDCl_3) 1.30-1.43 (m, 4H), 1.80-1.83 (m, 6H), 2.15-2.30 (m, 10H), 6.05-6.09 (m, 4H), 6.38 (t, $J = 10$ Hz, 2H), 6.63-6.66 (m, 2H), 6.73-6.82 (m, 4H), 7.14-7.16 (m, 2H), 7.27-7.41 (m, 10H).

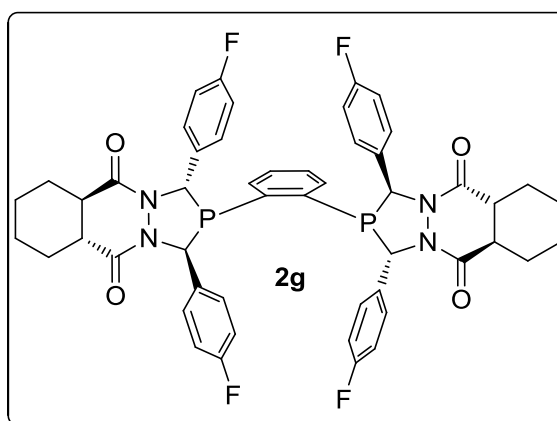
^{13}C NMR (100M, CDCl_3) 24.3, 24.4, 26.0, 26.4, 42.1, 42.2, 58.3 (m), 58.7 (t, $J = 17$ Hz), 125.2, 126.6, 127.2, 127.6, 128.1, 129.1, 129.4, 130.2, 131.4, 131.8, 131.9, 133.0, 135.6 (m), 139.6 (m), 165.6, 167.5.

^{31}P NMR (162M, CDCl_3) -14.77.

HRMS (ESI): calcd for $\text{C}_{50}\text{H}_{44}\text{Cl}_4\text{N}_4\text{O}_4\text{P}_2$ ($[\text{M}+\text{H}]$): 967.1592, found 969.1649.

$[\alpha]_{\text{D}}^{25} = 35.2^\circ$ ($c = 0.20$, acetone).

White solid (11 % yield); M.P. 240°C .



^1H NMR (400M, CDCl_3) 1.30-1.43 (m, 4H), 1.83-1.86 (m, 5H), 5.54-5.59 (m, 4H), 6.36-6.41 (m, 4H), 6.60-6.64 (m, 4H), 6.93-6.97 (m, 4H), 7.05 (t, $J = 8$ Hz, 4H), 7.42-7.44 (m, 2H), 7.56-7.58 (m, 2H).

^{13}C NMR (100M, CDCl_3) 24.2, 24.4, 25.7, 26.7, 41.5, 42.6, 59.4, 61.9 (t, $J = 8$ Hz, 2H), 7.63 (t, $J = 17$ Hz), 114.4 (d, $J = 21$ Hz), 116.1 (d, $J = 21$ Hz), 127.1 (d, $J = 9$ Hz), 128.6 (m), 131.2, 131.5, 134.3, 140.3, 160.6 (d, $J = 62$ Hz), 163.0 (d, $J = 62$ Hz), 164.6, 167.7.

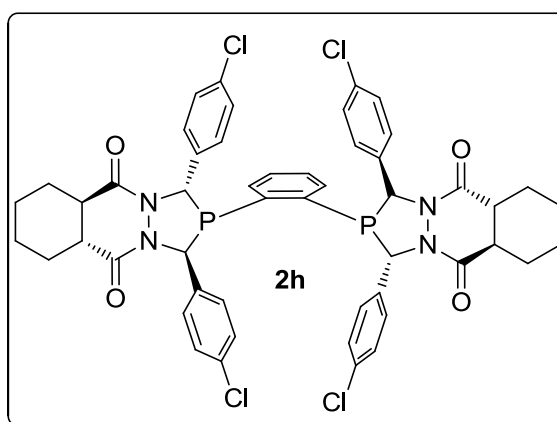
^{31}P NMR (162M, CDCl_3) -14.69.

^{19}F NMR (376M, CDCl_3) -113.6 (d, $J = 75$ Hz).

HRMS (ESI): calcd for $\text{C}_{50}\text{H}_{44}\text{F}_4\text{N}_4\text{O}_4\text{P}_2$ ($[\text{M}+\text{H}]$): 903.2774, found 903.2799.

$[\alpha]_{\text{D}}^{25} = 57.0^\circ$ (c = 0.21, acetone).

White solid (13 % yield); M.P. 210°C .



^1H NMR (400M, CDCl_3) 1.35-1.37 (m, 2H), 1.60 (m, 3H), 1.85-1.87 (m, 5H), 2.09-2.37 (m, 10H), 5.48-5.56 (m, 4H), 6.14-6.20 (m, 4H), 6.91-6.93 (m, 7H), 7.34-7.36 (m, 4H), 7.43-7.47 (m, 3H), 7.57-7.61 (m, 2H).

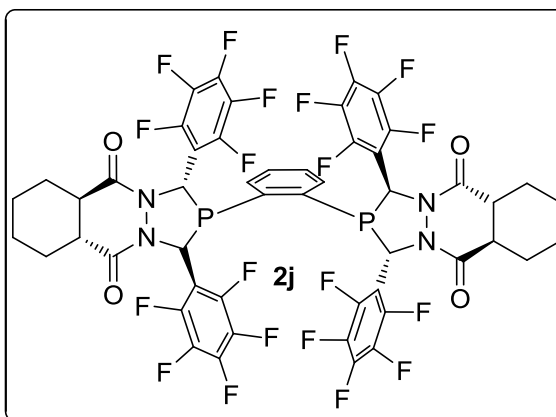
^{13}C NMR (100M, CDCl_3) 24.4, 24.6, 25.8, 26.8, 41.6, 42.7, 59.7, 62.0 (m), 126.8, 127.8, 128.5, 129.5, 131.5, 131.8, 133.2, 137.2, 140.2, 161.0, 162.0, 164.7, 167.9.

^{31}P NMR (162M, CDCl_3) -14.90

HRMS (ESI): calcd for $\text{C}_{50}\text{H}_{44}\text{Cl}_4\text{N}_4\text{O}_4\text{P}_2$ ($[\text{M}+\text{H}]$): 967.1592, found 969.1613.

$[\alpha]_{\text{D}}^{25} = 40.7^\circ$ ($c = 0.33$, acetone).

White solid (6 % yield); M.P. 285°C .



^1H NMR (400M, CDCl_3) 1.30-1.43 (m, 5H), 1.85-1.91 (m, 5H), 2.11-2.15 (m, 2H), 2.32-2.56 (m, 8H), 5.76 (s, 2H), 6.48 (s, 2H), 7.53-7.57 (m, 2H), 7.61-7.68 (m, 2H).

^{13}C NMR (100M, CDCl_3) 24.0, 24.5, 25.6, 26.9, 40.5, 41.5, 51.3 (m), 56.4 (m), 111.5-111.9 (m), 129.7, 133.2, 136.1 (m), 136.6 (m), 138.6 (m), 139.1 (m), 140.8 (m), 143.0 (m), 145.6 (m), 167.7, 168.2.

^{31}P NMR (162M, CDCl_3) 21.84 (m).

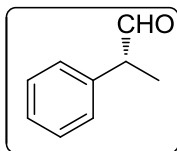
^{19}F NMR (376M, CDCl_3) -162.2 (m), -161.1 (m), -153.3 (m), -144.5.

HRMS (ESI): calcd for $\text{C}_{50}\text{H}_{28}\text{F}_{20}\text{N}_4\text{O}_4\text{P}_2$ ($[\text{M}+\text{H}]$): 1191.1266, found 1191.1305.

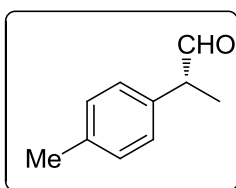
$[\alpha]_{\text{D}}^{25} = 14.6^\circ$ ($c = 1.6$, acetone).

White solid (11 % yield); M.P. 195°C.

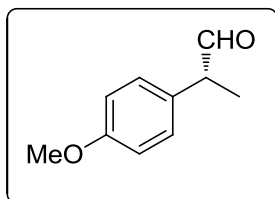
2.4.4 GC and HPLC analysis of the chiral aldehydes.



(*R*)-2-phenylpropanal **4a**: Enantiomeric excess was determined by GC with a Supelco's Beta Dex 225 column, Temperature program: 100 °C, stay 5 mins, 1 °C/min to 160 °C, stay 5 mins, Flow rate = 1.0 mL/min, $t_{\text{minor}} = 12.3$ min, $t_{\text{major}} = 12.4$ min; 85 %

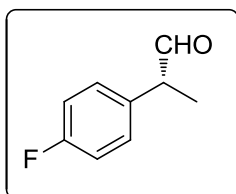


(*R*)-2-*p*-tolylpropanal **4b**: Enantiomeric excess was determined by GC with a Supelco's Beta Dex 225 column, Temperature program: 100 °C, stay 5 mins, 1.5 °C/min to 147 °C, stay 5 mins, Flow rate = 1.0 mL/min, $t_{\text{minor}} = 19.9$ min, $t_{\text{major}} = 20.0$ min; 80 % *ee*.

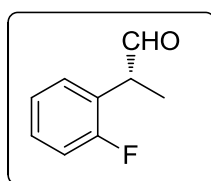


(*R*)-2-(4-methoxyphenyl)propanal **4c**: Enantiomeric excess was determined by GC with a Supelco's Beta Dex 225 column, Temperature program: 100 °C, stay 5 mins,

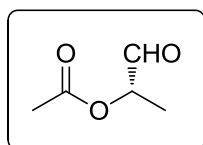
1.5 °C/min to 147 °C, stay 12 mins, Flow rate = 1.0 mL/min, $t_{\text{minor}} = 32.9$ min, $t_{\text{major}} = 33.2$ min; 77 % *ee*.



(*R*)-2-(4-fluorophenyl)propanal **4d**: Enantiomeric excess was determined by GC with a Supelco's Beta Dex 225 column, Temperature program: 60 °C, stay 2 mins, 0.9 °C/min to 120 °C, stay 5 mins, Flow rate = 1.0 mL/min, $t_{\text{minor}} = 59.6$ min, $t_{\text{major}} = 60.4$ min; 83 % *ee*.

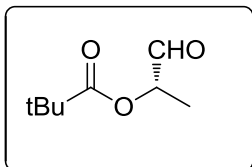


(*R*)-2-(2-fluorophenyl)propanal **4e**: Enantiomeric excess was determined by reducing it into alcohol with NaBH₄ and analyzing with HPLC: Daicel Chiralcel AS-H, hexane/*i*PrOH = 95:5, flow rate = 1.0 mL/min, $\lambda = 254$ nm, $t_{\text{minor}} = 8.7$ min, $t_{\text{major}} = 7.9$ min; 88 % *ee*.

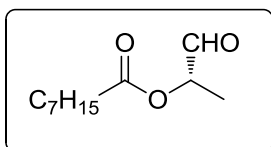


(*S*)-1-oxopropan-2-yl acetate **7a**: Enantiomeric excess was determined by GC with a Supelco's Beta Dex 225 column, Temperature program: 100 °C, stay 5 mins, 1 °C/min

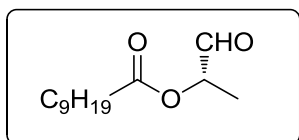
to 160 °C, stay 5 mins, Flow rate = 1.0 mL/min, $t_{\text{minor}} = 8.5$ min, $t_{\text{major}} = 6.4$ min; 91 % *ee*.



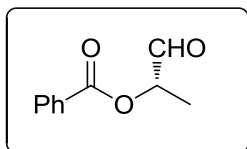
(*S*)-1-oxopropan-2-yl pivalate **7b**: Enantiomeric excess was determined by GC with a Supelco's Beta Dex 225 column, Temperature program: 50 °C, stay 5 mins, 1 °C/min to 100 °C, stay 5 mins, Flow rate = 1.0 mL/min, $t_{\text{minor}} = 42.1$ min, $t_{\text{major}} = 40.5$ min; 91 % *ee*.



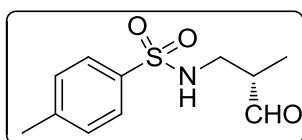
(*S*)-1-oxopropan-2-yl octanoate **7c**: Enantiomeric excess was determined by GC with a Supelco's Beta Dex 225 column, Temperature program: 130 °C, stay 30 mins, Flow rate = 1.0 mL/min, $t_{\text{minor}} = 23.0$ min, $t_{\text{major}} = 21.9$ min; 93 % *ee*.



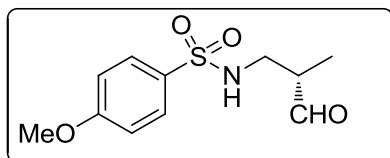
(*S*)-1-oxopropan-2-yl decanoate **7d**: Enantiomeric excess was determined by GC with a Supelco's Beta Dex 225 column, Temperature program: 130 °C, stay 70 mins, Flow rate = 1.0 mL/min, $t_{\text{minor}} = 63.5$ min, $t_{\text{major}} = 57.9$ min; 93 % *ee*.



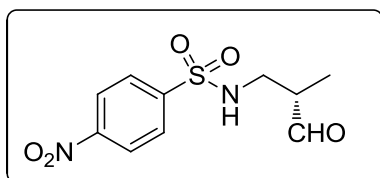
(*S*)-1-oxopropan-2-yl benzoate **7e**: Enantiomeric excess was determined by GC with a Supelco's Beta Dex 225 column, Temperature program: 135 °C, stay 36 mins, Flow rate = 1.0 mL/min, $t_{\text{minor}} = 23.8$ min, $t_{\text{major}} = 25.0$ min; 91 % *ee*.



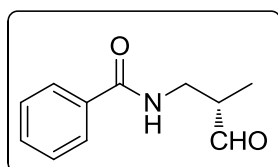
(*S*)-4-methyl-*N*-(2-methyl-3-oxopropyl)benzenesulfonamide **10a**: Enantiomeric excess was determined by reducing it into alcohol with NaBH₄ and analyzing with HPLC: Daicel Chiralcel AD-H, hexane/iPrOH = 90:10, flow rate = 1.0 mL/min, $\lambda = 254$ nm, $t_{\text{minor}} = 42.1$ min, $t_{\text{major}} = 29.7$ min; 88 % *ee*.



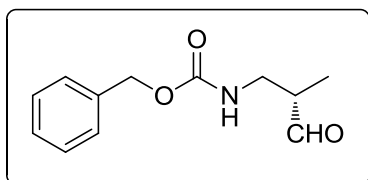
(*S*)-4-methoxy-*N*-(2-methyl-3-oxopropyl)benzenesulfonamide **10b**: Enantiomeric excess was determined by reducing it into alcohol with NaBH₄ and analyzing with HPLC: Daicel Chiralcel OD-H, hexane/iPrOH = 85:15, flow rate = 1.0 mL/min, $\lambda = 254$ nm, $t_{\text{minor}} = 31.4$ min, $t_{\text{major}} = 23.2$ min; 88 % *ee*.



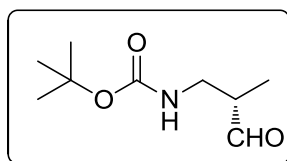
(*S*)-*N*-(2-methyl-3-oxopropyl)-4-nitrobenzenesulfonamide **10c**: Enantiomeric excess was determined by reducing it into alcohol with NaBH₄ and analyzing with HPLC: Daicel Chiralcel AD-H, hexane/iPrOH = 85:15, flow rate = 1.0 mL/min, λ = 254 nm, t_{minor} = 46.4 min, t_{major} = 37.1 min; 91 % *ee*.



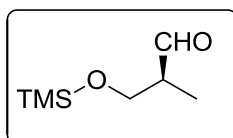
(*S*)-*N*-(2-methyl-3-oxopropyl)benzamide **10d**: Enantiomeric excess was determined by reducing it into alcohol with NaBH₄ and analyzing with HPLC: Daicel Chiralcel AD-H, hexane/iPrOH = 95:5, flow rate = 1.0 mL/min, λ = 254 nm, t_{minor} = 19.2 min, t_{major} = 20.2 min; 92 % *ee*.



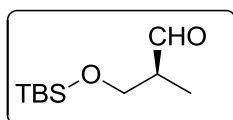
(*S*)-benzyl 2-methyl-3-oxopropylcarbamate **10e**: Enantiomeric excess was determined by reducing it into alcohol with NaBH₄ and analyzing with HPLC: Daicel Chiralcel AS-H, hexane/iPrOH = 90:10, flow rate = 1.0 mL/min, λ = 254 nm, t_{minor} = 15.1 min, t_{major} = 14.2 min; 92 % *ee*.



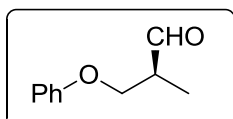
(*S*)-*tert*-butyl 2-methyl-3-oxopropylcarbamate **10f**: Enantiomeric excess was determined by GC with a Supelco's Beta Dex 225 column, Temperature program: 120 °C, stay 20 mins, 0.7 °C/min to 130 °C, stay 5 mins, 0.7 °C/min to 140 °C, stay 2 mins, Flow rate = 1.0 mL/min, $t_{\text{minor}} = 40.4$ min, $t_{\text{major}} = 40.7$ min; 85 % *ee*.



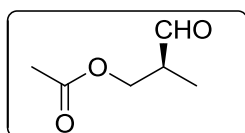
(*S*)-2-methyl-3-(trimethylsilyloxy)propanal **13a**: Enantiomeric excess was determined by GC with a Supelco's Beta Dex 225 column, Temperature program: 70 °C, stay 30 mins, Flow rate = 1.0 mL/min, $t_{\text{minor}} = 18.4$ min, $t_{\text{major}} = 18.5$ min; 94 % *ee*.



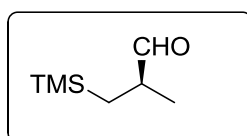
(*S*)-3-(*tert*-butyldimethylsilyloxy)-2-methylpropanal **13b**: Enantiomeric excess was determined by GC with a Supelco's Beta Dex 225 column, Temperature program: 65 °C, stay 30 mins, 0.7 °C/min to 80 °C, stay 10 mins, Flow rate = 1.0 mL/min, 0.7 °C/min to 90 °C, stay 10 mins, $t_{\text{minor}} = 63.2$ min, $t_{\text{major}} = 63.7$ min; 83 % *ee*.



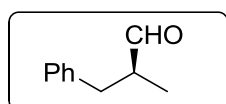
(*S*)-2-methyl-3-phenoxypropanal **13c**: Enantiomeric excess was determined by GC with a Supelco's Beta Dex 225 column, Temperature program: 90 °C, stay 1 mins, 0.8 °C/min to 160 °C, stay 1 mins, Flow rate = 1.0 mL/min, $t_{\text{minor}} = 51.3$ min, $t_{\text{major}} = 51.5$ min; 90 % *ee*.



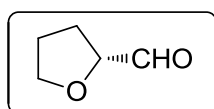
(*S*)-2-methyl-3-oxopropyl acetate **13d**: Enantiomeric excess was determined by GC with a Supelco's Beta Dex 225 column, Temperature program: 90 °C, stay 10 mins, 0.8 °C/min to 100 °C, stay 2 mins, 0.8 °C/min to 110 °C, stay 2 mins, Flow rate = 1.0 mL/min, $t_{\text{minor}} = 26.0$ min, $t_{\text{major}} = 24.9$ min; 92 % *ee*.



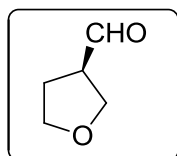
(*S*)-*tert*-butyl 2-methyl-3-oxopropylcarbamate **13e**: Enantiomeric excess was determined by GC with a Supelco's Beta Dex 225 column, Temperature program: 80 °C, stay 1 mins, 0.8 °C/min to 120 °C, stay 12 mins, Flow rate = 1.0 mL/min, $t_{\text{minor}} = 9.8$ min, $t_{\text{major}} = 9.5$ min; 91 % *ee*.



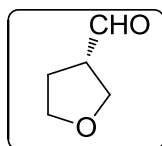
(*S*)-2-methyl-3-phenylpropanal **13f**: Enantiomeric excess was determined by reducing it into alcohol with NaBH₄ and analyzing with HPLC: Daicel Chiralcel OD-H, hexane/iPrOH = 95:5, flow rate = 1.0 mL/min, λ = 254 nm, t_{minor} = 10.4 min, t_{major} = 8.5 min; 90 % *ee*.



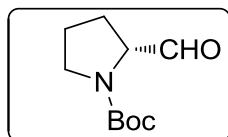
(*R*)-tetrahydrofuran-2-carbaldehyde **16**: Enantiomeric excess was determined by GC with a Supelco's Beta Dex 225 column, Temperature program: 50 °C, stay 1 mins, 15 °C/min to 150 °C, stay 10 mins, Flow rate = 1.0 mL/min, t_{minor} = 7.5 min, t_{major} = 7.2 min; 92 % *ee*.



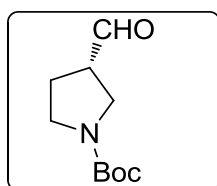
(*R*)-tetrahydrofuran-3-carbaldehyde **17a**: Enantiomeric excess was determined by GC with a Supelco's Beta Dex 225 column, Temperature program: 50 °C, stay 1 mins, 15 °C/min to 150 °C, stay 10 mins, Flow rate = 1.0 mL/min, t_{minor} = 8.1 min, t_{major} = 8.6 min; 93 % *ee*.



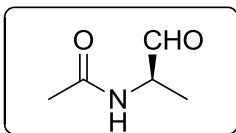
(*S*)-tetrahydrofuran-3-carbaldehyde **17b**: Enantiomeric excess was determined by GC with a Supelco's Beta Dex 225 column, Temperature program: 50 °C, stay 1 mins, 15 °C/min to 150 °C, stay 10 mins, Flow rate = 1.0 mL/min, $t_{\text{minor}} = 8.6$ min, $t_{\text{major}} = 8.1$ min; 92 % *ee*.



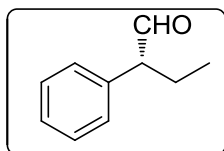
(*R*)-tetrahydrofuran-2-carbaldehyde **21**: Enantiomeric excess was determined by GC with a Supelco's Beta Dex 225 column, Temperature program: 120 °C, stay 30 mins, 0.8 °C/min to 130 °C, stay 10 mins, 0.8 °C/min to 140 °C, stay 10 mins, Flow rate = 1.0 mL/min, $t_{\text{minor}} = 31.5$ min, $t_{\text{major}} = 31.7$ min; 95 % *ee*.



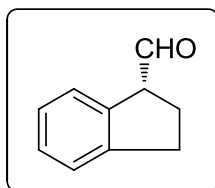
(*S*)-*tert*-butyl 3-formylpyrrolidine-1-carboxylate **22**: Enantiomeric excess was determined by GC with a Supelco's Beta Dex 225 column, Temperature program: 120 °C, stay 30 mins, 0.8 °C/min to 130 °C, stay 10 mins, 0.8 °C/min to 140 °C, stay 10 mins, Flow rate = 1.0 mL/min, $t_{\text{minor}} = 61.3$ min, $t_{\text{major}} = 61.6$ min; 91 % *ee*.



(*R*)-*N*-(1-oxopropan-2-yl)acetamide **23b**: Enantiomeric excess was determined by GC with a Supelco's Beta Dex 225 column, Temperature program: 100 °C, stay 5 mins, 1.5 °C/min to 160 °C, stay 5 mins, Flow rate = 1.0 mL/min, $t_{\text{minor}} = 40.9$ min, $t_{\text{major}} = 35.6$ min; 88 % *ee*.

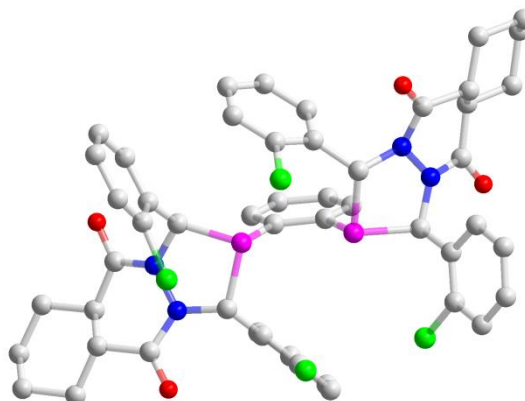


(*R*)-2-phenylbutanal **24b**: Enantiomeric excess was determined by GC with a Supelco's Beta Dex 225 column, Temperature program: 80 °C, stay 5 mins, 1.5 °C/min to 107 °C, stay 17 mins, Flow rate = 1.0 mL/min, $t_{\text{minor}} = 29.3$ min, $t_{\text{major}} = 29.6$ min; 89 % *ee*.



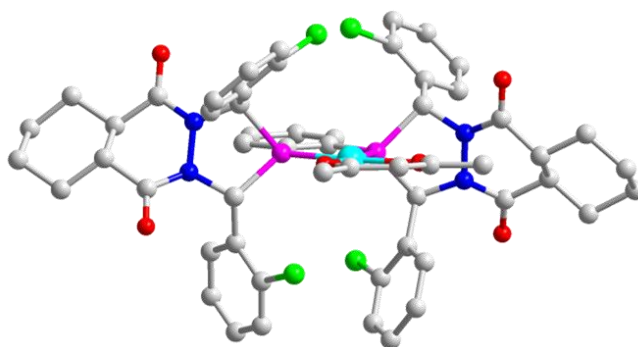
(*R*)-2,3-dihydro-1H-indene-1-carbaldehyde **25b**: Enantiomeric excess was determined by GC with a Supelco's Beta Dex 225 column, Temperature program: 100 °C, stay 10 mins, 3 °C/min to 130 °C, stay 15 mins, Flow rate = 1.0 mL/min, $t_{\text{minor}} = 25.5$ min, $t_{\text{major}} = 26.0$ min; 71% *ee*.

2.4.5. Single crystal X-ray diffraction structure of ligand 1c (CCDC 955452)



Chemical formula	$C_{50}H_{48}Cl_4N_4O_6P_2 \cdot C_1H_4O_1$
FW	1036.74
Crystal system	orthorhombic
Space group	$P2_12_12_1$
T, K	100(2)
a/Å	9.8323(9)
b/Å	11.4917(11)
c/Å	42.543(4)
$\alpha/^\circ$	90.00
$\beta/^\circ$	90.00
$\gamma/^\circ$	90.00
V, Å ³	4807.0(8)
Z	4
Goodness of fit	1.006

2.4.6 Single crystal structure of complex A (CCDC 955453)



Chemical formula	C ₅₅ H ₅₁ Cl ₄ N ₄ O ₆ P ₂ Rh ₁
FW	1170.68
Crystal system	monoclinic
Space group	P2 ₁
T, K	100(2)
a/Å	12.6276(9)
b/Å	37.908(3)
c/Å	13.1171(9)
α /°	90.00
β /°	101.3640(10)
γ /°	90.00
V, Å ³	6155.8(8)
Z	4
Goodness of fit	0.967

Reference

1. a) B. M. Trost, M. L. Crawley, *Chem. Rev.* **2003**, *103*, 2921; b) Y. Zhang, M. S. Sigman, *J. Am. Chem. Soc.* **2007**, *129*, 3076; c) B. Li, Y. Zhao, Y. Lai, T. P. Loh, *Angew. Chem.* **2012**, *124*, 8165; *Angew. Chem. Int. Ed.*, **2012**, *32*, 8041; d) C. Zheng, D. Wang, S. S. Stahl, *J. Am. Chem. Soc.* **2012**, *134*, 16496.
2. For selected reviews, see: a) B. Breit, W. Seiche, *Synthesis* **2001**, 1; b) B. Breit, *Angew. Chem.* **2005**, *117*, 6976; *Angew. Chem. Int. Ed.*, **2005**, *44*, 6816; c) P. W. N. M. van Leeuwen, C. Claver, Rhodium Catalyzed Hydroformylation; Springer: Berlin, Heidelberg, **2008**; d) R. Franke, D. Selent, A. Börner, *Chem. Rev.* **2012**, *112*, 5675; e) J. Pospech, I. Fleischer, R. Franke, S. Buchholz, M. Beller, *Angew. Chem.* **2013**, *125*, 2922; *Angew. Chem. Int. Ed.* **2013**, *52*, 2852. For selected examples on linear selectivity, see: f) A. Seayad, M. Ahmed, H. Klein, R. Jackstell, T. Gross, M. Beller, *Science*, **2002**, *297*, 1676; g) I. Piras, R. Jennerjahn, R. Jackstell, A. Spannenberg, R. Franke, M. Beller, *Angew. Chem.* **2011**, *123*, 294; *Angew. Chem. Int. Ed.* **2011**, *50*, 280; h) L. Wu, I. Fleischer, R. Jackstell, I. Profir, R. Franke, M. Beller, *J. Am. Chem. Soc.* **2013**, *135*, 14306; i) C. Grünanger, B. Breit, *Angew. Chem.* **2010**, *122*, 979; *Angew. Chem. Int. Ed.* **2010**, *49*, 967; j) D. Fuchs, G. Rousseau, L. Diab, U. Gellrich, B. Breit, *Angew. Chem.* **2012**, *124*, 2220; *Angew. Chem. Int. Ed.* **2012**, *51*, 2178; k) U. Gellrich, W. Seiche, M. Keller, B. Breit, *Angew. Chem.* **2012**, *124*, 11195; *Angew. Chem. Int. Ed.* **2012**, *51*, 11033; l) K. Takahashi, M. Yamashita, T. Ichihara, K. Nakano, K. Nozaki, *Angew. Chem.* **2010**, *122*, 4590; *Angew. Chem. Int. Ed.* **2010**, *49*, 4488; m) K. Takahashi, M. Yamashita, K. Nozaki, *J. Am. Chem. Soc.* **2012**, *134*, 18746.

3. For selected reviews on AHF, see: a) F. Agbossou, J. F. Carpentier, A. Mortreux, *Chem. Rev.* **1995**, 95, 2485; b) B. Breit, *Acc. Chem. Res.* **2003**, 36, 264; c) M. Diéguez, O. Pamies, C. Claver, *Tetrahedron: Asymmetry* **2004**, 15, 2113; d) M. L. Clarke, *Curr. Org. Chem.* **2005**, 9, 701; e) J. Klosin, C. R. Landin, *Acc. Chem. Res.* **2007**, 40, 1251; f) H. Fernández-Pérez, P. Etayo, A. Panossian, A. Vidal-Ferran, *Chem. Rev.* **2011**, 111, 2119.
4. For the selected applications of AHF in the constructing of pharmaceutical building blocks, see: a) R. V. Chaudhari, *Curr. Opin. Drug Discovery Dev.* **2008**, 11, 820; b) W. H. Chiou, G. H. Lin, C. C. Hsu, S. J. Chaterpaul, I. Ojima, *Org. Lett.* **2009**, 11, 2659; c) Airiau, E.; Girard, N.; Mann, A.; Salvadori, J.; Taddei, M. *Org. Lett.* **2009**, 11, 5314.
5. a) N. Sakai, K. Nozaki, H. Takaya, *J. Chem. Soc. Chem. Commun.* **1994**, 395; b) K. Nozaki, N. Sakai, T. Nanno, T. Higashijima, S. Mano, T. Horiuchi, H. Takaya, *J. Am. Chem. Soc.* **1997**, 119, 4413; c) K. Nozaki, Y. Ito, F. Shibahara, E. Shirakawa, T. Otha, H. Takaya, T. Hiyama, *J. Am. Chem. Soc.* **1998**, 120, 4051; d) R. Tanaka, K. Nakano, K. Nozaki, *J. Org. Chem.* **2007**, 72, 8671; e) D. A. Castillo Molina, C. P. Casey, I. Müller, K. Nozaki, C. Jäkel, *Organometallics* **2010**, 29, 3362.
6. a) J. E. Babin, G. T. Whiteker, PCT Int. Appl. WO 9303839, **1993**; b) C. J. Cogley, J. Klosin, C. Qin, G. T. Whiteker, *Org. Lett.* **2004**, 6, 3277.
7. a) S. Breeden, M. Wills, *J. Org. Chem.* **1999**, 64, 9735; b) S. Breeden, D. J. Cole-Hamilton, D. F. Foster, G. J. Schwarz, M. Wills, *Angew. Chem.* **2000**, 112, 4272; *Angew. Chem. Int. Ed.* **2000**, 39, 4106.
8. a) S. Deerenberg, P. C. J. Kamer, P. W. N. M. van Leeuwen, *Organometallics* **2000**, 19, 2065; b) S. Deerenberg, O. Pamies, M. Dieguez, C. Claver, P. C. J.

- Kamer, P. W. N. M. van Leeuwen, *J. Org. Chem.* **2001**, *66*, 7626; c) F. Doro, J. N. H. Reek, P. W. N. M. van Leeuwen, *Organometallics*, **2010**, *29*, 4440.
9. a) M. Diéguez, O. Pamies, A. Ruiz, S. Castillon, C. Claver, *Chem. Eur. J.* **2001**, *7*, 3086; b) M. Diéguez, O. Pamies, C. Claver, *Chem. Commun.* **2005**, 1221.
10. a) J. Wassenaar, B. de Bruin, J. N. H. Reek, *Organometallics* **2010**, *29*, 2767; b) S. H. Chikkali, R. Bellini, G. Berthon-Gelloz, J. I. van der Vlugt, B. de Bruin, J. N. H. Reek, *Chem. Commun.* **2010**, *46*, 1244; c) R. Bellini, S. H. Chikkali, G. Berthon-Gelloz, J. N. H. Reek, *Angew. Chem.* **2011**, *123*, 7480; *Angew. Chem. Int. Ed.* **2011**, *50*, 7342; d) S. H. Chikkali, R. Bellini, B. Bruin, J. I. Vlugt, J. N. H. Reek, *J. Am. Chem. Soc.* **2012**, *134*, 6607; e) R. Bellini, J. N. H. Reek, *Chem. Eur. J.* **2012**, *18*, 13510; f) R. Bellini, J. N. H. Reek, *Chem. Eur. J.* **2012**, *18*, 7091.
11. Worthy, A. D.; Joe, C. L.; Lightburn, T. E.; Tan, K. L. *J. Am. Chem. Soc.* **2010**, *132*, 14757.
12. a) S. L. Buchwald, *J. Am. Chem. Soc.* **2011**, *133*, 19080; b) X. Wang, S. L. Buchwald, *J. Org. Chem.* **2013**, *78*, 3429.
13. G. M. Noonan, J. A. Fuentes, C. J. Cobley, M. L. Clarke, *Angew. Chem.* **2012**, *124*, 2527–2530; *Angew. Chem. Int. Ed.* **2012**, *51*, 2477.
14. B. Zhang, X. Peng, Z. Wang, C. Xia, K. Ding, *Chem. Eur. J.* **2008**, *14*, 7847.
15. a) Y. Yan, X. Zhang, *J. Am. Chem. Soc.* **2006**, *128*, 7198-7202; b) X. Zhang, B. Cao, S. Yu, X. Zhang, *Angew. Chem.* **2010**, *122*, 4141; *Angew. Chem. Int. Ed.* **2010**, *49*, 4047.
16. a) M. Rubio, A. Suarez, E. Alvarez, C. Bianchini, W. Oberhauser, M. Peruzzini, A. Pizzano, *Organometallics* **2007**, *26*, 6428; b) J. Mazuelaa, O.

- Pàmies, M. Diéguez, L. Palais, S. Rosset, A. Alexakis, *Tetrahedron: Asymmetry* **2010**, *21*, 2153; d) J. Mazuelaa, M. Coll, O. Pàmies, M. Diéguez, *J. Org. Chem.* **2009**, *74*, 5440; e) H. Fernández-Pérez, J. Benet-Buchholz, A. Vidal-Ferran, *Org. Lett.* **2013**, *15*, 3634.
17. a) A. T. Axtell, C. J. Cobley, J. Klosin, G. T. Whiteker, A. Zanotti-Gerosa, K. A. Abboud, *Angew. Chem.* **2005**, *117*, 5984; *Angew. Chem. Int. Ed.* **2005**, *44*, 5834; For Klosin's other important works on AHF, see: b) P. J. Thomas, A. T. Axtell, J. Klosin, W. Peng, C. L. Rand, T. P. Clark, C. R. Landis, K. A. Abboud, *Org. Lett.* **2007**, *9*, 2665; c) A. T. Axtell, J. Klosin, *Organometallics* **2006**, *25*, 5003.
18. a) T. P. Clark, C. R. Landis, S. L. Freed, J. Klosin, K. A. Abboud, *J. Am. Chem. Soc.* **2005**, *127*, 5040; b) A. L. Watkins, B. G. Hashiguchi, C. R. Landis, *Org. Lett.* **2008**, *10*, 4553; c) R. I. McDonald, G. W. Wong, R. P. Neupane, S. S. Stahl, C. R. Landis, *J. Am. Chem. Soc.* **2010**, *132*, 14027; d) A. L. Watkins, C. R. Landis, *Org. Lett.* **2011**, *13*, 164; e) T. T. Adint, G. W. Wong, C. R. Landis, *J. Org. Chem.* **2013**, *78*, 4231; f) E. R. Nelsen, C. R. Landis, *J. Am. Chem. Soc.* **2013**, *135*, 9636.
19. CCDC-955452 (**1c**) and CCDC-955453 (complex **A**, [Rh(**1c**)(acac)]) contain the supplementary crystallographic data for this paper. These data can be obtained free of charge from The Cambridge Crystallographic Data Centre via www.ccdc.cam.ac.uk/data_request/cif.
20. The configuration of ligand **2c** was determined by analogy. From the ¹H and ¹³C NMR experiments, the spectra are similar with ligand **1c**. From the ³¹P NMR experiment, only one single peak was observed (δ= -14.8 ppm), which showed that the two P atoms were equivalent.

21. a) R. A. Barrow, T. Hemscheidt, J. Liang, S. Paik, R. E. Moore, M. A. Tius, *J. Am. Chem. Soc.* **1995**, *117*, 2479; b) J. D. White, J. Hong, L. A. Robage, *J. Org. Chem.* **1999**, *64*, 6206.
22. a) Chikkali, S.H.; Bellini, R.; de Bruin, B.; van der Vlugt, J. I.; Reek, J. N. H. J. W. J. *Am. Chem. Soc.* **2012**, *134*, 6607; b) Song, S.; Zhu, S.; Pu, L.; Zhou, Q. *Angew. Chem. Int. Ed.* **2013**, *52*, 6072; c) Al-Farhan, E.; Deininger, D. D.; McGhie, S.; O'Callaghan, J.; Robertson, M. S.; Rodgers, K.; Rout, S. J.; Singh, H.; Tung, R. D. PCT Int. Appl. WO 9948885, **1999**; d) Huang, X.; Brien, E.; Thai, F.; Cooper, G. *Org. Process Res. Dev.* **2010**, *14*, 592; e) Zhang, M.; Tamiya, J.; Nguyen, L.; Rowbottom, M. W.; Dyck, B.; Vickers, T. D.; Grey, J.; Schwarz, D. A.; Heise, C. E.; Haelewyn, J.; Mistry, M. S.; Goodfellow, V. S. *Bioorg. Med. Chem. Lett.* **2007**, *17*, 2535; f) Sharma, R.; Lubell, W. D. *J. Org. Chem.* **1996**, *61*, 202; g) Zhang, H.; Mifsud, M.; Tanaka, F.; Barbas, C. F. *J. Am. Chem. Soc.* **2006**, *128*, 9630.
23. Adint, T. T.; Landis, C. R. *J. Am. Chem. Soc.* **2014**, *136*, 7943.
24. The stereochemistry can be retained via Baeyer-Villiger oxidation process according to many previous reports. A similar process has been reported, see ref [2b] and references therein.
25. a) Al-Farhan, E.; Deininger, D. D.; McGhie, S.; O'Callaghan, J.; Robertson, M. S. Rodgers, K.; Rout, S. J.; Singh, H.; Tung, R. D. PCT Int. Appl. WO 9948885, **1999**; b) Kim, B. M.; Bae, S. J.; So, S. M.; Yoo, H. T.; Chang, S. K.; Lee, J. H.; Kang, J. S. *Org. Lett.* **2001**, *3*, 2349.
26. The two P atoms are diastereotopic and so are the two C atoms of CO; however, only one P atom and one C atom were observed from NMR analysis due to the fast exchange. The Rh-C coupling and P-C coupling (for terminal CO) were

not observed due to the fast exchange. Therefore, only an average coupling was left.

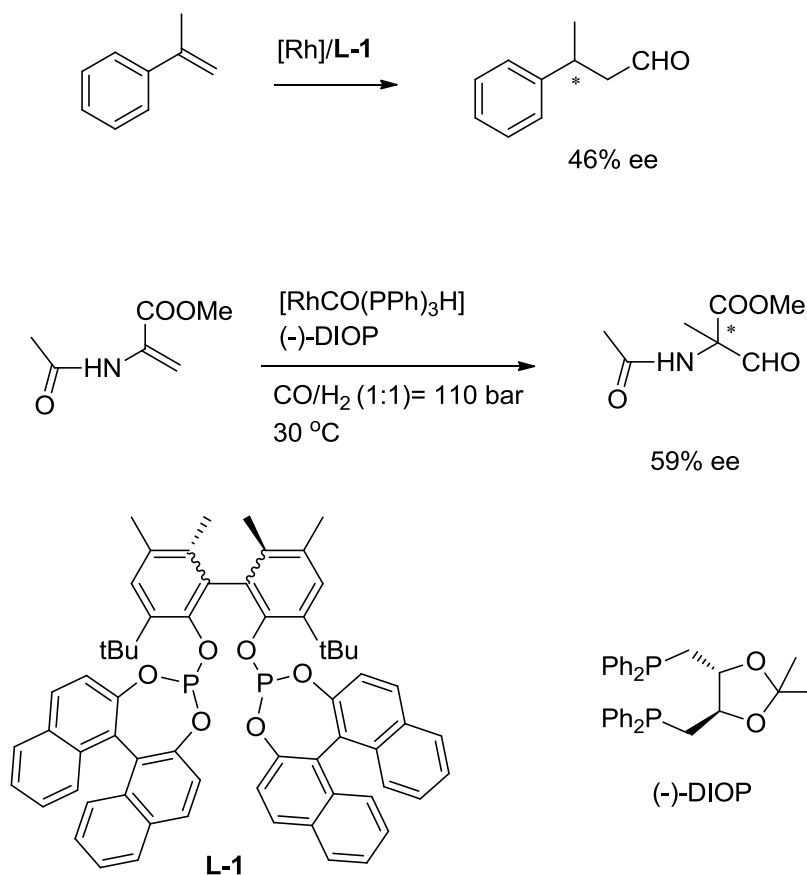
27. Van Rooy, A.; Kamer, P.C.J.; van Leeuwen, P.W.N.W. *J. Chem. Soc., Dalton Trans.*, **1995**, 409.

Chapter 3

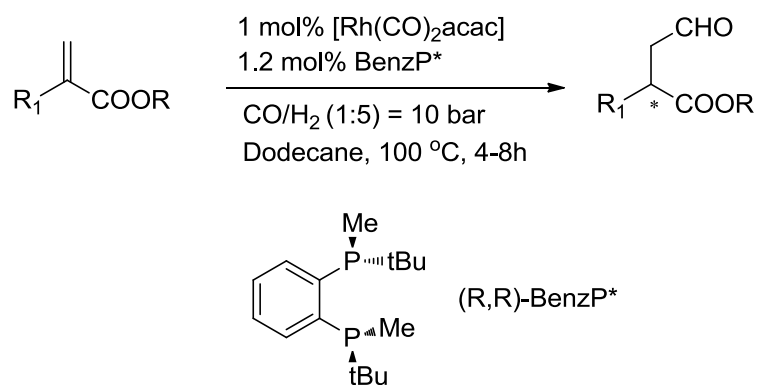
Rh-catalyzed Asymmetric Hydroformylation of 1,1-Disubstituted Allylphthalimides

3.1 Introduction

Asymmetric hydroformylation has been proven to be a straightforward and powerful homogeneously catalyzed process in fine chemicals, as it converts olefins into enantiomerically pure aldehydes in only one step.¹ Although a number of chiral phosphorus ligands have been developed to enhance both regio- and enantioselectivity in AHF,² the scope of substrates is still limited to monosubstituted³ and 1, 2-disubstituted olefins.⁴ Particularly, 1, 1-disubstituted olefin has been much less investigated due to difficulty controlling the enantioselectivity and reactivity.^{5,4f} The AHF of α -methylstyrene using diphosphite ligand to yield the linear product in moderate enantioselectivity (46%).⁴ⁱ The (R,R)-DIOP ligand has been applied in the AHF of amido acrylate. It was obtained exclusively the quaternary aldehyde in high yield but moderate enantioselectivity (up to 59%) (Scheme 3-1). Recently, Buchwald's group reported the AHF of functionalized 1,1-disubstituted alkenes under mild reaction conditions by using (R,R)-BenzP* ligand in good yields, excellent regioselectivity and enantioselectivity (Scheme 3-2).^{4f,6} However, the scope of 1,1-disubstituted alkenes is still quite limited and needs further exploration.



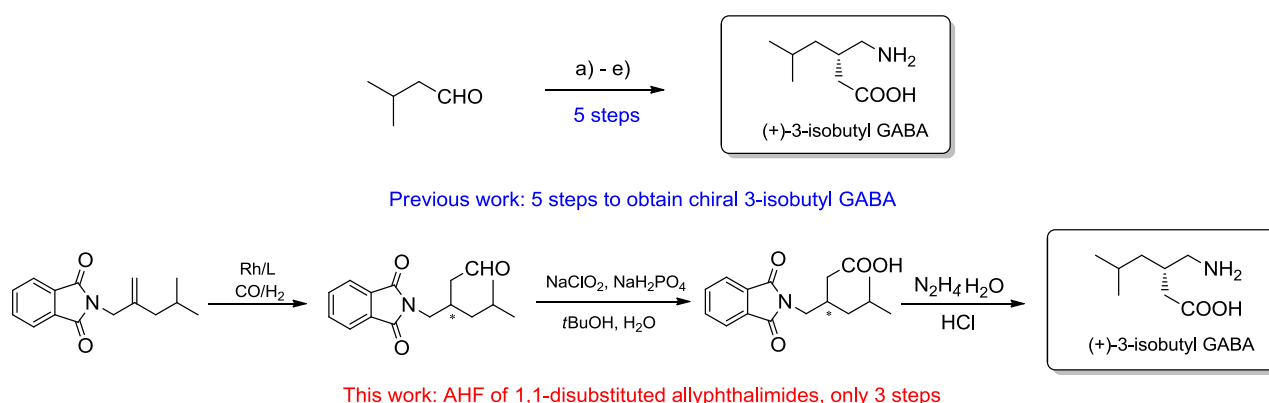
Scheme 3-1. The AHF of 1,1-disubstituted alkenes by ligand **1** and DIOP



Scheme 3-2. The AHF of α -alkylacrylates by ligand (R,R)-BenzP*

β -amino acids are key structural elements of many peptides and natural products.⁷ Chiral β^3 -amino acids are also universal in nature and play a crucial role in biochemical processes and overall physiological metabolism in human beings.⁸ For

instance, chiral γ -aminobutyric acid (GABA), its general formula $\text{NH}_2(\text{CH}_2)_3\text{COOH}$, is one of the most widely distributed inhibitory calming neurotransmitter to regulate brain and nerve cell activity by inhibiting the number of neurons firing in the brain⁹. GABA promotes healthy sleep and support healthy resting and a relaxed state of mind. Its derivatives from *S*-(+)-3-isobutyl GABA (Pregabalin) is a novel anticonvulsant drug which traditionally requires at least five steps, then applying resolution to obtain the final product (Scheme 3-3).¹⁰

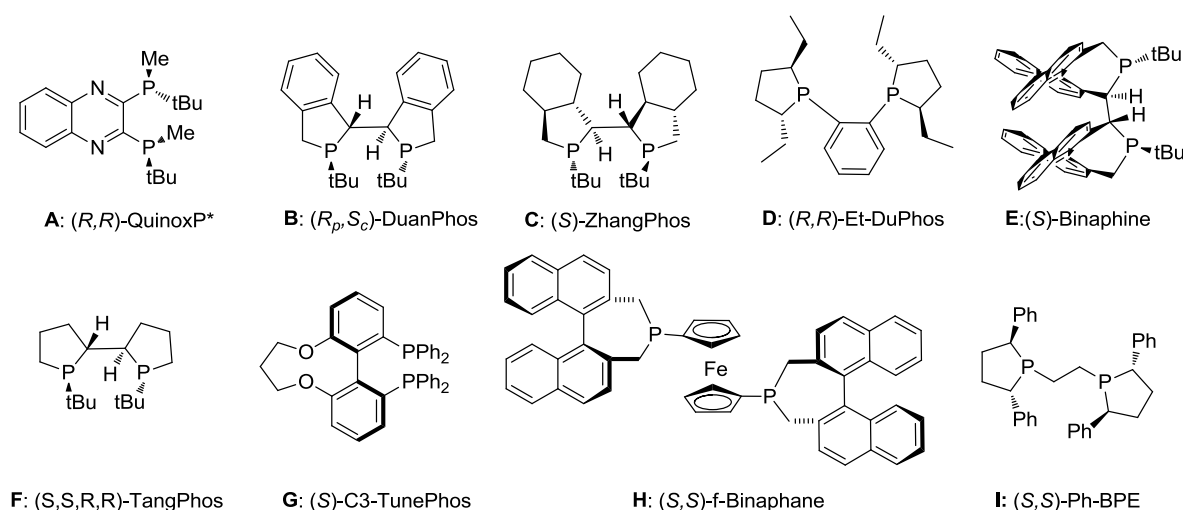


Scheme 3-3. Synthesis of (+)-3-isobutyl GABA.¹⁰ a) $n\text{Pr}_2\text{NH}$, HOAc ; b) KCN , ROH ; c) 1). KOH , MeOH 2). H_2 , Ni 3). HOAc ; d) 1) IPA , H_2O 2) recryst e) 1) $\text{THF}/\text{H}_2\text{O}$ 2) recryst

The low efficiency of this synthesis prompted us to seek an alternative approach by the AHF of 1,1-disubstituted allylphthalimides. It is a remarkably valuable transformation to afford optically pure linear phthalimide aldehydes (as indicated by Keulemans' rule)^{1g,11} in a single step, following two additional steps to provide the chiral β^3 -aminoaldehydes, which are valuable precursors for the synthesis of nonproteinogenic amino acids^{1g,4f} (Scheme 3-3). Herein, we disclose rhodium-catalyzed asymmetric hydroformylation of 1,1-disubstituted allylphthalimides with excellent enantioselectivity (up to 95% ee).

3.2 Results and Discussion

Initially, we investigated asymmetric hydroformylation of *N*-2-ethylallylphalimide (**1a**) as a model reaction by screening several known catalysts¹² (Scheme 3-4). Since the asymmetric hydroformylation using chiral phosphine/Rh complexes is well known, a diverse array of bisphosphine/Rh complexes were applied in this reaction. Some representative results are shown in Table 3-1.

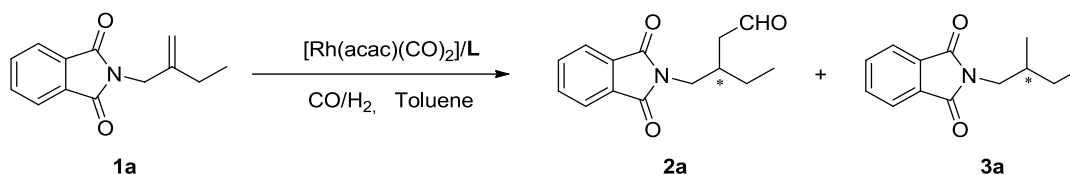


Scheme 3-4. Chiral ligands for the asymmetric hydroformylation reaction

The use of P-chirogenic diphosphine QuinoxP (**A**), which efficient for the AHF of α -alkylacrylate,⁶ gave both poor yield and ee value (Table 3-1, entry 1). When employing Binaphine (**E**), f-Binaphane (**H**) and TangPhos (**F**) with a 2.0 mol % loading of the rhodium catalyst at 90°C, they also displayed poor reactivity (Table 3-1, entries 5-6, 8). Application of biaryl diphosphine ligand C₃-TunePhos (**G**) provided **2a** in poor conversion with 36% ee (Table 3-1, entry 7). However, when employing phosphocyclic ligands like ligands **B**, **C** and **D**, the desired product **2a** could be obtained up to 61% ee (Table 3-1, entries 2-4). Furthermore, we discovered that by

using ligand (S,S)-Ph-BPE (**I**) gave desired product **2a** with higher enantiomeric excess (77%, Table 3-1, entry 9).

Table 3-1. Asymmetric hydroformylation of **1a**^a



Entry	Ligand (L)	Conv. [%] ^b	2a/3a ^b	<i>ee</i> [%] ^c
1	A	21	30/70	5
2	B	31	52/48	61
3	C	22	47/53	51
4	D	27	51/49	60
5	E	46	56/44	0
6	F	47	59/41	0
7	G	9	18/82	36
8	H	24	32/68	5
9	I	29	55/45	77

^a All reactions were performed at 90 °C in toluene under 20 bar of 1:1 CO/H₂, 2.0 mol % Rh(CO)₂acac, 8 mol % ligand, and 20 h reaction time.

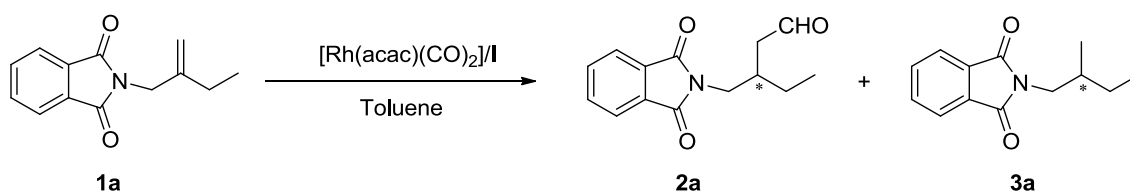
^b Conversions and **2a/3a** ratio were determined on the basis of ¹H NMR spectroscopy.

^c Determined by converting the aldehyde to the corresponding alcohol with NaBH(OAc)₃ followed by HPLC analysis.

With this promising result in hand, we next screened the ratio of CO/H₂ and Rh/ligand in order to enhance the conversion of **2a** and to minimize the hydrogenation

by-product **3a**. In Table 3-2, when we increased the CO/H₂ ratio to 3:1, the decreased enantiomeric excess was observed (Table 3-2, entry 2). However, under the same total pressure but varying CO/H₂ ratio from 1:3 to 1:5, the reaction afforded the desired product **2a** in 63% conversion, >99/1 **2a/3a** ratio with up to 81% ee (Table 3-2, entries 3-4). The use of lower total syngas pressure (6 bar) at the same ratio CO/H₂ (1:5) led to 60% conversion and 78% ee (Table 3-2, entry 5). In contrast, increased total syngas pressure to 40 bar led to drastically decrease conversion and enantioselectivity to 18% and 76% respectively (Table 3-2, entry 6). Under the total syngas 20 bar, the reaction afforded **2a** up to 82% ee by increasing the ratio of Rh/I to 1:5 (Table 3-2, entry 8). Further increasing or decreasing the ratio of Rh/I has no effect on conversion but enantioselectivities slightly went down.

Table 3-2. Syngas pressure screening for the Rh-catalyzed asymmetric hydroformylation of **1a**^a



Entry	CO/H ₂ [bar]	Rh/I	Conv. [%] ^b	2a/3a ^b	ee [%] ^c
1	20(1/1)	1/4	29	55/45	77
2	20(3/1)	1/4	22	52/48	75
3	20(1/3)	1/4	57	84/16	78
4	20(1/5)	1/4	63	>99/1	81
5	6(1/5)	1/4	60	61/39	78
6	40(1/5)	1/4	18	44/56	76
7	20(1/5)	1/3	54	>99/1	81

8	20(1/5)	1/5	80	>99/1	82
9	20(1/5)	1/6	78	>99/1	80

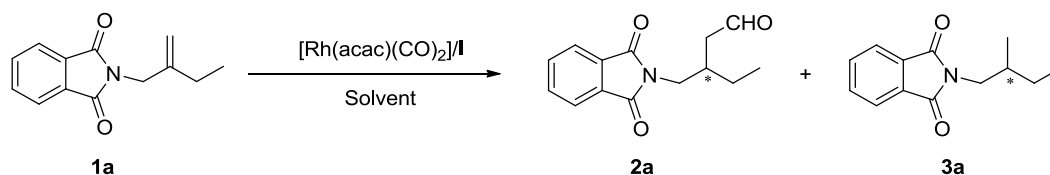
^a All reactions were performed at 90 °C in toluene, 2.0 mol % Rh(CO)₂(acac), and 20 h reaction time.

^b Conversions and **2a/3a** ratio were determined on the basis of ¹H NMR spectroscopy.

^c Determined by converting the aldehyde to the corresponding alcohol with NaBH(OAc)₃ followed by HPLC analysis.

Solvent is also a very important factor for this AHF reaction. In our screening of various solvents, full conversion and >99/1 **2a/3a** ratio were achieved by using cyclohexane and heptane as solvents (Table 3-3, entries 5-6). It was noteworthy that, when heptane was employed as the solvent, 90% enantioselectivity of the desired product **2a** with full conversion was obtained (Table 3-3, entry 6).

Table 3-3. Solvent screening for the Rh-catalyzed asymmetric hydroformylation of **1a**^a



Entry	Solvent	Conv. [%] ^b	2a/3a ^b	<i>ee</i> [%] ^c
1	EtOAc	89	89/11	75
2	THF	40	78/22	85
3	Undecane	72	90/10	83
4	Dodecane	50	93/7	84
5	Cyclohexane	100	>99/1	86
6	Heptane	100	>99/1	90

7	Acetone	75	88/12	77
8	CH ₃ CN	35	71/29	60
9	Toluene	80	>99/1	82

^a All reactions were performed at 90 °C under 20 bar of 1:5 CO/H₂, 2.0 mol % Rh(CO)₂acac, 10 mol % ligand **I** and 20 h reaction time.

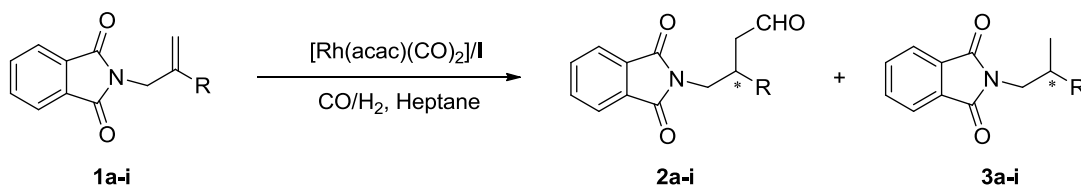
^b Conversions and **2a/3a** ratio were determined on the basis of ¹H NMR spectroscopy.

^c Determined by converting the aldehyde to the corresponding alcohol with NaBH(OAc)₃ followed by HPLC analysis.

With the optimized reaction conditions in hand (Table 3-3, entry 6), a series of **1a** derivatives were successfully converted to desired aldehydes with good conversion (up to 100%), >99/1 **2/3** ratio and excellent enantioselectivity (up to 95%). The AHF of butyl, isobutyl, propyl, benzyl and cyclopentyl substituted substrates only showed modest enantioselectivities and conversions (Table 3-4, entries 2-4, 7, 9). Possibly, the length of the aliphatic chain and the flexibility of the substrates significantly affected the stereo control in the transition state. However, the AHF reaction worked particularly well for methyl substituted substrate, with excellent conversion and 90% ee (Table 3-4, entry 6). The substrate bearing cyclohexyl group gave comparable enantioselectivity results to methyl substrate (90% ee), though its conversion was low (Table 3-4, entry 8). Notably, 95% ee was achieved in the asymmetric hydroformylation of isopropylphthalimide (Table 3-4, entry 5). The increased steric bulk of isopropyl group significantly improved the enantioselectivity of this reaction. Furthermore, this isopropyl structure is a considerably essential building block in a number of natural products and pharmaceutical ingredients (Scheme 3-5), such as agonists of the thrombopoietin (TPO) which are the promoters of thrombopoiesis and

megakaryocytopoiesis.¹³ This AHF procedure reported here delivers significant conversion to these valuable products in a direct manner.

Table 3-4. Asymmetric hydroformylation of allylphthalimide^a

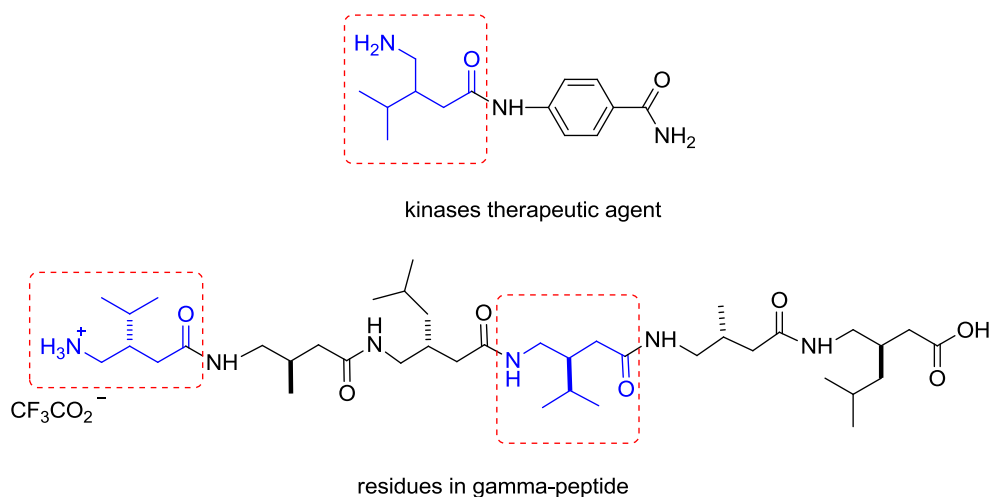


Entry	R	Conv. [%] ^b	2/3 ^b	<i>ee</i> [%] (config.) ^c
1	Et (1a)	100	>99/1	90 (-)
2	<i>n</i> Bu (1b)	54	97/3	77 (-)
3	<i>i</i> Bu (1c)	22	86/14	55 (+)
4	<i>n</i> Pr (1d)	36	>99/1	75 (-)
5	<i>i</i> Pr (1e)	45	>99/1	95 (-)
6	Me (1f)	88	>99/1	90 (+)
7	Bn (1g)	83	92/8	57 (-)
8	cyclohexyl(1h)	13	72/28	90(-)
9	cyclopentyl(1i)	36	>99/1	57(+)

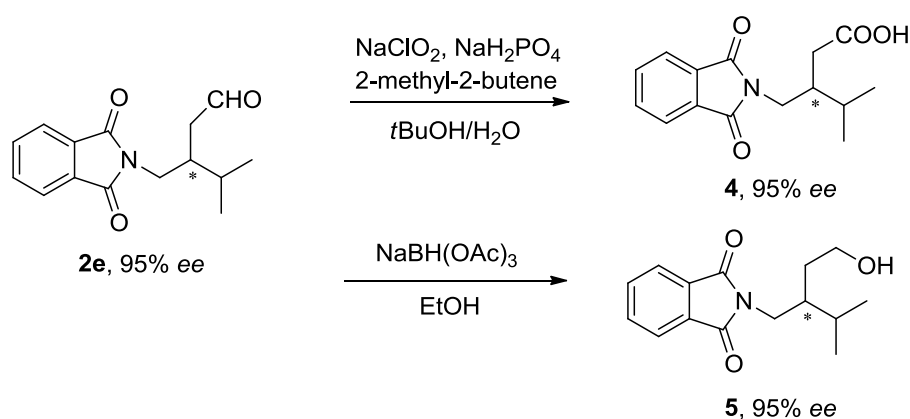
^a All reactions were performed at 90 °C in heptane under 20 bar of 1:5 CO/H₂, 2.0 mol % Rh(CO)₂acac, 10 mol % ligand **I** and 20 h reaction time.

^b Conversions and **2/3** ratio were determined on the basis of ¹H NMR spectroscopy.

^c Determined by converting the aldehyde to the corresponding alcohol with NaBH(OAc)₃ followed by HPLC analysis.



Scheme 3-5. Biologically active compounds containing isopropyl moiety



Scheme 3-6. Synthesis of β^3 -amino acids and alcohols

Asymmetric hydroformylation of 1, 1-disubstituted allylphthalimides allows the asymmetric synthesis of β^3 -amino acid from allylic compounds using three consecutive catalytic transformations. The subsequent oxidation and reduction of *N*-phthalimide-protected β^3 -aminoaldehyde did not affect the stereochemistry. *N*-phthalimide-protected β^3 -amino acid **4** was obtained by flash chromatography after treatment of **2d** with NaClO_2 . Reduction of aldehyde **2d** provided β^3 -amino alcohol **5** with 95% ee (Scheme 3-6).

3.3 Conclusion

In summary, we have demonstrated that the high efficient Rh-catalyzed asymmetric hydroformylation of 1, 1-disubstituted allylphthalimides. A variety of aliphatic allylic substrates have been successfully investigated under optimized conditions with up to 95% ee and 100% conversion. This asymmetric transformation provides an alternative route to current methods to prepare chiral β^3 -aminoaldehydes, acids and alcohols.

3.4 Experiment Section

3.4.1 General Remarks

All reagents were received from commercial source and used without further purification. All of the reactions were carried out in the nitrogen-filled glovebox. Purifications of the ligands were carried out by flash chromatography using silica gel. ^1H NMR, ^{13}C NMR and ^{31}P NMR spectra were recorded on a Bruker Avance (400 MHz) spectrometer with CDCl_3 as the solvent and tetramethylsilane (TMS) as the internal standard. Chemical shifts are reported in parts per million (ppm, δ scale) downfield from TMS at 0.00 ppm and referenced to the CDCl_3 at 7.26 ppm (for ^1H NMR) or 77.16 ppm (for deuteriochloroform). GC analysis was carried out on Agilent gas chromatography using chiral capillary columns. HPLC analysis was carried out on Agilent 1200 series. New compounds were further characterized by high resolution mass spectra (HRMS) on a Waters Q-ToF Ultima mass spectrometer with an electrospray ionization source (University of Illinois, SCS, Mass Spectrometry Lab). Optical rotations $[\alpha]_D$ were measured on a JASCO P-2000 polarimeter.

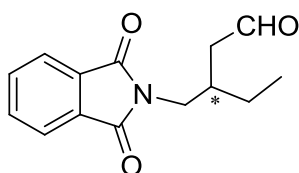
3.4.2 General Procedure for the Synthesis of Substrates 1a-1i

To a suspension of phthalimide (4.41 g, 30 mmol), triphenylphosphine (7.86 g, 30 mmol) and allyl alcohol (30 mmol) was added dropwise diethyl azodicarboxylate (4.72 mL, 30 mmol) at 0 °C. The reaction mixture was allowed to warm to room temperature and stirred for 18 h. The solvent was evaporated, and the residue was slurried in diethyl ether. The solids were removed by filtered and washed with ether, and the filtrate was evaporated. The residue was purified by silica gel chromatography to give the corresponding allyl phthalimide in about 75-85% yield.

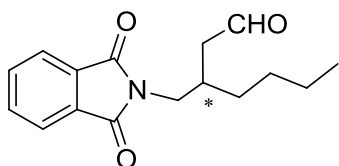
3.4.3 General Procedure for the Asymmetric Hydroformylation of Allylphthalimides.

In a glovebox filled with nitrogen, ligand L (0.005 mmol) and [Rh(acac)(CO)₂] (0.001 mmol in 0.2 mL toluene) were added to a 2 mL vial. After stirring for 10 minutes, the substrate (0.05 mmol) and additional solvent were added to bring the total volume of the reaction mixture to 1.0 mL. The vial was transferred into an autoclave and taken out of the glovebox. Carbon monoxide and hydrogen were added sequentially. The reaction mixture was stirred at 90 °C for 20 hours. The reaction was cooled and the pressure was carefully released in a well-ventilated fume hood. The conversion of this reaction was determined by ¹H NMR spectroscopy from the crude reaction mixture. The enantiomeric excess was determined by reducing the aldehyde to the corresponding alcohol with NaBH(OAc)₃. The crude reaction mixture was purified by column chromatography on silic gel (R_f = 0.3 in hexane/EtOAc = 3/2), followed by HPLC analysis.

3-ethyl-4-(1,3-dioxoisindolin-2-yl)butanal (2a)

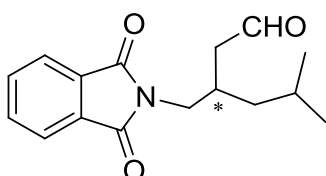


^1H NMR (CDCl_3 , TMS, 400 MHz) δ : 9.63 (s, 1H), 7.72-7.61 (m, 4H), 3.62-3.48 (m, 2H), 2.37-2.31 (m, 3H), 1.41-1.23 (m, 2H), 0.87 (t, $J = 7.4$ Hz, 3H); ^{13}C NMR (CDCl_3 , TMS, 100 MHz) δ : 201.40, 168.48, 133.96, 131.82, 123.15, 46.03, 41.31, 33.99, 24.98, 10.88.



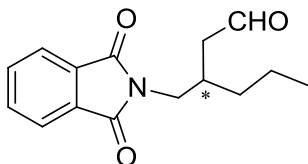
3-butyl-4-(1,3-dioxoisindolin-2-yl)butanal (2b)

^1H NMR (CDCl_3 , TMS, 400 MHz) δ : 9.73 (s, 1H), 7.85-7.71 (m, 4H), 3.70-3.59 (m, 2H), 2.51-2.40 (m, 3H), 1.40-1.35 (m, 6H), 0.89 (t, $J = 4$ Hz, 3H); ^{13}C NMR (CDCl_3 , TMS, 100 MHz) δ : 201.33, 168.53, 133.98, 131.91, 123.22, 46.62, 41.74, 32.63, 32.08, 28.72, 22.67, 13.87.



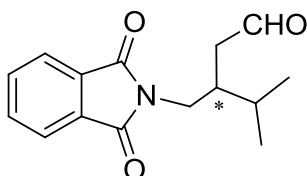
3-isobutyl-4-(1,3-dioxoisindolin-2-yl)butanal (2c)

^1H NMR (CDCl_3 , TMS, 400 MHz) δ : 9.72 (s, 1H), 7.84-7.72 (m, 4H), 3.73-3.57 (m, 2H), 2.60-2.35 (m, 3H), 1.79-1.69 (m, 1H), 1.32-1.16 (m, 2H), 0.97-0.96 (d, $J = 6.6$ Hz, 3H), 0.91-0.89 (d, $J = 6.6$ Hz, 3H); ^{13}C NMR (CDCl_3 , TMS, 100 MHz) δ : 201.26, 168.54, 133.97, 131.90, 123.21, 47.04, 41.91, 41.83, 30.58, 25.26, 22.58, 22.51.



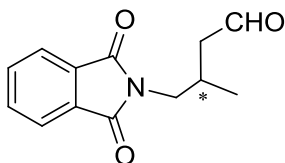
3-propyl-4-(1,3-dioxisoindolin-2-yl)butanal (2d)

^1H NMR (CDCl_3 , TMS, 400 MHz) δ : 9.73(s, 1H), 7.85-7.71 (m, 4H), 3.74-3.59 (m, 2H), 2.54-2.40 (m, 3H), 1.46-1.26 (m, 4H), 0.93 (t, $J = 7.0$ Hz, 3H); ^{13}C NMR (CDCl_3 , TMS, 100 MHz) δ : 201.35, 168.59, 134.01, 131.95, 123.28, 46.65, 41.77, 34.62, 32.48, 19.79, 14.06.



3-isopropyl-4-(1,3-dioxisoindolin-2-yl)butanal (2e)

^1H NMR (CDCl_3 , TMS, 400 MHz) δ : 9.69 (s, 1H), 7.82-7.71 (m, 4H), 3.73-3.58 (m, 2H), 2.53-2.38 (m, 3H), 1.85-1.77 (m, 1H), 0.99-0.96 (dd, $J = 5.2, 6.9$ Hz, 6H); ^{13}C



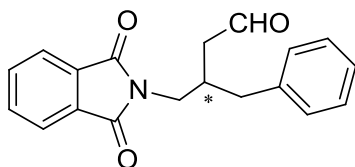
NMR (CDCl_3 , TMS, 100 MHz) δ : 201.38, 168.35, 133.89, 131.86, 123.09, 43.64, 40.63, 37.50, 29.22, 19.54, 18.32.

3-methyl-4-(1,3-dioxisoindolin-2-yl)butanal (2f)

^1H NMR (CDCl_3 , TMS, 400 MHz) δ : 9.74 (s, 1H), 7.84-7.73 (m, 4H), 3.62-3.61 (d, J

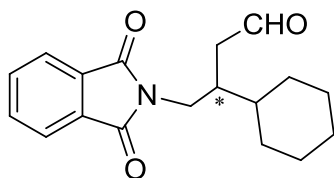
= 6.8 Hz, 2H), 2.62-2.52 (m, 2H), 2.38-2.32 (m, 1H), 1.03-1.03 (d, J = 6.8 Hz, 3H);

^{13}C NMR (CDCl_3 , TMS, 100 MHz) δ : 200.99, 168.37, 133.96, 131.83, 123.16, 48.35, 43.19, 27.82, 17.88.



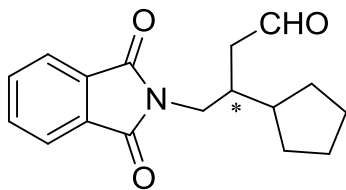
3-benzyl-4-(1,3-dioxoisindolin-2-yl)butanal (2g)

^1H NMR (CDCl_3 , TMS, 400 MHz) δ : 9.59 (s, 1H), 7.80-7.66 (m, 4H), 7.25-7.11 (m, 5H), 3.73-3.68 (m, 2H), 2.90-2.88 (m, 1H), 2.81-2.58 (m, 2H), 2.44-2.41 (m, 2H); ^{13}C NMR (CDCl_3 , TMS, 100 MHz) δ : 200.82, 168.49, 138.70, 133.98, 131.89, 129.02, 128.49, 126.40, 123.22, 45.91, 41.93, 38.78, 34.13.



3-cyclohexyl-4-(1,3-dioxoisindolin-2-yl)butanal (2h)

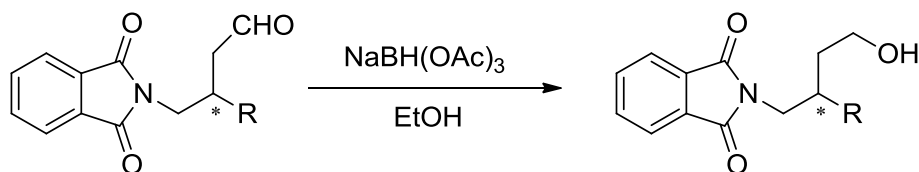
^1H NMR (CDCl_3 , TMS, 400 MHz) δ : 9.67 (s, 1H), 7.85-7.70 (m, 4H), 4.01-3.95 (m, 1H), 3.78-3.65 (m, 1H), 2.91-2.84 (m, 1H), 1.80-1.60 (m, 6H), 1.38-1.29 (m, 2H), 1.28-1.08 (m, 4H), 0.92-0.83 (m, 1H); ^{13}C NMR (CDCl_3 , TMS, 100 MHz) δ : 202.73, 168.11, 134.11, 131.87, 123.40, 48.89, 37.41, 35.13, 34.75, 33.48, 33.01, 26.33, 26.10, 26.04.



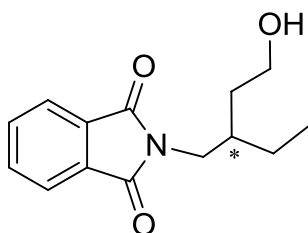
3-cyclopentyl-4-(1,3-dioxoisindolin-2-yl)butanal (2i)

^1H NMR (CDCl_3 , TMS, 400 MHz) δ : 9.70 (s, 1H), 7.84-7.71 (m, 4H), 3.78-3.63 (m, 2H), 2.51-2.45 (m, 2H), 1.96-1.52 (m, 10H); ^{13}C NMR (CDCl_3 , TMS, 100 MHz) δ : 201.48, 168.56, 133.95, 131.91, 123.19, 45.60, 42.55, 41.46, 37.51, 30.50, 30.31, 25.32, 25.15.

Conversions of amino aldehydes to amino alcohols

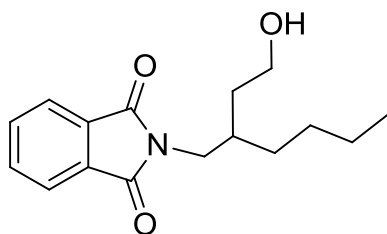


To a solution of the corresponding aldehyde (0.01mmol) in EtOH at rt, sodium triacetoxyborohydride (0.05mmol) was added. After reflux overnight, the reaction was quenched with aq. saturated solution of ammonium chloride and extracted with ethyl acetate. The organic layers were dried over Na_2SO_4 , the solvent was removed in vacuum and the residue was purified by flash column chromatography (R_f = 0.15 in hexane/EtOAc = 3/2).



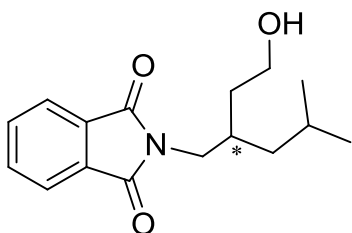
2-(2-ethyl-4-hydroxybutyl)-phthalimide

$[\alpha]_D^{25} = -17.4$ (c 0.80, CHCl_3); ^1H NMR (CDCl_3 , TMS, 400 MHz) δ : 7.54-7.27 (m, 4H), 3.76-3.60 (m, 2H), 3.45-3.28 (m, 2H), 1.64-1.50 (m, 3H), 1.41-1.37 (m, 2H), 0.93 (t, $J = 7.5$ Hz, 3H); ^{13}C NMR (CDCl_3 , TMS, 100 MHz) δ : 170.26, 139.40, 135.94, 130.89, 130.59, 128.10, 127.94, 64.37, 60.52, 43.41, 37.34, 25.42, 11.17 ; ESI-MS : m/z : calcd. for $\text{C}_{14}\text{H}_{17}\text{NO}_3$ found $[\text{M}+\text{H}]^+$ 248.29; found: 248.35. The product was analyzed by HPLC to determine the enantiomeric excess: 90% ee (Chiralcel AD-H, *i*-propanol/hexane = 10/90, flow rate 1.0 mL/min, $\lambda = 254$ nm); $t_r = 14.87$ and 17.22 min.



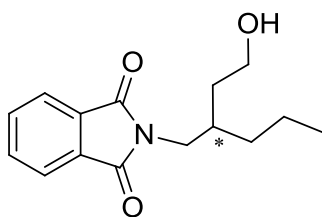
2-(2-butyl-4-hydroxybutyl)-phthalimide

$[\alpha]_D^{25} = -38.5$ (c 0.97, CHCl_3); ^1H NMR (CDCl_3 , TMS, 400 MHz) δ : 7.85-7.70 (m, 4H), 3.77-3.64 (m, 4H), 2.04-1.99 (m, 2H), 1.63-1.54 (m, 1H), 1.39-1.26 (m, 6H), 0.88 (t, $J = 7.1$ Hz, 3H); ^{13}C NMR (CDCl_3 , TMS, 100 MHz) δ : 168.83, 133.92, 132.05, 123.22, 60.63, 42.08, 34.79, 34.33, 31.6, 28.58, 25.31, 22.87, 13.94; ESI-MS: m/z : calcd. for $\text{C}_{16}\text{H}_{20}\text{NO}_3$ found $[\text{M}+\text{H}]^+$ 276.34; found: 276.31. The product was analyzed by HPLC to determine the enantiomeric excess: 77% ee (Chiralcel AD-H, *i*-propanol/hexane = 2/98, flow rate 1.0 mL/min, $\lambda = 254$ nm); $t_r = 93.70$ and 108.38 min.



2-(2-isobutyl-4-hydroxybutyl)-phthalimide

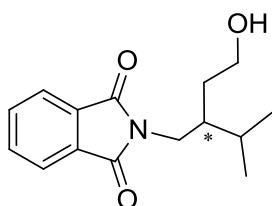
$[\alpha]_D^{25} = +1.87$ (c 0.19, CHCl_3); ^1H NMR (CDCl_3 , TMS, 400 MHz) δ : 7.78-7.63 (m, 4H), 3.73-3.56 (m, 4H), 2.02-1.96 (m, 1H), 1.68-1.46 (m, 2H), 1.18-1.11 (m, 2H), 0.86-0.78 (dd, $J = 23.8, 6.6$ Hz, 6H); ^{13}C NMR (CDCl_3 , TMS, 100 MHz) δ : 167.89, 132.95, 131.05, 122.25, 59.59, 41.39, 40.83, 33.79, 31.78, 24.38, 21.83, 21.62; ESI-MS: m/z : calcd. for $\text{C}_{16}\text{H}_{20}\text{NO}_3$ found $[\text{M}+\text{H}]^+$ 276.34; found: 276.26. The product was analyzed by HPLC to determine the enantiomeric excess: 55% ee (Chiralcel AD-H, *i*-propanol/hexane = 10/90, flow rate 1.0 mL/min, $\lambda = 254$ nm); $t_r = 14.48$ and 16.20 min.



2-(2-propyl-4-hydroxybutyl)-phthalimide

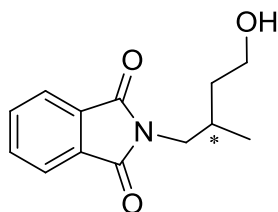
$[\alpha]_D^{25} = -12.6$ (c 0.56, CHCl_3); ^1H NMR (CDCl_3 , TMS, 400 MHz) δ : 7.85-7.71 (m, 4H), 3.81-3.63 (m, 4H), 2.04-1.98 (m, 1H), 1.61-1.54 (m, 1H), 1.45-1.29 (m, 5H), 0.90 (t, $J = 7.0$ Hz, 3H); ^{13}C NMR (CDCl_3 , TMS, 100 MHz) δ : 168.86, 134.03, 133.95, 132.05, 123.31, 123.25, 60.71, 42.04, 34.27, 32.49, 29.68, 19.61, 14.27; ESI-

MS: m/z : calcd. for $C_{15}H_{18}NO_3$ found $[M+H]^+$ 262.32; found: 262.30. The product was analyzed by HPLC to determine the enantiomeric excess: 75% ee (Chiralcel AD-H, *i*-propanol/hexane = 10/90, flow rate 1.0 mL/min, λ = 254 nm); t_r = 16.56 and 19.53 min.



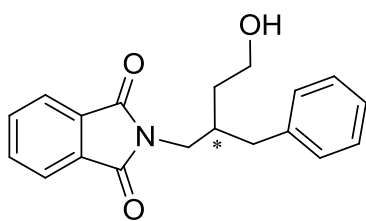
2-(2-isopropyl-4-hydroxybutyl)-phthalimide

$[\alpha]_D^{25}$ = -33.13 (c 0.71, $CHCl_3$); 1H NMR ($CDCl_3$, TMS, 400 MHz) δ : 7.75-7.62 (m, 4H), 3.68-3.45 (m, 4H), 1.84-1.79 (m, 1H), 1.69-1.53 (m, 2H), 1.39-1.30 (m, 1H), 0.92-0.83 (dd, J = 15.8, 6.8 Hz, 6H); ^{13}C NMR ($CDCl_3$, TMS, 100 MHz) δ : 168.81, 133.92, 132.05, 123.20, 61.31, 40.02, 39.79, 30.89, 28.37, 19.52, 17.79; ESI-MS: m/z : calcd. for $C_{15}H_{18}NO_3$ found $[M+H]^+$ 262.32; found: 262.27. The product was analyzed by HPLC to determine the enantiomeric excess: 95% ee (Chiralcel AD-H, *i*-propanol/hexane = 10/90, flow rate 1.0 mL/min, λ = 254 nm); t_r = 15.71 and 17.91 min.



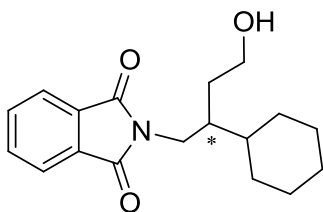
2-(2-methyl-4-hydroxybutyl)-phthalimide

$[\alpha]_D^{25} = +10.3$ (c 0.09, CHCl_3); ^1H NMR (CDCl_3 , TMS, 400 MHz) δ : 7.85-7.71 (m, 4H), 3.81-3.54 (m, 4H), 2.18-2.12 (m, 1H), 1.51-1.44 (m, 1H), 1.26-1.25 (m, 2H), 0.98-0.96 (d, $J = 6.8$ Hz, 3H); ^{13}C NMR (CDCl_3 , TMS, 100 MHz) δ : 220.12, 173.06, 139.23, 137.22, 131.60, 129.52, 128.68, 128.55, 127.20, 127.17, 72.98, 66.01, 65.06, 52.31, 37.70, 32.30, 18.54; ESI-MS: m/z : calcd. for $\text{C}_{13}\text{H}_{14}\text{NO}_3$ found $[\text{M}+\text{H}]^+$ 234.26; found: 234.27. The product was analyzed by HPLC to determine the enantiomeric excess: 90% ee (Chiralcel AD-H, *i*-propanol/hexane = 5/95, flow rate 1.0 mL/min, $\lambda = 254$ nm); $t_r = 18.46$ and 21.51 min.



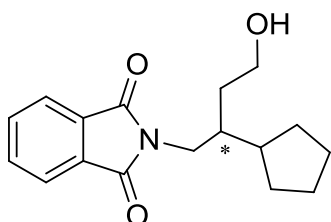
2-(2-benzyl-4-hydroxybutyl)-phthalimide

$[\alpha]_D^{25} = -18.3$ (c 0.46, CHCl_3); ^1H NMR (CDCl_3 , TMS, 400 MHz) δ : 7.81-7.68 (m, 4H), 7.21-7.05 (m, 5H), 3.78-3.66 (m, 4H), 2.73-2.58 (m, 2H), 2.53-2.42 (m, 1H), 1.66-1.53 (m, 2H); ^{13}C NMR (CDCl_3 , TMS, 100 MHz) δ : 168.74, 139.61, 133.88, 131.98, 128.86, 128.30, 125.97, 123.17, 60.62, 42.30, 39.07, 36.01, 34.46, 29.68; ESI-MS: m/z : calcd. for $\text{C}_{19}\text{H}_{18}\text{NO}_3$ found $[\text{M}+\text{H}]^+$ 310.36; found: 310.29. The product was analyzed by HPLC to determine the enantiomeric excess: 90% ee (Chiralcel AD-H, *i*-propanol/hexane = 10/90, flow rate 1.0 mL/min, $\lambda = 254$ nm); $t_r = 26.05$ and 30.05 min.



2-(2-cyclohexyl-4-hydroxybutyl)-phthalimide

$[\alpha]_D^{25} = -10.14$ (c 1.44, CHCl_3); ^1H NMR (CDCl_3 , TMS, 400 MHz) δ : 7.78-7.63 (m, 4H), 3.70-3.49 (m, 4H), 1.80-1.56 (m, 6H), 1.51-1.48 (m, 1H), 1.40-1.38 (m, 2H), 1.36-1.16 (m, 5H); ^{13}C NMR (CDCl_3 , TMS, 100 MHz) δ : 167.83, 132.92, 131.10, 122.23, 38.87, 38.72, 38.26, 30.53, 29.00, 27.64, 25.74, 25.68, 25.64; ESI-MS: m/z : calcd. for $\text{C}_{18}\text{H}_{22}\text{NO}_3$ found $[\text{M}+\text{H}]^+$ 302.37; found: 302.28. The product was analyzed by HPLC to determine the enantiomeric excess: 90% ee (Chiralcel AS-H, *i*-propanol/hexane = 10/90, flow rate 1.0 mL/min, λ = 254 nm); t_r = 17.27 and 19.83 min.

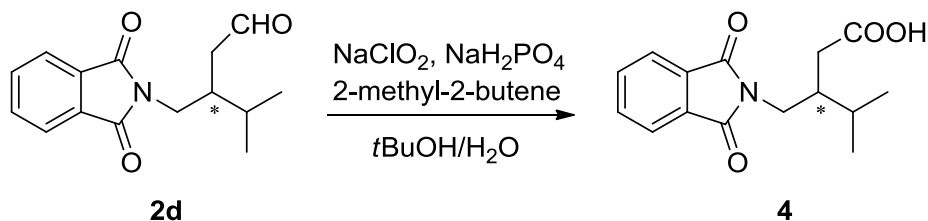


2-(2-cyclopentyl-4-hydroxybutyl)-phthalimide

$[\alpha]_D^{25} = +1.23$ (c 1.22, CHCl_3); ^1H NMR (CDCl_3 , TMS, 400 MHz) δ : 7.85-7.71 (m, 4H), 3.85-3.71 (m, 4H), 1.92-1.51 (m, 5H), 1.35-1.24 (m, 7H); ^{13}C NMR (CDCl_3 , TMS, 100 MHz) δ : 168.97, 133.97, 132.07, 123.26, 61.01, 42.02, 41.40, 39.68, 32.53, 30.38, 29.73, 25.51, 25.342; ESI-MS: m/z : calcd. for $\text{C}_{17}\text{H}_{20}\text{NO}_3$ found $[\text{M}+\text{H}]^+$ 288.35; found: 288.32. The product was analyzed by HPLC to determine the enantiomeric excess: 90% ee (Chiralcel AS-H, *i*-propanol/hexane = 10/90, flow rate

1.0 mL/min, $\lambda = 254$ nm); $t_r = 21.74$ and 78.26 min.

Conversions of amino aldehydes to amino acid (compound **4**)



To a stirred solution of **2d** (2.0 mmol) in tert-butyl alcohol/water (5:1, 10 mL) were added successively $\text{NaH}_2\text{PO}_4 \cdot 2\text{H}_2\text{O}$ (3.4 mmol), 2-methyl-2-butene (14.0 mmol), and NaClO_2 (7.0 mmol). The resulting mixture was stirred for 5 h. The solvent was removed under reduced pressure. The residue was extracted with ethyl acetate, washed with water and brine, and dried over MgSO_4 . The combined organic layers were concentrated under reduced pressure to give **4** as viscous oil. $[\alpha]_D^{25} = -5.9$ (c 0.78, CHCl_3); ^1H NMR (CDCl_3 , TMS, 400 MHz) δ : 9.71 (br, 1H), 7.74–7.61 (m, 4H), 3.57 (m, 2H), 2.24–2.17 (m, 3H), 1.71 (m, 1H), 0.89 (d, 6H); ^{13}C NMR (CDCl_3 , TMS, 100 MHz) δ : 178.45, 168.53, 133.88, 131.93, 123.20, 39.84, 39.75, 33.97, 29.21, 19.13, 18.48; ESI-MS : m/z : calcd. for $\text{C}_{15}\text{H}_{17}\text{NO}_4$ found $[\text{M}+\text{H}]^+$ 276.12; found: 276.15. The product was analyzed by HPLC to determine the enantiomeric excess: 95% ee (Chiralcel OJ-H, *i*-propanol/hexane = 10/90, flow rate 1.0 mL/min, $\lambda = 254$ nm); $t_r = 10.49$ and 12.89 min.

Reference

- For reviews, see: a) K. Nozaki, I. Ojima, in: *Catalytic Asymmetric Synthesis*, 2nd edn., (Ed.: I. Ojima), WileyVCH, New York, **2000**, chap. 7; b) R. Franke, D. Selent, A. Boerner, *Chem. Rev.* **2012**, *112*, 5675, and references cited

therein.

2. For selective ligands used in AHF reactions, see: a) N. Sakai, S. Mano, K. Nozaki, H. Takaya, *J. Am. Chem. Soc.* **1993**, *115*, 7033; b) J. E. Babin, G. T. Whiteker, (Union Carbide Corporation), Patent WO 9303839, **1993**; c) S. Breeden, D. J. Cole-Hamilton, D. F. Foster, G. J. Schwarz, M. Wills, *Angew. Chem.* **2000**, *112*, 4272; *Angew. Chem. Int. Ed.* **2000**, *39*, 4106; d) C. J. Cobley, K. Gardner, J. Klosin, C. Praquin, C. Hill, G. T. Whiteker, A. Zanotti-Gerosa, J. L. Petersen, K. A. Abboud, *J. Org. Chem.* **2004**, *69*, 4031; e) C. J. Cobley, J. Klosin, C. Qin, G. T. Whiteker, *Org. Lett.* **2004**, *6*, 3277; f) T. P. Clark, C. R. Landis, S. L. Freed, J. Klosin, K. Abboud, *J. Am. Chem. Soc.* **2005**, *127*, 5040; g) A. T. Axtell, C. J. Cobley, J. Klosin, G. T. Whiteker, A. Zanotti-Gerosa, K. A. Abboud, *Angew. Chem.* **2005**, *117*, 5984; *Angew. Chem. Int. Ed.* **2005**, *44*, 5834; h) B. Zhao, X. Peng, Z. Wang, C. Xia, K. Ding, *Chem. Eur. J.* **2008**, *14*, 7847; i) Y. Yan, X. Zhang, *J. Am. Chem. Soc.* **2006**, *128*, 7198; j) X. Zhang, B. Cao, Y. Yan, S. Yu, B. Ji, X. Zhang, *Chem. Eur. J.* **2010**, *16*, 871; k) X. Zhang, B. Cao, S. Yu, X. Zhang, *Angew. Chem.* **2010**, *122*, 4141; *Angew. Chem. Int. Ed.* **2010**, *49*, 4047; l) G. M. Noonan, J. A. Fuentes, C. J. Cobley, M. L. Clarke, *Angew. Chem.* **2012**, *124*, 2527; *Angew. Chem. Int. Ed.* **2012**, *51*, 2477.
3. a) K. Nozaki, N. Sakai, T. Nanno, T. Higashijima, S. Mano, T. Horiuchi, H. Takaya, *J. Am. Chem. Soc.* **1997**, *119*, 4413; b) K. Nozaki, Y. Ito, F. Shibahara, E. Shirakawa, T. Otha, H. Takaya, T. Hiyama, *J. Am. Chem. Soc.* **1998**, *120*, 4051; c) J. Klosin, C. R. Landis, *Acc. Chem. Res.* **2007**, *40*, 1251; d) A. T. Axtell, J. Klosin, G. T. Whiteker, C. J. Cobley, M. E. Fox, M. Jackson, K. A. Abboud, *Organometallics*. **2009**, *28*, 2993; e) C. J. Cobley, K. Gardner, J.

- Klosin, C. Praquin, C. Hill, G. T. Whiteker, A. Zanotti-Gerosa, *J. Org. Chem.* **2004**, *69*, 4031; f) C. J. Cobley, R. D. J. Froese, J. Klosin, C. Qin, G. T. Whiteker, K. A. Abboud, *Organometallics*. **2007**, *26*, 2986; g) G. Erre, S. Enthaler, K. Junge, S. Gladiali, M. Beller, *J. Mol. Catal. A* **2008**, *280*, 148; h) T. Robert, J. W. Abiri, A. J. Sandee, S. Romanski, J.-M. Neudörfl, H.-G. Schmalz, J. N. H. Reek, *Organometallics*. **2010**, *29*, 478; i) J. Wassenaar, B. de Bruin, J. N. H. Reek, *Organometallics*. **2010**, *29*, 2767.
4. a) N. Sakai, K. Nozaki, T. Takaya, *J. Chem. Soc. Chem. Commun.* **1994**, 395; b) L. Kollar, E. Farkas, J. Batiu, *J. Mol. Catal. A: Chem.* **1997**, *115*, 283; c) A. L. Watkins, B. G. Hashiguchi, C. R. Landis, *Org. Lett.* **2008**, *10*, 4553; d) J. Mazuela, M. Coll, O. Pamies, M. Dieguez, *J. Org. Chem.* **2009**, *74*, 5440; e) A. D. Worthy, C. L. Joe, T. E. Lightburn, K. L. Tan, *J. Am. Chem. Soc.* **2010**, *132*, 14757; f) R. I. McDonald, G. W. Wong, R. P. Neupane, S. S. Stahl, C. R. Landis, *J. Am. Chem. Soc.* **2010**, *132*, 14027; g) S. H. Chikkali, R. Bellini, G. Berthon-Gelloz, J. I. van der Vlugt, B. de Bruin, J. N. H. Reek, *Chem. Commun.* **2010**, *46*, 1244; h) A. J. L. Clemens, S. D. Burke, *J. Org. Chem.* **2012**, *77*, 2983; i) Ojima, I.; Takai, M.; Takahashi, T. Patent WO 078766, 2004.
5. a) K. Nozaki, W.-G. Li, T. Horiuchi, H. Takaya, *Tetrahedron Lett.* **1997**, *38*, 4611; b) C. Botteghi, T. Corrias, M. Marchetti, S. Paganelli, O. Piccolo, *Org. Process Res. Dev.* **2002**, *6*, 379; c) I. Ojima, M. Takai, T. Takahashi, Patent WO 078766, **2004**; d) T. Doi, H. Komatsu, K. Yamamoto, *Tetrahedron Lett.* **1996**, *37*, 6877; e) B. Breit, *Angew. Chem.* **1996**, *108*, 3021; *Angew. Chem. Int. Ed. Engl.* **1996**, *35*, 2835; f) J. L. Leighton, D. N. O'Neil, *J. Am. Chem. Soc.* **1997**, *119*, 11118; g) I. J. Krauss, C. C.-Y. Wang, J. L. Leighton, *J. Am. Chem.*

- Soc.* **2001**, *123*, 11514; h) L. Ren, C. M. Crudden, *J. Org. Chem.* **2002**, *67*, 1746.
6. X. Wang, S. L. Buchwald, *J. Am. Chem. Soc.* **2011**, *133*, 19080.
 7. a) D. Seebach, J. Gardiner, *Acc. Chem. Res.* **2008**, *41*, 1366; b) R. P. Cheng, S. H. Gellman, W. F. DeGrado, *Chem. Rev.* **2001**, *101*, 3219.
 8. B. Weiner, A. Baeza, T. Jerphagnon, B. L. Feringa, *J. Am. Chem. Soc.* **2009**, *131*, 9473.
 9. a) J. Frackenpohl, P. Arvidsson, J. V. Schreiber, D. Seebach, *Chem. Bio. Chem.* **2001**, *2*, 445; b) M. Watanabe; K. Maemura, K. Kanbara, T. Tamayama, H. Hayasaki, *Int. Rev. Cytol.* **2002**, *213*, 1.
 10. M. S. Hoekstra, D. M. Sobieray, M. A. Schwindt, et al. *Org. Process Res. Dev.* **1997**, *1*, 26.
 11. a) A. I. M. Keuelemans, A. Kwantes, T. van Bavel, *Recl. Trav. Chim. Pays-Bas*, **1948**, *67*, 298; b) M. L. Clarke, G. J. Roff, *Chem. Eur. J.* **2006**, *12*, 7978; c) M. Uhlemann; A. Bärner, *ChemCatChem.* **2012**, *4*, 753.
 12. For QuinoxP*, see: T. Imamoto, K. Tamura, Z. Zhang, Y. Horiuchi, M. Sugiya, K. Yoshida, A. Yanagisawa, I. D. Gridnev, *J. Am. Chem. Soc.* **2012**, *134*, 1754, and references cited therein. For (Rp,Sc)-DuanPhos, see: H. Geng, K. Huang, T. Sun, W. Li, X. Zhang, L. Zou, W. Wu, X. Zhang, *J. Org. Chem.* **2011**, *76*, 332, and references cited therein. For ZhangPhos, see: K. Huang, X. Zhang, H. Geng, S. Li, X. Zhang, *ACS Catal.* **2012**, *2*, 1343, and references cited therein. For Et-DuPhos, see: M. J. Burk, C. S. Kalbery, A. Pizzano, *J. Am. Chem. Soc.* **1998**, *120*, 4345, and references cited therein. For TangPhos. see: J. Chen, Q. Liu, W. Zhang, S. Spinella, A. Lei, X. Zhang, *Org. Lett.* **2008**, *10*, 3033, and references cited therein. For C₃-TunePhos, see: Q. Yang, W. Gao, J. Deng, X.

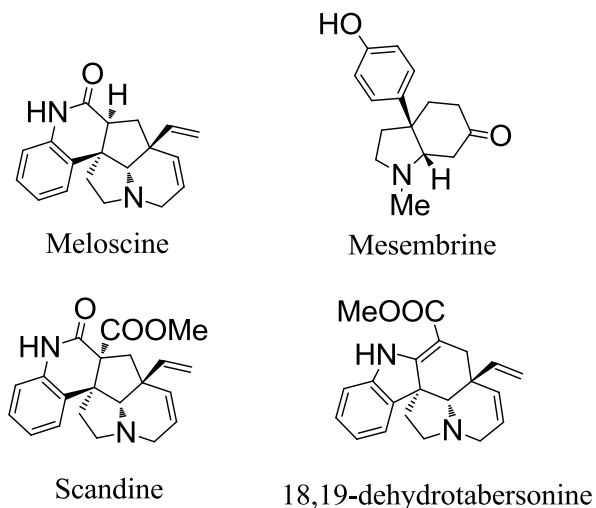
- Zhang, *Tetrahedron Lett.* **2006**, 47, 81, and references cited therein. For f-Binaphane, see: M. Chang, W. Li, X. Zhang, *Angew. Chem.* **2011**, 123, 10867; *Angew. Chem. Int. Ed.* **2011**, 50, 10679 and references cited therein. For (S,S)-Ph-BPE, see: M. Iwata, R. Yazaki, I. H. Chen, D. Sureshkumar, N. Kumagai, M. Shibasaki, *J. Am. Chem. Soc.* **2011**, 133, 5554, and references cited therein.
13. L. C. Blumberg, M. F. Brown, M. J. Munchhof, L. A. Reiter, Patent WO 004038, **2007**.

Chapter 4

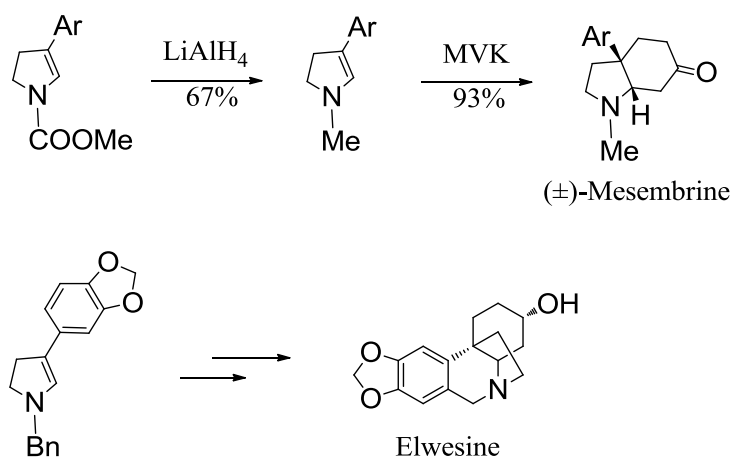
Synthesis of 4-Aryl-2,3-Dihydropyrrole Derivatives by Rh-Catalyzed Intramolecular Hydroaminomethylation Reaction

4.1 Introduction

N-Heterocyclic moieties are universal skeletons in biologically and physiologically active alkaloids¹ (Scheme 4-1). 4-aryl-2,3-dihydropyrrole derivatives are the key intermediates in the synthesis of (±)-Mesembrine,² Elwesine³ and other bioactive alkaloids (Scheme 4-2). Numerous organic methodologies have been reported in the past decades. Most of them involved multisteps with low yields. None of them could establish 4-aryl-2,3-dihydropyrroles only in one step.⁴ Long reaction procedures limited the application of these valuable building blocks in total synthesis.



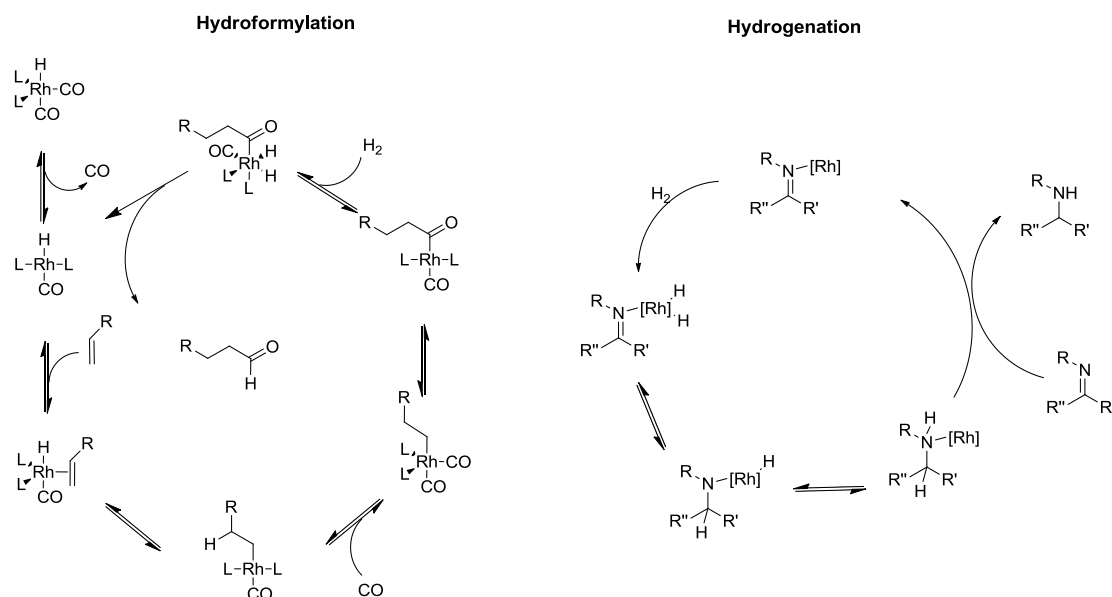
Scheme 4-1. Structures of biologically active alkaloids with pyrrolidine moieties



Scheme 4-2. Transformation of 3-aryl dihydropyrrole into bioactive alkaloids

Hydroaminomethylation is a one-pot tandem reaction, which is superior methodology over conventional ones from economical and environmental aspects.⁵ It was first discovered by Reppe that carbon monoxide reacted with acetylenic compounds in the presence of ammonia and water. And then, transition metals were applied in the catalytic process, such as manganese, cobalt, nickel. Recently, rhodium, ruthenium and iridium precursors have also been employed to provide interesting performance under milder reaction conditions.

The reaction mechanism is the first step of hydroformylation of the olefins, which is already well-established and has been described in Chapter 1. As soon as the aldehydes are produced, they react with the primary or secondary amine to generate the corresponding imine or enamine with the loss of water. The hydrogenation of the enamine or imine takes place on Rh center, and then oxidative addition of dihydrogen, hydride transfer generating an alkyl moiety. The last step is reductive elimination leading to the final product amine (Scheme 4-3). Generally, the electron-donating substituted olefins generate more quantities of the linear aldehydes; while the electron-withdrawing olefins prefer branched products. It has also been observed that the linear aldehydes react faster than the branched ones with amine.



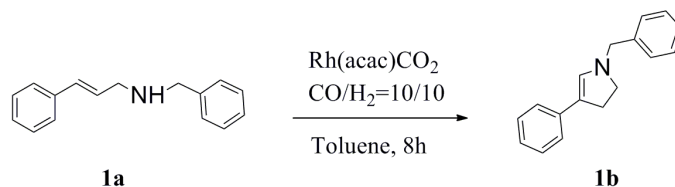
Scheme 4-3. General catalytic cycle for hydroaminomethylation

Intramolecular hydroaminomethylation can be used to synthesize cyclic amine. The intramolecular hydroaminomethylation of 2-isopropenylanilines access to 1,2,3,4-tetrahydroquinolines, which are of great interest for the preparation of pharmaceuticals and agrochemicals. The seven-membered-ring 2-benzazepines and 1-benzazepines, which have proven to be interesting for their biological activity, can be also synthesized by this reaction. Furthermore, hydroaminomethylation of the substituted cinnamylamine is a remarkable method to access dihydropyrrole derivatives only in one step. Busacca and coworkers have reported a facile synthesis of 4-aryl-2,3-dihydropyrroles via hydroformylation of *N*-allylsulfonamides. However, the limitations of this methodology are extremely slow reaction rate and quite narrow scope of substrates. Therefore, in this chapter, we disclose a more practical approach to reach this useful target compounds by rhodium-catalyzed intramolecular hydroaminomethylation.

4.2 Results and Discussion

The hydroaminomethylation of (E)-*N*-benylcinnamylamine **1a** was initially investigated as a model reaction catalyzed by rhodium complexes bearing representative bidentate or monodentate phosphorous ligands. When **1a** was catalyzed by Xantphos at 80 °C, only 1% expected product **2a** was yielded (Table 4-1, entry 1). Other two bidentate ligands Bisbi and dppb also displayed poor reactivities (Table 4-1, entries 2 and 3). In order to improving the yield, several monodentate phosphorous ligands were chosen for this reaction. No desired product was detected when carrying out with P(OPh)₃ ligand. A remarkable improvement of the yield to 83% was observed by employing PPh₃ as ligand (Table 4-1, entry 6). Further changing PPh₃/Rh(acac)CO₂ ratio (L/Rh) to either 15 or 5 cannot improve the reaction yield (Table 4-1, entries 7 and 8).

Table 4-1. Rh-catalyzed hydroaminomethylation of **1a** with different ligands^a



Entry	Ligand	L/Rh	Yield ^b (%)
1	Xantphos	10	1
2	Bisbi	10	57
3	dppb	10	3
4	P(OPh) ₃	10	NR
5	P(<i>o</i> -toyl) ₃	10	11
6	PPh ₃	10	83

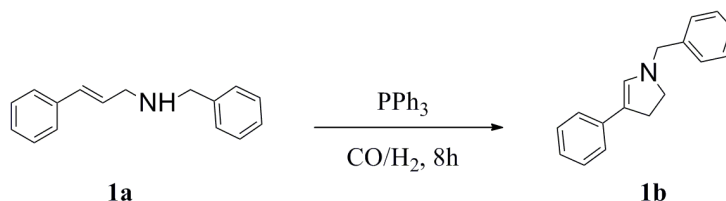
7	PPh ₃	5	78
8	PPh ₃	15	67

^a Reaction conditions: **1a** (1mmol), Rh(acac)CO₂ (0.2 mol%), ligand (2 mol%), total 0.5 mL in toluene at 80 °C for 8 h.

^b Isolated yield.

Solvent, as a crucial factor for hydroaminomethylation, was also screened. The results were summarized in Table 4-2. Toluene was finally chosen as the best solvent (Table 4-2, entry 1). On the basis of these results, different H₂/CO pressure ratios were tested. When increase the total pressure to 30 bar, the yield was slightly decreased to 81% (Table 4-2, entry 7). The similar result was obtained when the total pressure decrease to 10 bar. Under 20 bar total syngas pressure constantly, H₂/CO ratio was varied to 1/2, yielding the comparable result as ratio 1/1 (Table 4-2, entry 8). Increasing H₂ partial pressure cannot further hydrogenate dihydropyrrole to pyrrole, but led to dramatically drop yield to 68% (Table 4-2, entry 9). Herein, the 1/1 of H₂/CO ratio was the best for this reaction.

Table 4-2. Optimization of reaction conditions^a



Entry	Solvent	Temp (°C)	[Rh]	H ₂ /CO (bar)	Yield (%)
1	Toluene	80	0.002	20 (1/1)	83
2	EtOAc	80	0.002	20 (1/1)	71

3	Acetone	80	0.002	20 (1/1)	60
4	THF	80	0.002	20 (1/1)	60
5	DCM	80	0.002	20 (1/1)	5
6	Toluene	80	0.002	10 (1/1)	76
7	Toluene	80	0.002	30 (1/1)	81
8	Toluene	80	0.002	20 (1/2)	82
9	Toluene	80	0.002	20 (2/1)	68
10	Toluene	60	0.002	20 (1/1)	40
11	Toluene	80	0.002	20 (1/1)	83
12	Toluene	80	0.002	20 (1/1)	83
13 ^b	Toluene	80	0.001	20 (1/1)	99
14 ^c	Toluene	80	0.004	20 (1/1)	68

^a Reaction conditions: **1a** (1mmol), PPh₃ (2 mol%), total 0.5 mL for 8 h.

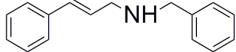
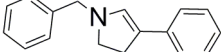
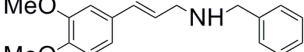
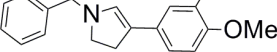
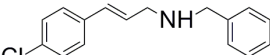
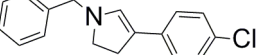
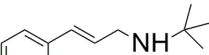
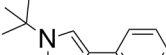
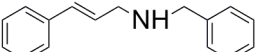
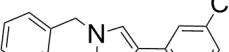
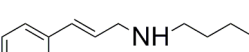
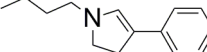
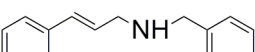
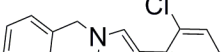
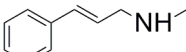
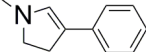
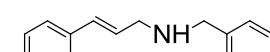
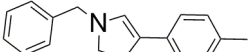
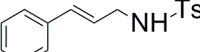
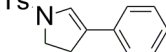
^b PPh₃ 1 mol%

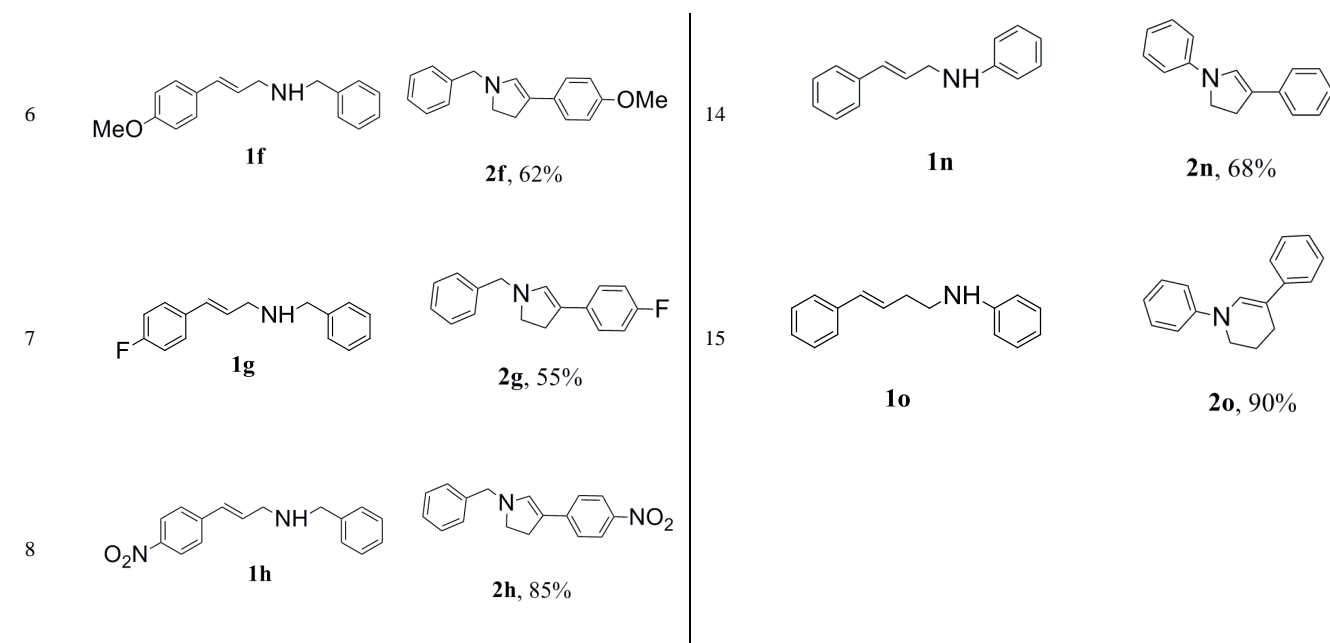
^c PPh₃ 4 mol%

Lower temperature from 80 °C to 60 °C furnished the **2a** in 40% yield (Table 4-2, entry 10). Surprisingly, decreasing Rh concentration from 0.2 mol% to 0.1 mol% considerably increased the yield to 99% (Table 4-2, entry 13). However, doubling the metal concentration led to drop of yield dramatically (Table 4-2, entry 14). Therefore, the optimal reaction condition was carried out by rhodium complex bearing PPh₃ ligand (1 mol %) in toluene at 80 °C under 10/10 of H₂/CO.

With the optimized reaction conditions in hand, a series of **1a** derivatives was successfully converted to desired 4-aryl-2,3-dihydropyrroles with moderate to excellent yields (Table 4-3). Most of electron-withdrawing substituents at the phenyl

$$\text{R}_1\text{-CH=CH-CH}_2\text{-NH-R}_2 \xrightarrow[\text{Toluene, 8h}]{\text{PPh}_3, \text{Rh(acac)CO}_2, \text{CO/H}_2=10/10} \text{R}_1\text{-CH}_2\text{-CH(R}_2\text{)-CH(R}_1\text{)-NH-R}_2$$

Entry	Substrate	Product	Entry	Substrate	Product
1	 1a	 2a , 99%	9	 1i	 2i , 52%
2	 1b	 2b , 84%	10	 1j	 2j , 83%
3	 1c	 2c , 65%	11	 1k	 2k , 92%
4	 1d	 2d , 95%	12	 1l	 2l , 88%
5	 1e	 2e , 64%	13	 1m	 2m , 86%



^a Reaction conditions: **1** (1mmol), Rh(acac)CO₂ (0.1 mol%), PPh₃ (1 mol%), CO/H₂=10/10, total 0.5 mL in toluene at 80°C for 8 h.

4.3 Conclusion

In summary, intramolecular hydroaminomethylation provides an efficient alternative approach in the synthesis of 4-aryl-2,3-dihydropyrroles in only one step with mild reaction conditions.

4.4 Experimental Section

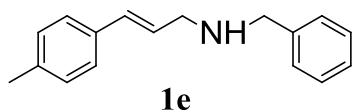
4.4.1 General Remarks

All reagents were received from commercial source and used without further purification. All of the reactions were carried out in the nitrogen-filled glovebox. Purifications of the ligands were carried out by flash chromatography using silica gel. ¹H NMR, ¹³C NMR and ³¹P NMR spectra were recorded on a Bruker Avance (400 MHz) spectrometer with CDCl₃ as the solvent and tetramethylsilane (TMS) as the internal standard. Chemical shifts are reported in parts per million (ppm, δ scale) downfield from TMS at 0.00 ppm and referenced to the CDCl₃ at 7.26 ppm (for ¹H

NMR) or 77.16 ppm (for deuteriochloroform).

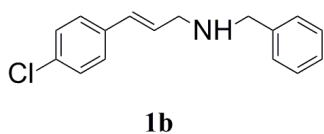
4.4.2 General procedure for hydroaminomethylation reactions

In a glovebox filled with nitrogen, to a 5 mL vial equipped with a magnetic bar was added ligand (1 mol%) and Rh(acac)(CO)₂ (0.1 mol%). After stirring for 10 min, substrate (1.0 mmol) and additional toluene was charged to bring the total volume of the reaction mixture to 0.5 mL. The vial was transferred into an autoclave and taken out of the glovebox. Carbon monoxide (10 bar) and hydrogen (10 bar) were charged in sequence. The reaction mixture was stirred at 80 °C (oil bath) for 8 h. The reaction was cooled and the pressure was carefully released in a well ventilated hood. The crude product was purified with column chromatography to yield desired product.



N-[(2E)-3-phenyl-2-propen-1-yl]-Benzenemethanamine:

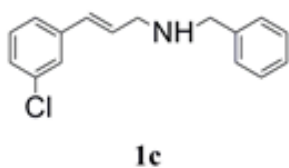
¹H NMR (400 MHz, CDCl₃): δ 7.42-7.25 (m, 10H), 7.60-7.55 (d, 1H, J=15 Hz), 6.40-6.30 (m, 1H), 3.88 (s, 2H), 3.48-3.46 (d, 2H, J=6 Hz).



N-[(2E)-3-(4-chlorophenyl)-2-propen-1-yl]-Benzenemethanamine:

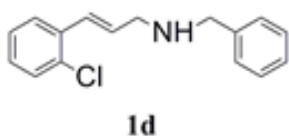
¹H NMR (400 MHz, CDCl₃): δ 7.11-7.20 (m, 9H), 6.31-6.34 (d, 1H, J=12 Hz), 6.11-6.14 (d, 1H, J=12 Hz), 3.68 (s, 2H), 3.26-3.27 (d, 2H, J=4 Hz); ¹³C NMR (100 MHz, CDCl₃) δ 139.17, 134.64, 131.81, 128.91, 128.23, 127.60, 127.37, 127.09,

126.40, 125.93, 52.33, 50.00



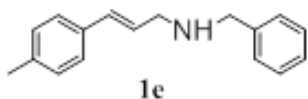
N-[(2E)-3-(3-chlorophenyl)-2-propen-1-yl]-Benzenemethanamine:

^1H NMR (400 MHz, CDCl_3): δ 7.07-7.23 (m, 9H), 6.34-6.38 (d, 1H, $J=16$ Hz), 6.18-6.22 (d, 1H, $J=16$ Hz), 3.71 (s, 2H), 3.30-3.32 (d, 2H, $J=8$ Hz); ^{13}C NMR (100 MHz, CDCl_3): δ 139.11, 138.03, 133.43, 129.10, 129.03, 128.87, 128.69, 127.41, 127.13, 126.21, 125.99, 125.19, 123.39, 52.30, 49.92



N-[(2E)-3-(2-chlorophenyl)-2-propen-1-yl]-Benzenemethanamine:

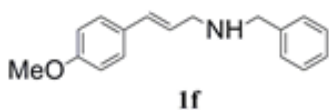
^1H NMR (400 MHz, CDCl_3): δ 7.03-7.45 (m, 9H), 6.19-6.24 (m, 2H), 3.76 (s, 2H), 3.37-3.38 (d, 2H, $J=4$ Hz); ^{13}C NMR (100 MHz, CDCl_3): δ 140.39, 135.42, 132.97, 131.69, 129.76, 128.55, 128.47, 128.35, 127.56, 127.11, 126.98, 126.96, 53.42, 51.31



N-[(2E)-3-(4-methylphenyl)-2-propen-1-yl]-Benzenemethanamine:

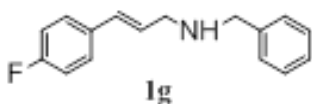
^1H NMR (400 MHz, CDCl_3): δ 7.04-7.28 (m, 9H), 6.43-6.47 (d, 1H, $J=12$ Hz), 6.20-6.24 (d, 1H, $J=16$ Hz), 3.75 (s, 2H), 3.34-3.35 (d, 2H, $J=4$ Hz); ^{13}C NMR (100 MHz, CDCl_3) δ 139.29, 135.94, 133.37, 130.20, 128.24, 128.16, 127.32, 127.10, 126.35,

125.85, 125.18, 125.14, 52.24, 50.18, 20.07



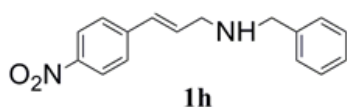
N-[(2E)-3-(4-methoxyphenyl)-2-propen-1-yl]-Benzenemethanamine:

^1H NMR (400 MHz, CDCl_3): δ 7.16-7.27 (m, 7H), 6.76-6.78 (m, 2H), 6.38-6.42 (d, 1H, $J=16$ Hz), 6.08-6.13 (m, 1H), 3.72 (s, 2H), 3.63 (s, 2H), 3.30 -3.31 (d, 2H, $J=4$ Hz); ^{13}C NMR (100 MHz, CDCl_3) δ 159.23, 140.54, 130.97, 130.13, 128.50, 128.30, 127.65, 127.56, 127.03, 126.37, 114.24, 114.14, 55.22, 53.40, 51.41



N-[(2E)-3-(4-fluorophenyl)-2-propen-1-yl]-Benzenemethanamine:

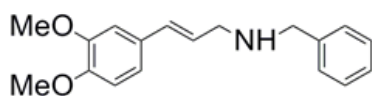
^1H NMR (400 MHz, CDCl_3): δ 7.11-7.20 (m, 9H), 6.31-6.34 (d, 1H, $J=12$ Hz), 6.11-6.14 (d, 1H, $J=12$ Hz), 3.68 (s, 2H), 3.26-3.27 (d, 2H, $J=4$ Hz); ^{13}C NMR (100 MHz, CDCl_3) δ 139.17, 134.64, 131.81, 128.91, 128.23, 127.60, 127.37, 127.09, 126.40, 125.93, 52.33, 50.73



N-[(2E)-3-(4-nitrophenyl)-2-propen-1-yl]-Benzenemethanamine:

^1H NMR (400 MHz, CDCl_3): δ 7.11-7.20 (m, 9H), 6.31-6.34 (d, 1H, $J=12$ Hz), 6.11-6.14 (d, 1H, $J=12$ Hz), 3.68 (s, 2H), 3.26-3.27 (d, 2H, $J=4$ Hz); ^{13}C NMR (100 MHz, CDCl_3) δ 139.17, 134.64, 131.81, 128.91, 128.23, 127.60, 127.37, 127.09, 126.40,

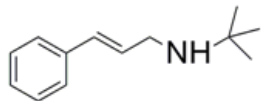
125.93, 52.33, 49.93



1i

N-[(2E)-3-(3,4-methoxyphenyl)-2-propen-1-yl]-Benzenemethanamine:

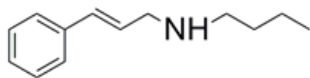
^1H NMR (400 MHz, CDCl_3): δ 7.18-7.29 (m, 5H), 6.72-6.90 (m, 3H), 6.41-6.45 (d, 1H, $J=16$ Hz), 6.16-6.19 (d, 1H, $J=12$ Hz), 3.81 (s, 2H), 3.80 (s, 3H), 3.78 (s, 3H), 3.36-3.37 (d, 2H, $J=4$ Hz); ^{13}C NMR (100 MHz, CDCl_3) δ 149.06, 148.67, 140.32, 131.01, 130.29, 128.32, 128.09, 126.86, 126.53, 119.26, 111.26, 108.85, 55.80, 55.70, 53.29, 51.21



1j

(E)-N-tButylcinnamylamine:

^1H NMR (400 MHz, CDCl_3): δ 7.17-7.35 (m, 9H), 6.48-6.52 (d, 1H, $J=16$ Hz), 6.29-6.34 (m, 1H), 3.33-3.35 (d, 2H, $J=8$ Hz), 1.14 (m, 9H); ^{13}C NMR (100 MHz, CDCl_3) δ 137.31, 130.79, 129.41, 128.48, 127.21, 126.24, 50.46, 45.16, 29.10

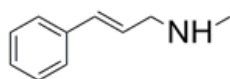


1k

(E)-N-Butylcinnamylamine:

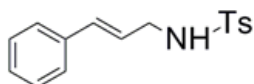
^1H NMR (400 MHz, CDCl_3): δ 7.21-7.35 (m, 9H), 6.50-6.54 (d, 1H, $J=16$ Hz), 6.28-

6.33 (d, 1H, J=20 Hz), 3.40 -3.42 (d, 2H, J=8 Hz), 2.64-2.67 (d, 2H, J=12 Hz), 1.46-1.52 (m, 2H), 1.33-1.39 (m, 2H), 0.90-0.94 (m, 3H); ^{13}C NMR (100 MHz, CDCl_3) δ 137.27, 131.13, 128.78, 128.54, 127.31, 126.28, 52.02, 49.27, 32.36, 20.53, 14.02

**1l**

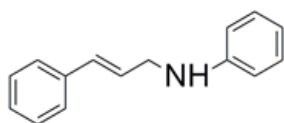
(E)-N-methylcinnamylamine:

^1H NMR (400 MHz, CDCl_3): δ 7.22-7.39 (m, 9H), 6.51-6.55 (d, 1H, J=16 Hz), 6.30-6.33 (d, 1H, J=12 Hz), 3.20 -3.22 (d, 2H, J=8 Hz), 2.30 (s, 3H); ^{13}C NMR (100 MHz, CDCl_3) δ 137.05, 132.83, 128.51, 127.44, 127.22, 126.32, 59.80, 42.14

**1m**

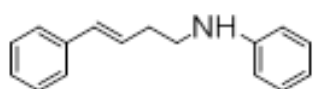
N-[(3E)-4-phenyl-3-buten-1-yl]-Benzenemethanamine:

^1H NMR (400 MHz, CDCl_3): δ 7.07-7.26 (m, 10H), 6.33-6.37 (d, 1H, J=16 Hz), 6.06-6.11 (d, 1H, J=20 Hz), 3.65(s, 2H), 2.62-2.65 (m, 2H), 2.29 -2.32 (m, 2H); ^{13}C NMR (100 MHz, CDCl_3) δ 140.40, 140.38, 137.43, 131.36, 128.37, 128.30, 128.22, 128.14, 127.98, 127.82, 127.80, 126.91, 126.85, 126.78, 126.74, 126.54, 125.94, 53.70, 48.55, 33.52

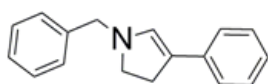
**1n**

(E)-N-phenylcinnamylamine:

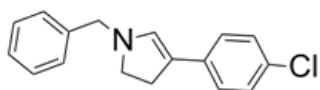
^1H NMR (400 MHz, CDCl_3): δ 7.15-7.30 (m, 7H), 6.69-6.73 (d, 1H, $J=16$ Hz), 6.58 - 6.66 (m, 3H), 6.28 - 6.32 (d, 1H, $J=16$ Hz), 3.90-3.92 (d, 2H, $J=8$ Hz); ^{13}C NMR (100 MHz, CDCl_3) δ 148.08, 136.91, 131.55, 129.27, 128.57, 127.52, 127.10, 126.34, 117.65, 113.08

**1o****N-[(3E)-4-phenyl-3-buten-1-yl]-Benzenemethanamine:**

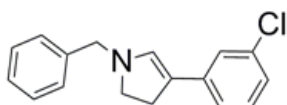
^1H NMR (400 MHz, CDCl_3): δ 7.07-7.26 (m, 10H), 6.33-6.37 (d, 1H, $J=16$ Hz), 6.06-6.11 (d, 1H, $J=20$ Hz), 3.65(s, 2H), 2.62-2.65 (m, 2H), 2.29-2.32 (m, 2H); ^{13}C NMR (100 MHz, CDCl_3) δ 140.40, 140.38, 137.43, 131.36, 128.37, 128.30, 128.22, 128.14, 127.98, 127.82, 127.80, 126.91, 126.85, 126.78, 126.74, 126.54, 125.94, 53.70, 48.55, 33.52

**2a, 99%****2,3-dihydro-4-phenyl-1-(phenylmethyl)-1H-pyrrole**

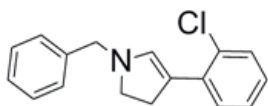
^1H NMR (400 MHz, CDCl_3): δ 7.09-7.24 (m, 10H), 6.13 (s, 1H), 3.58 (s, 2H), 3.24-3.31 (m, 2H), 2.23-2.28 (m, 2H); ^{13}C NMR (100 MHz, CDCl_3) δ 145.73, 139.37, 128.80, 128.37, 128.25, 127.90, 127.34, 126.90, 126.03, 117.08, 62.32, 54.65, 33.32

**2b**, 84%**4-(4-chlorophenyl)-2,3-dihydro-1-(phenylmethyl)-1H-pyrrole**

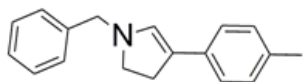
^1H NMR (400 MHz, CDCl_3): δ 7.09-7.24 (m, 9H), 6.15 (s, 1H), 4.26 (s, 2H), 3.65 (m, 2H), 2.23 (m, 2H); ^{13}C NMR (100 MHz, CDCl_3) δ 139.37, 137.12, 136.4, 128.80, 128.37, 128.25, 127.90, 127.34, 126.90, 117.08, 62.32, 54.65, 33.32

**2c**, 65%**4-(3-chlorophenyl)-2,3-dihydro-1-(phenylmethyl)-1H-pyrrole**

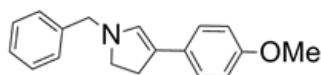
^1H NMR (400 MHz, CDCl_3): δ 7.09-7.24 (m, 9H), 6.15 (s, 1H), 4.26 (s, 2H), 3.65 (m, 2H), 2.23 (m, 2H); ^{13}C NMR (100 MHz, CDCl_3) δ 139.37, 137.12, 136.4, 134.20, 128.80, 128.37, 128.25, 127.90, 127.34, 127.12, 126.90, 117.08, 62.32, 54.65, 33.32

**2d**, 95%**4-(2-chlorophenyl)-2,3-dihydro-1-(phenylmethyl)-1H-pyrrole**

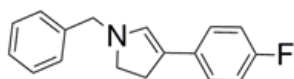
^1H NMR (400 MHz, CDCl_3): δ 7.19-7.24 (m, 9H), 6.15 (s, 1H), 4.26 (s, 2H), 3.65 (m, 2H), 2.23 (m, 2H); ^{13}C NMR (100 MHz, CDCl_3) δ 137.12, 136.4, 129.90, 129.34, 128.80, 128.37, 128.25, 127.90, 127.65, 127.34, 126.90, 118.08, 62.32, 54.65, 33.32

**2e**, 64%**4-(4-methylphenyl)-2,3-dihydro-1-(phenylmethyl)-1H-pyrrole**

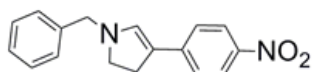
^1H NMR (400 MHz, CDCl_3): δ 7.19-7.24 (m, 5H), 7.08-6.87 (dd, 4H), 6.15 (s, 1H), 4.26 (s, 2H), 3.65 (m, 2H), 2.40 (s, 3H), 2.23 (m, 2H); ^{13}C NMR (100 MHz, CDCl_3) δ 139.37, 137.12, 136.4, 128.80, 128.37, 128.25, 127.90, 127.65, 127.34, 126.90, 117.08, 62.32, 54.65, 38.2, 21.3

**2f**, 62%**4-(4-methoxyphenyl)-2,3-dihydro-1-(phenylmethyl)-1H-pyrrole**

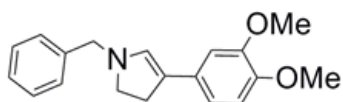
^1H NMR (400 MHz, CDCl_3): δ 7.19-7.24 (m, 5H), 7.08-6.87 (dd, 4H), 6.15 (s, 1H), 4.26 (s, 2H), 3.83 (s, 3H), 3.65 (m, 2H), 2.23 (m, 2H); ^{13}C NMR (100 MHz, CDCl_3) δ 159.37, 136.4, 131.71, 128.80, 128.37, 128.25, 127.90, 127.65, 127.34, 126.90, 117.08, 62.32, 55.8, 54.65, 38.2

**2g**, 55%**4-(4-fluorophenyl)-2,3-dihydro-1-(phenylmethyl)-1H-pyrrole**

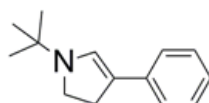
^1H NMR (400 MHz, CDCl_3): δ 7.09-7.24 (m, 9H), 6.15 (s, 1H), 4.26 (s, 2H), 3.65 (m, 2H), 2.23 (m, 2H); ^{13}C NMR (100 MHz, CDCl_3) δ 140.37, 137.12, 136.4, 128.80, 128.37, 128.85, 127.90, 127.34, 126.90, 117.18, 62.32, 54.65, 33.32

**2h**, 85%**4-(4-nitrophenyl)-2,3-dihydro-1-(phenylmethyl)-1H-pyrrole**

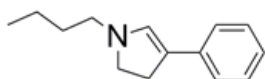
^1H NMR (400 MHz, CDCl_3): δ 8.21-7.64 (dd, 4H), 7.09-7.24 (m, 5H), 6.15 (s, 1H), 4.26 (s, 2H), 3.65 (m, 2H), 2.23 (m, 2H); ^{13}C NMR (100 MHz, CDCl_3) δ 147.37, 145.12, 136.4, 128.80, 128.37, 128.85, 127.90, 127.34, 126.90, 117.18, 62.32, 54.65, 33.32

**2i**, 52%**4-(3,4-dimethoxyphenyl)-2,3-dihydro-1-(phenylmethyl)-1H-pyrrole**

^1H NMR (400 MHz, CDCl_3): δ 7.19-7.24 (m, 8H), 7.08-6.87 (dd, 4H), 6.15 (s, 1H), 4.26 (s, 2H), 3.83 (s, 6H), 3.65 (m, 2H), 2.23 (m, 2H); ^{13}C NMR (100 MHz, CDCl_3) δ 149.37, 149.10, 136.4, 131.71, 128.80, 128.37, 128.25, 127.90, 127.65, 127.34, 127.09, 117.08, 58.8, 56.1, 51.65, 38.2

**2j**, 83%**4-phenyl-2,3-dihydro-1-(t-butyl)-1H-pyrrole**

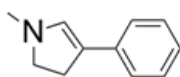
^1H NMR (400 MHz, CDCl_3): δ 7.09-7.24 (m, 5H), 6.15 (s, 1H), 3.65 (m, 2H), 2.23 (m, 2H), 1.28 (s, 9H); ^{13}C NMR (100 MHz, CDCl_3) δ 139.37, 128.80, 128.37, 128.10, 127.90, 117.08, 62.32, 54.65, 38.32, 28.8



2k, 92%

4-phenyl-2,3-dihydro-1-butyl-1H-pyrrole

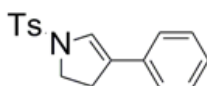
^1H NMR (400 MHz, CDCl_3): δ 7.09-7.24 (m, 5H), 6.15 (s, 1H), 3.65 (m, 2H), 2.55 (t, 2H), 2.08 (t, 3H), 1.38 (m, 2H), 1.31 (m, 2H), 0.90 (t, 3H); ^{13}C NMR (100 MHz, CDCl_3) δ 139.37, 128.61, 128.12, 127.4, 126.80, 117.08, 57.32, 51.65, 38.32, 30.6, 20.5, 13.8



2l, 88%

4-phenyl-2,3-dihydro-1-methyl-1H-pyrrole

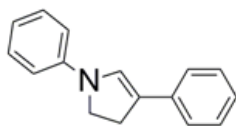
^1H NMR (400 MHz, CDCl_3): δ 7.09-7.24 (m, 5H), 6.15 (s, 1H), 3.65 (m, 2H), 3.04 (s, 3H), 2.23 (m, 2H); ^{13}C NMR (100 MHz, CDCl_3) δ 139.37, 128.64, 127.90, 126.65, 117.08, 53.32, 43.5, 37.9



2m, 86%

4-phenyl-2,3-dihydro-1-tosyl-1H-pyrrole

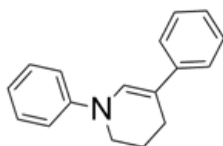
^1H NMR (400 MHz, CDCl_3): δ 7.40-7.74 (dd, 4H), 7.09-7.24 (m, 5H), 6.15 (s, 1H), 4.26 (s, 2H), 3.65 (m, 2H), 2.34 (s, 3H), 2.23 (m, 2H); ^{13}C NMR (100 MHz, CDCl_3) δ 139.37, 137.12, 133.4, 129.80, 128.37, 128.25, 127.90, 127.65, 126.90, 117.08, 44.32, 36.65, 21.32



2n, 68%

1,4-diphenyl-2,3-dihydro-1H-pyrrole

^1H NMR (400 MHz, CDCl_3): δ 7.09-7.24 (m, 10H), 6.15 (s, 1H), 3.65 (m, 2H), 2.23 (m, 2H); ^{13}C NMR (100 MHz, CDCl_3) δ 144.42, 139.37, 129.12, 128.4, 126.80, 120.37, 120.15, 119.25, 117.08, 48.32, 37.32



2o, 90%

1,5-diphenyl-1,2,3,4-tetrahydropyridine

^1H NMR (400 MHz, CDCl_3): 6.89-7.24 (m, 10H), 6.15 (s, 1H), 4.04 (t, 2H), 1.96 (t, 2H), 1.56 (m, 2H); ^{13}C NMR (100 MHz, CDCl_3) δ 139.37, 137.12, 136.4, 128.70, 128.37, 128.25, 127.90, 127.65, 127.34, 126.90, 120.08, 119.41, 51.00, 28.67, 20.32

Reference

1. a) Spande, T. F.; Garaffo, H. M.; Edwards, M. W.; Yeh, H.J. C.; Pannell, L.; Daly, J. W. *J. Am. Chem. Soc.* **1992**, *114*, 3475; b) Li, S.; Huang, K.; Zhang, J.; Wu, W.; Zhang, X. *Org. Lett.* **2013**, *15*, 1036; c) Li, S.; Huang, K.; Zhang, J.; Wu, W.; Zhang, X. *Org. Lett.* **2013**, *15*, 3078; d) Schneider, M. J.; Lijewski, M.; Woelfel, R.; Haumann, M.; Wasserscheid, P. *Angew. Chem. Int. Ed.* **2013**, *52*, 6996.
2. Zhang, H.; Curran, D.P. *J. Am. Chem. Soc.* **2011**, *133*, 10376.

3. Matsumura, Y.; Terauchi, J.; Yamamoto, T.; Konno, T.; Shono, T. *Tetrahedron*. **1993**, *49*, 8503.
4. a) Kwok, S. W.; Zhang, L.; Grimster, N. P.; Fokin, V. V. *Angew. Chem. Int. Ed.* **2014**, *53*, 3452; b) Schwalm, C. S.; Castro, I. B. D.; Ferrari, J.; Olivera, F. L.; Aparicio, R.; Correia, C. R. D. *Tetrahedron Lett.* **2012**, *53*, 1660; c) Busacca, C. A.; Dong, Y. *Tetrahedron Lett.* **1996**, *37*, 3947; d) Nairoukh, Z.; Blum, J. *J. Org. Chem.* **2014**, *79*, 2397; e) Wu, L.; Fleischer, I.; Jackstell, R.; Beller, M. *J. Am. Chem. Soc.* **2013**, *135*, 3989.
5. Crozet, D.; Urrutigoity, M.; Kalck, P. *ChemCatChem*, **2011**, *3*, 1102.